

Beamforming Technologies for Ultra-Massive MIMO in Terahertz Communications

Chong Han

Shanghai Jiao Tong University

chong.han@sjtu.edu.cn

Linglong Dai

Tsinghua University

dail@tsinghua.edu.cn

Zhi Chen

University of Electronic Science and
Technology of China

chenzhi@uestc.edu.cn

Outline



- **Chapter 1: Introduction**
 - i. Evolution to 6G
 - ii. Applications
 - iii. Motivations for THz UM-MIMO
- **Chapter 2: THz UM-MIMO Systems**
 - i. Electronic and photonic approaches
 - ii. New material approaches
 - iii. THz UM-MIMO channel
- **Chapter 3: THz Beamforming Technologies**
 - i. Fundamentals of beamforming
 - ii. State-of-the-art and challenges on beamforming
 - iii. Far-field beamforming
 - iv. Near-field beamforming/beamfocusing
- **Chapter 4: THz Beam Management**
 - i. Fundamentals of beam management
 - ii. State-of-the-art and challenges on beam management
 - iii. Beam estimation/alignment
 - iv. Beam tracking
 - v. Beam-guided medium access
- **Chapter 5: Future Directions**
 - i. Cross far- and near-field beamforming
 - ii. IRS-assisted hybrid beamforming
 - iii. Beam management in IRS assisted systems
- **Conclusion**

6G Key Capability Vision



- 6G Application scenarios: "Broadband, ubiquitous, smart"



Metaverse



AR automatic drive



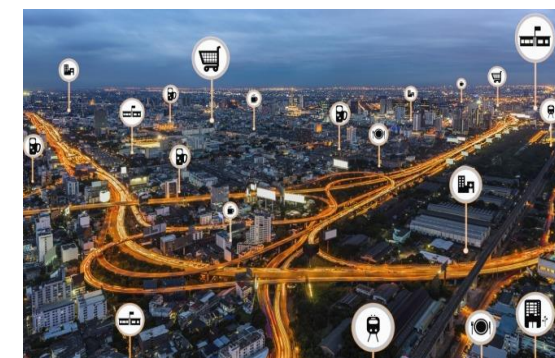
Intelligent manufacturing 2025



Holographic intelligent medical service



Networked UAV



Smart city

6G Key Capability Vision



	Peak rate	User data rate	Delay	Reliability	Spectral efficiency	Connection density
5G	0.01Tbit/s	0.1-0.5 Gbit/s	1 ms	99.999%	30 bps/Hz	10^2 devices/100 m ²
6G	1 Tbit/s	10 Gbit/s	0.1 ms	99.99999%	100 bps/Hz	10^3 devices/100 m ²

Rich spectrum resources

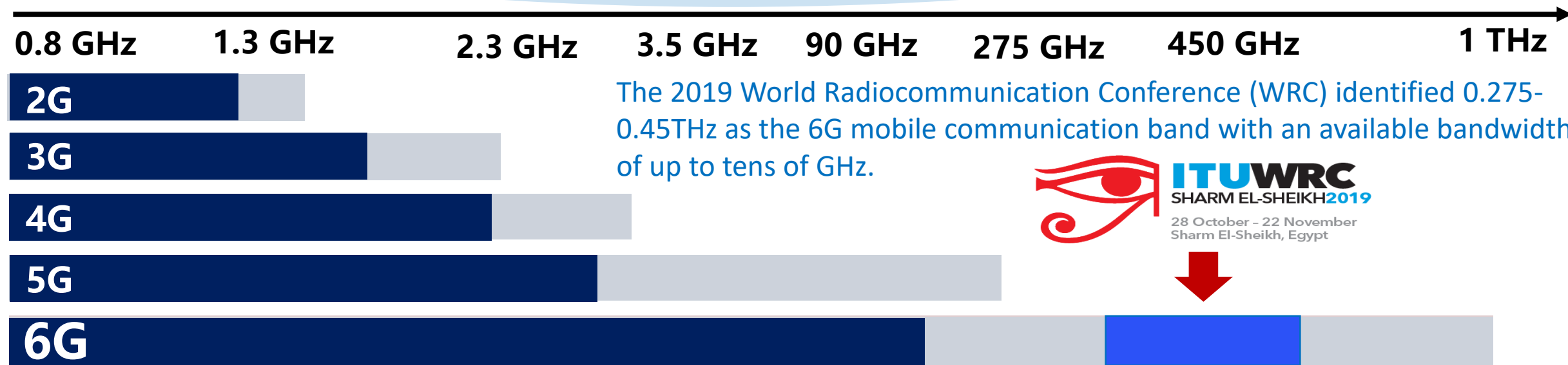
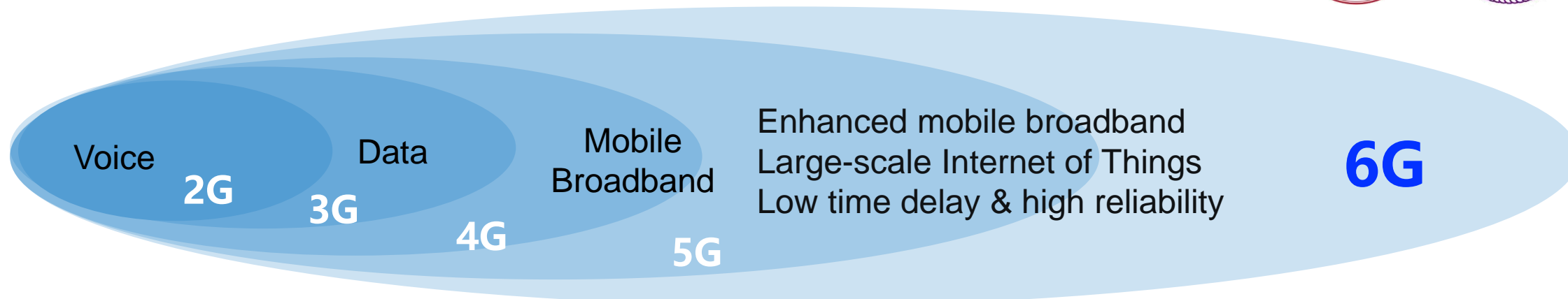
Ultra-high frequency (mmWave, THz)

Ultra-massive MIMO (256 and above)

Multiple times of spectral efficiency

Ultra-high frequency and ultra-large scale MIMO are recognized as key technologies

Trend One: Higher Carrier Band



Ultra-high frequency band (millimeter wave, terahertz) will become important supports for 6G communication ultra-wideband real-time service.

Trend Two: Larger Antenna Array Scale



1G

2G

3G

4G

5G

6G

Omni-directional antenna

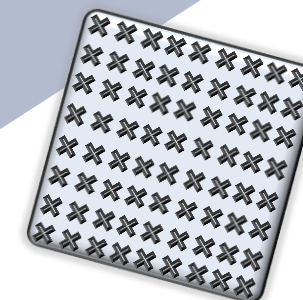
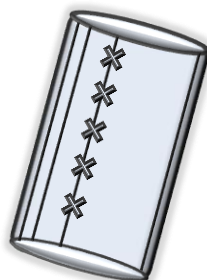
Single-polarized directional antenna

Bipolar antenna

MIMO antennas (2 – 8)

Massive MIMO antennas (64 – 128)

Ultra-massive MIMO antennas (256 – 1024)

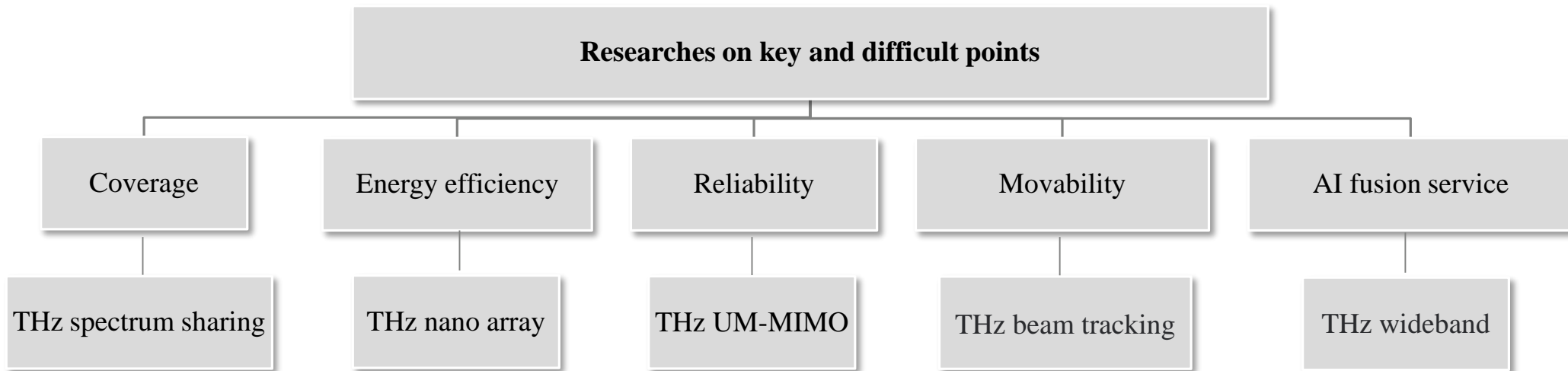
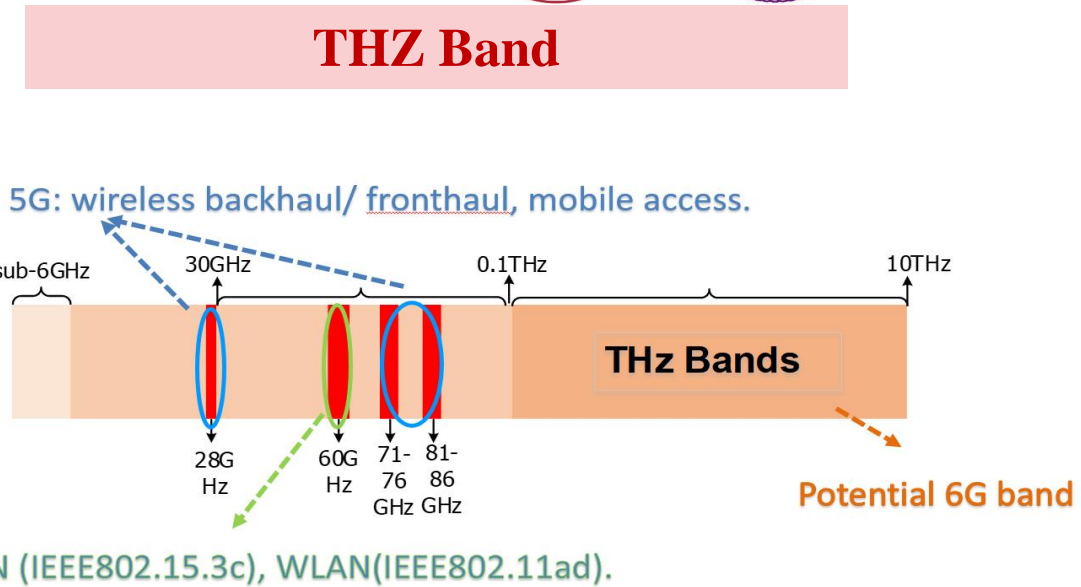


Very large scale MIMO (256 and above) will become an important support for 6G multi-mode intensive deployment

Motivations for Terahertz



- THz has **ultra-wideband, high-speed communication capability and high precision sensing imaging capability**, which is an important candidate technology for 6G
- Key technologies to meet the requirements of 6G communication scenarios become research hotspots



Research Progress of THz



Europe

- **Eu framework programme:** Horizon 2020、Horizon Europe
- **Transnational terahertz project:** Heterogeneous networking
Ultra-high capacity sending

China

- Terahertz research launched at the "Terahertz Science and Technology" conference in 2005
- "Terahertz Wireless Communication Technology and System" major project of Ministry of Science and Technology in 2018
- Terahertz Core Devices and Transceiver Chips in 2019
- Domestic universities, research institutes and other joint research institutions, close to or part of the world's advanced level in 2020

America

- DARPA and NASA launched the terahertz system Bell LABS 0.625 THz communication system is the highest frequency fully electronic architecture terahertz communication system realized to date in 2009.
- The FCC approved the opening of future wireless mobile communications research in August 2020.

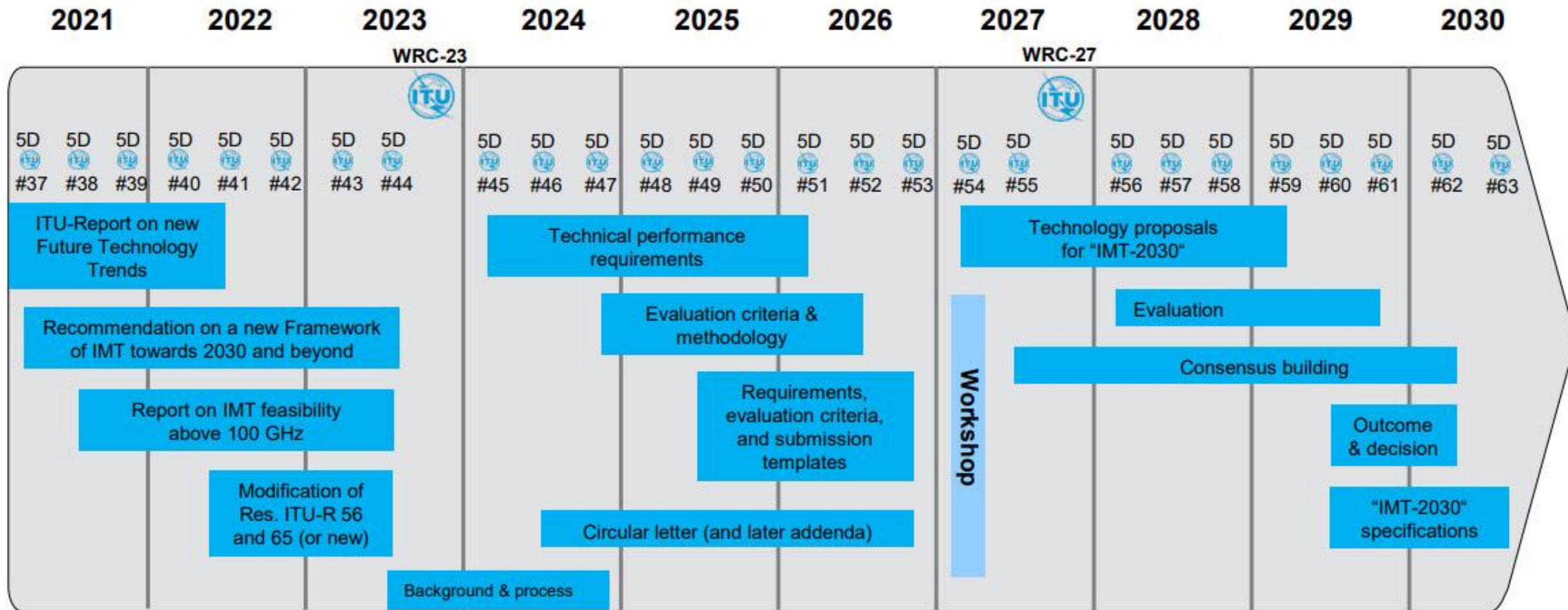
Japan

- Terahertz technology ranks first among the top ten technologies in the strategic planning of future science and technology
- In 2006, NTT demonstrated the first terahertz communication
The government and the people will work together to formulate the 2030 "post-5G" strategy

International Telecommunication Union ITU

- In 2019, ITU WRC-19 allocated bands 0.275 - 0.296 THz, 0.306 - 0.313 THz, 0.318 - 0.333 THz, and 0.356 - 0.45 THz for land mobile and fixed services
- August 2021 "IMT Above 100GHz" to explore the feasibility of frequency band above 100GHz
- In 2021, IEEE ComSoc RCC Terahertz Special Interest Group was established

ITU-R timeline for IMT-2030



Note 1: WP 5D #59 will additionally organize a workshop involving the Proponents and registered Independent Evaluation Groups (IEGs) to support the evaluation process

Note 2: While not expected to change, details may be adjusted if warranted. Content of deliverables to be defined by responsible WP 5D groups

Note by the ITU-R Radiocommunication Bureaux: This document is taken from Attachment 2.12 to Chapter 2 of Document 5D/1361 (Meeting report WP 5D #41, June 2022) and adjustments could be made in the future. ITU holds copyright in the information – when used, reference to the source shall be done.

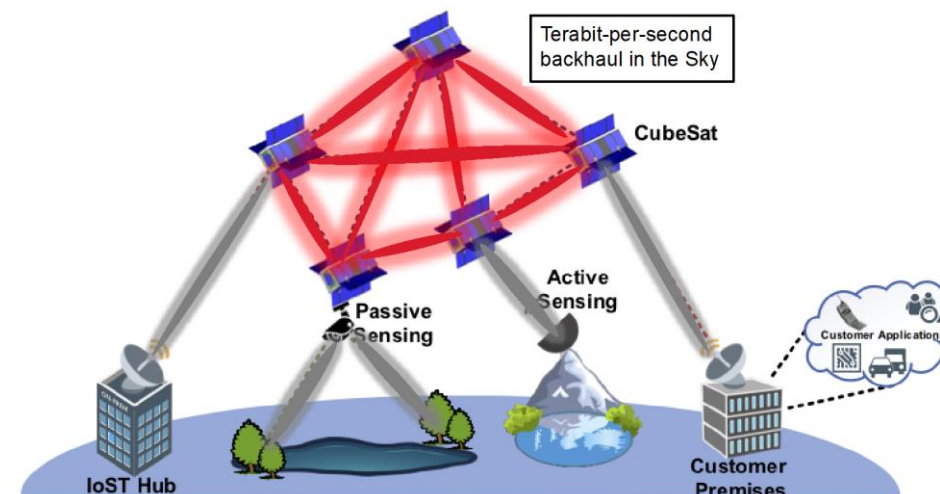
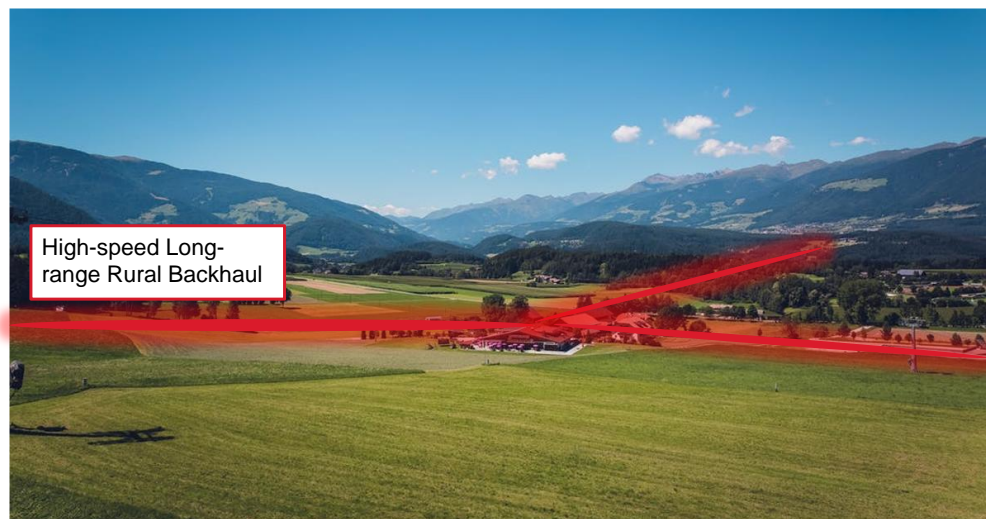
THz Application Scenarios



- **Tbps** wireless communications rate



Tbps MR and metaverse



THz Application: Practical Example



- **Tbps** wireless communications rate
 - Sports event broadcasting: Ultra-low latency, uncompressed 8K ultra HD video

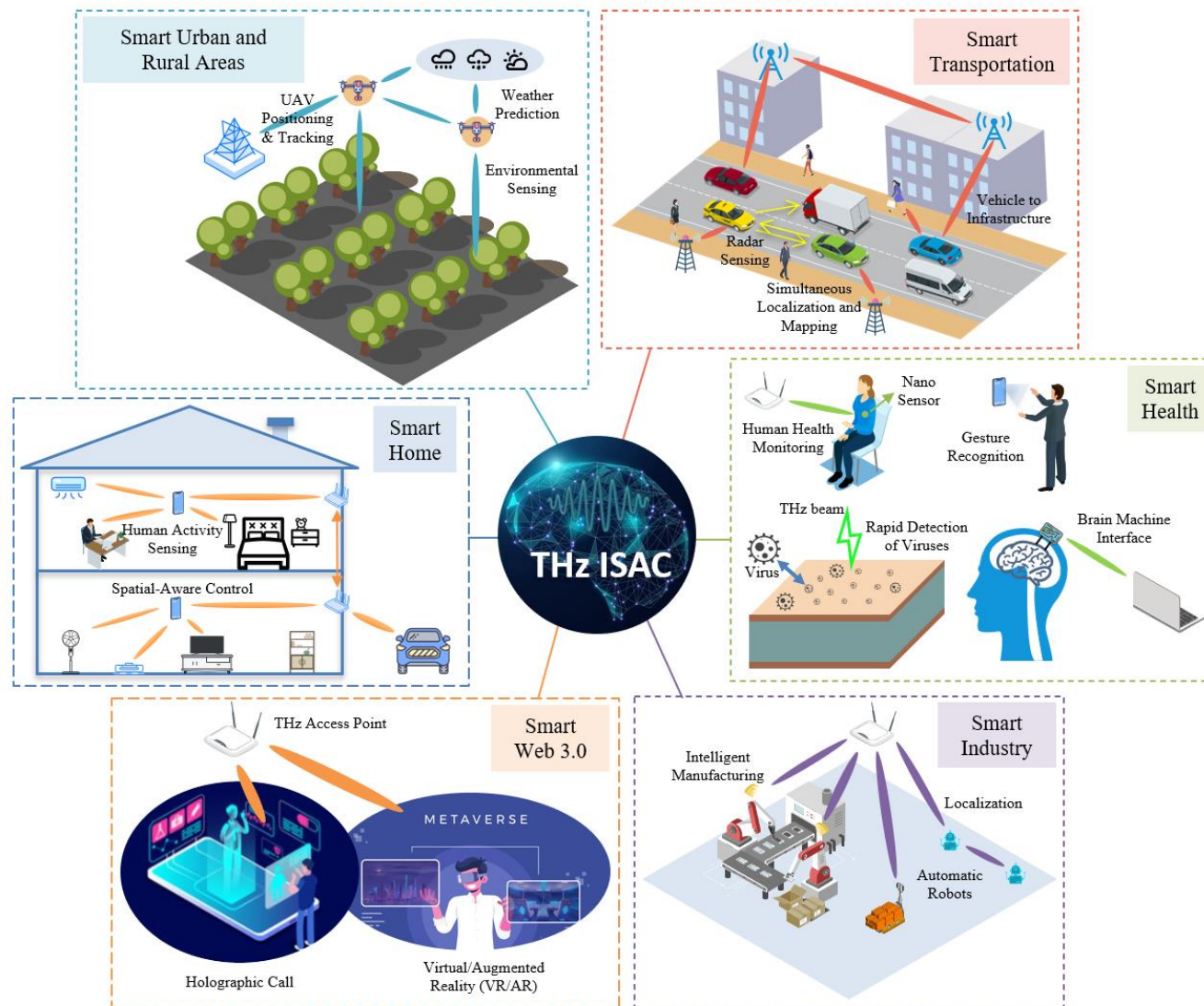


- Real-time transmission rate exceeding 80Gbps
- Distance coverage of over 1 kilometer
- New milestone in real-time transmission distance

THz Application Scenarios



- **Tbps** wireless communications rate and **millimeter-level** sensing accuracy

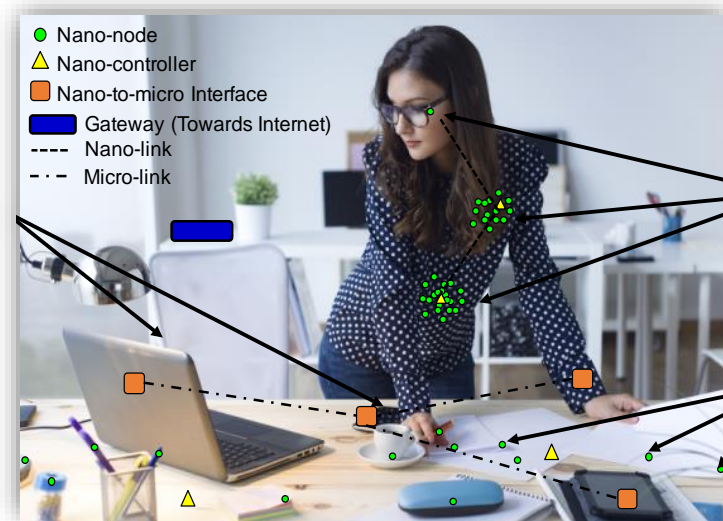


C. Han, Y. Wu, Z. Chen, Y. Chen, and G. Wang, "THz ISAC: A Physical Layer Perspective of Terahertz Integrated Sensing and Communication," IEEE Communications Magazine, 2023

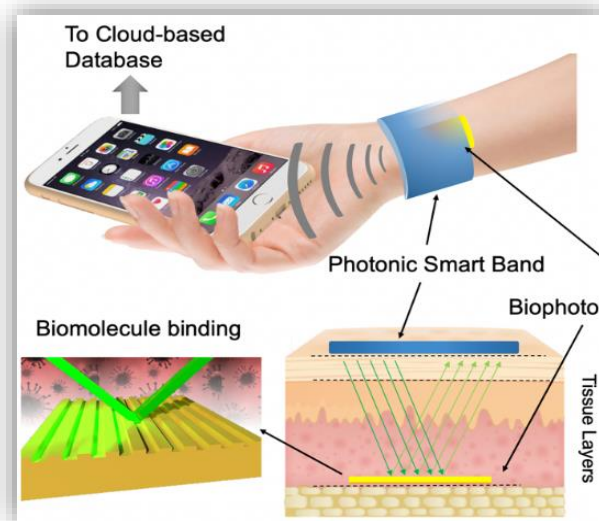
THz Application Scenarios



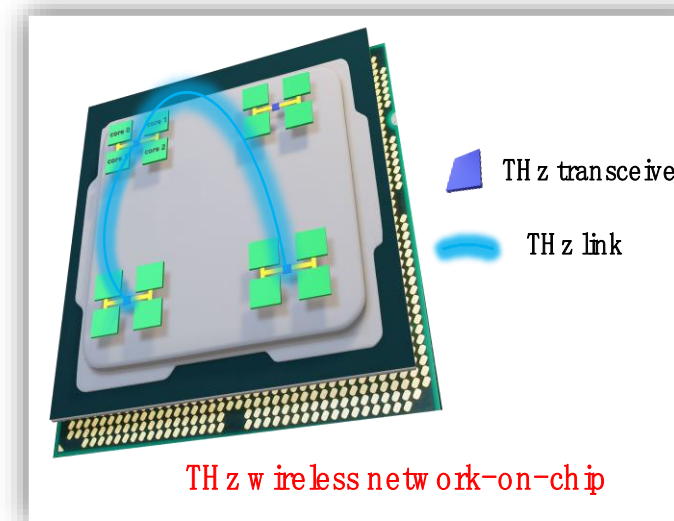
- Terahertz **nano-micro-scale** communication scenarios



Smart Wearable Device



In Vivo Nanocommunication



On-chip Communication

Motivations for THz Ultra-Massive MIMO



- Coverage challenge for THz communications

High frequency



- Large free space loss
- Large reflection and diffraction loss
- Huge molecular absorption loss



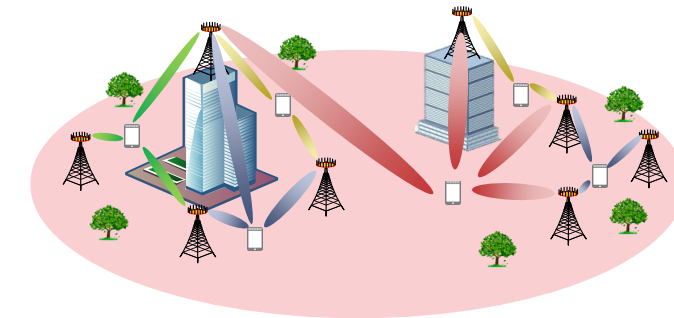
Short wavelength

Short transmission distance

- **Solution: THz ultra-massive MIMO (UM-MIMO) systems**

Decreasing size of THz antennas → use large number of antennas to compose a large-scale antenna array, e.g., 1024 antennas

- Provide **high-speed mobile access services**
- Improve **system capacity** and **signal quality** through centralized deployment of UM-MIMO and beamforming technology
- Improves **signal coverage** and **transmission rate** through distributed deployment of UM-MIMO
- Improve the accuracy of **3D location service** and realize **spatial positioning and perception**



Outline



- **Chapter 1: Introduction**
 - i. Evolution to 6G
 - ii. Applications
 - iii. Motivations for THz UM-MIMO
- **Chapter 2: THz UM-MIMO Systems**
 - i. Electronic and photonic approaches
 - ii. New material approaches
 - iii. THz UM-MIMO channel
- **Chapter 3: THz Beamforming Technologies**
 - i. Fundamentals of beamforming
 - ii. State-of-the-art and challenges on beamforming
 - iii. Far-field beamforming
 - iv. Near-field beamforming/beamfocusing
- **Chapter 4: THz Beam Management**
 - i. Fundamentals of beam management
 - ii. State-of-the-art and challenges on beam management
 - iii. Beam estimation/alignment
 - iv. Beam tracking
 - v. Beam-guided medium access
- **Chapter 5: Future Directions**
 - i. Cross far- and near-field beamforming
 - ii. IRS-assisted hybrid beamforming
 - iii. Beam management in IRS assisted systems
- **Conclusion**

THz UM-MIMO Systems



Fabrication can be roughly divided into three categories:

- **Electronic-based**

- horns, reflectors
- cavity-backed slot antenna arrays

- **Photonics-based**

- photo-conductive antennas
- silicon-based lenses

- **New materials-based**

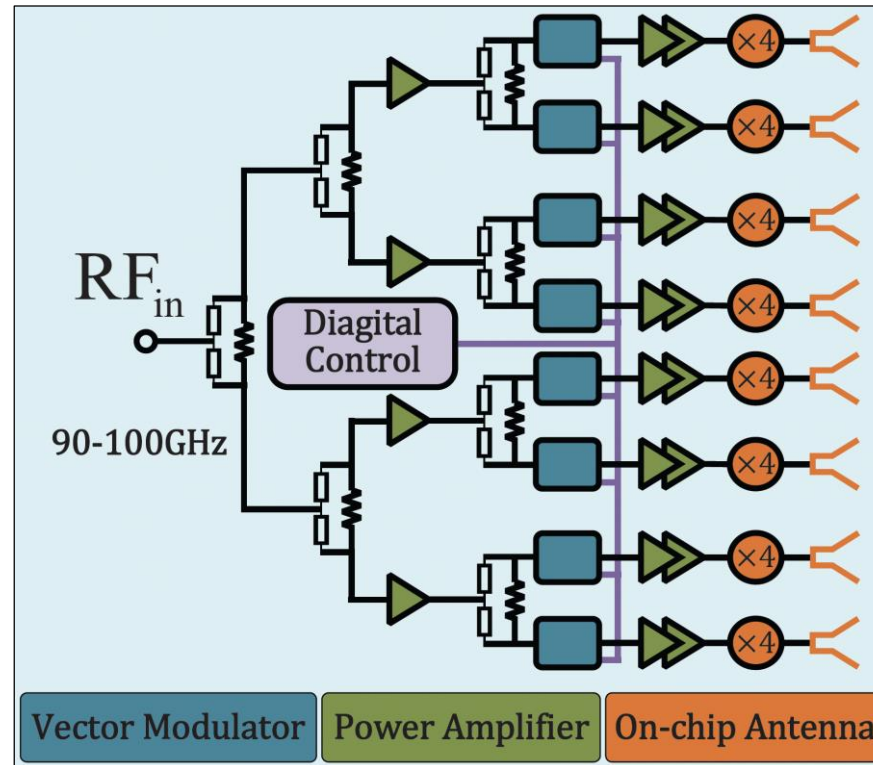
- vanadium dioxide (VO₂)
- graphene and liquid crystal (LC)

B. Ning, Z. Tian, Z. Chen, C. Han, S. Li, J. Yuan, and R. Zhang, “**Prospective Beamforming Technologies for Ultra-Massive MIMO in Terahertz Communications: A Tutorial,**” IEEE Open Journal of the Communications Society, 2023

Electronic approaches



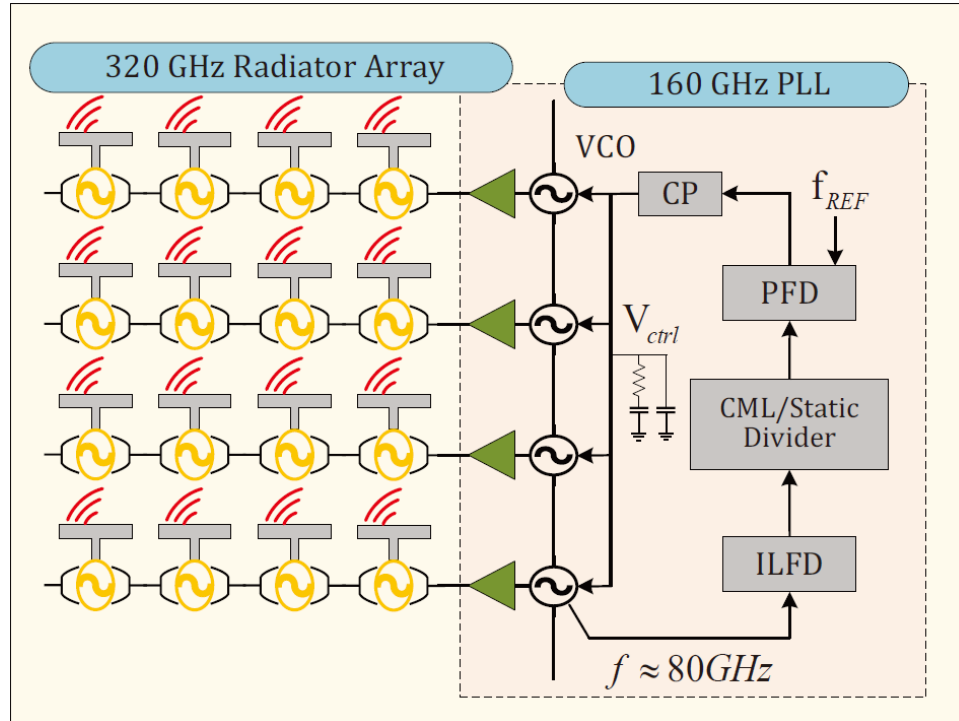
- As the efficacy of electronic components is constrained in the THz band, a feasible solution is to **modulate the phase in the lower frequency** and then **convert to the THz region**



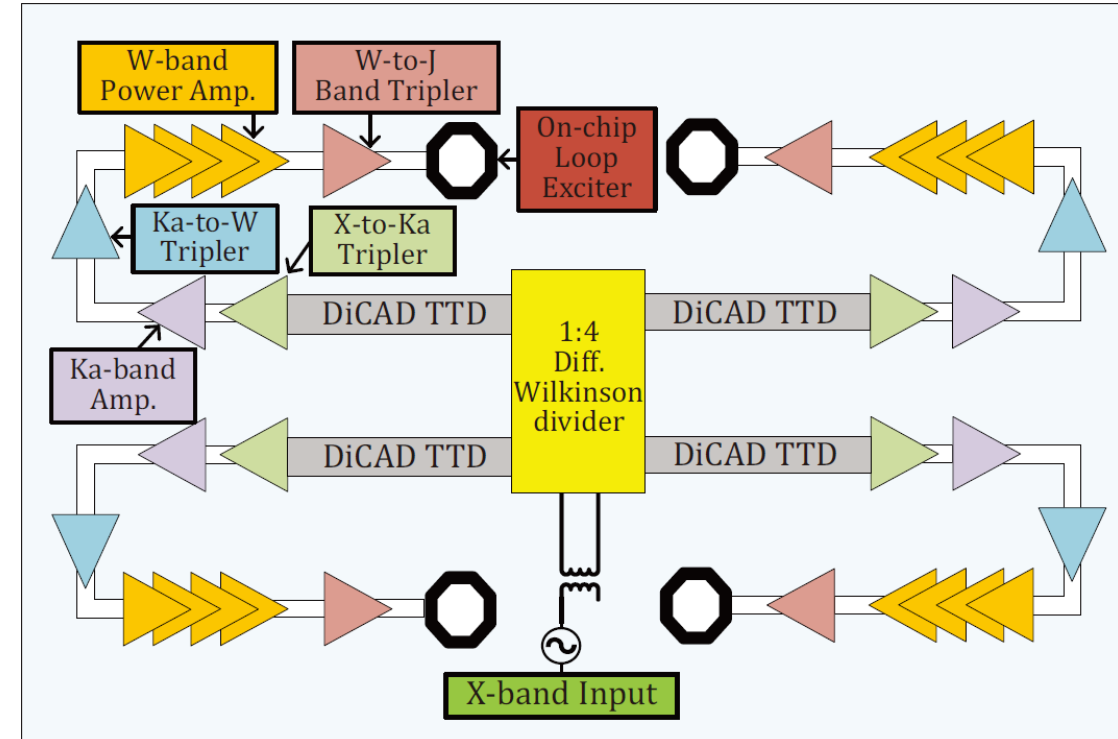
370 – 410 GHz 8 × 1 ULA

Y. Yang et al., “An Eight-Element 370-410-GHz Phased-Array Transmitter in 45-nm CMOS SOI with Peak EIRP of 8–8.5 dBm,” IEEE Trans. Microwave Theory Tech., vol. 64, no. 12, Dec. 2016, pp. 4241–49.

Electronic approaches



4 × 4 URPA using 130 nm SiGe bipolar-CMOS (BiCMOS) technology at 320 GHz [a]



280 GHz 2 × 2 chip-scale dielectric resonator antenna array [b]

[a] R. Han et al., “A SiGe Terahertz Heterodyne Imaging Transmitter with 3.3 mW Radiated Power and Fully-Integrated Phase-Locked Loop,” IEEE J. Solid-State Circuits, vol. 50, no. 12, Dec. 2015, pp. 2935–47.

[b] N. Buadana et al., “A 280-GHz Digitally Controlled Four Port Chip-Scale Dielectric Resonator Antenna Transmitter with DiCAD True Time Delay,” IEEE Solid-State Circuits Lett., vol. 3, 2020, pp. 454–57

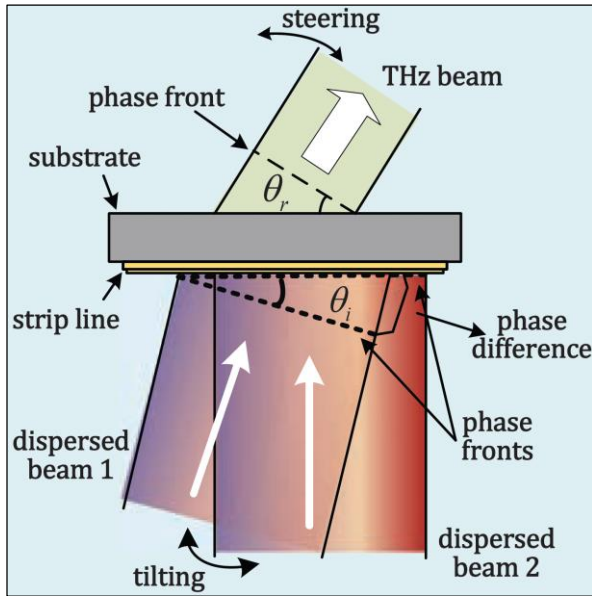
Photonic approaches



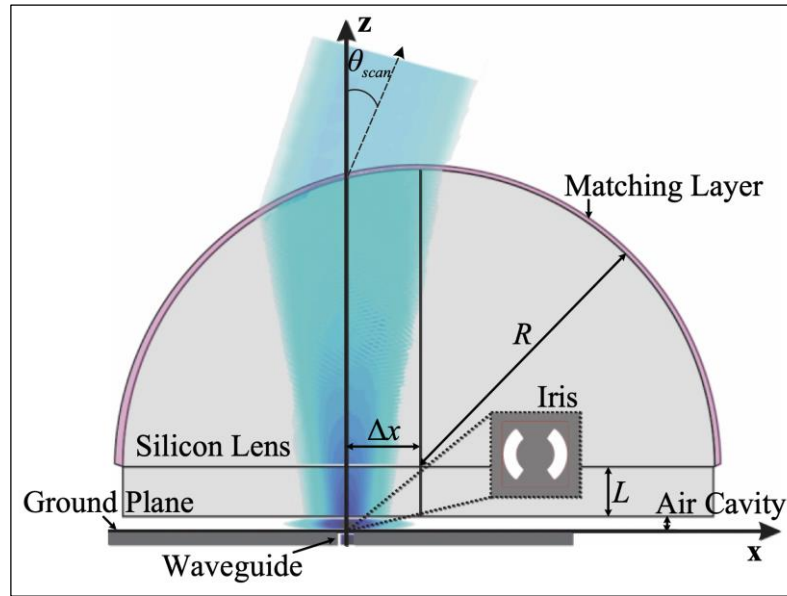
In **the photonic approach**, schemes for THz dynamic beam scanning are designed.

- Frequency-scanning antennas can be used to control **THz beam steering**
- A proposed photoelectric phase shifter can control **300 GHz** beam scanning within 50 degree
- The optical **TTD phase shifters** are also employed to offer stable time delay for wideband communications

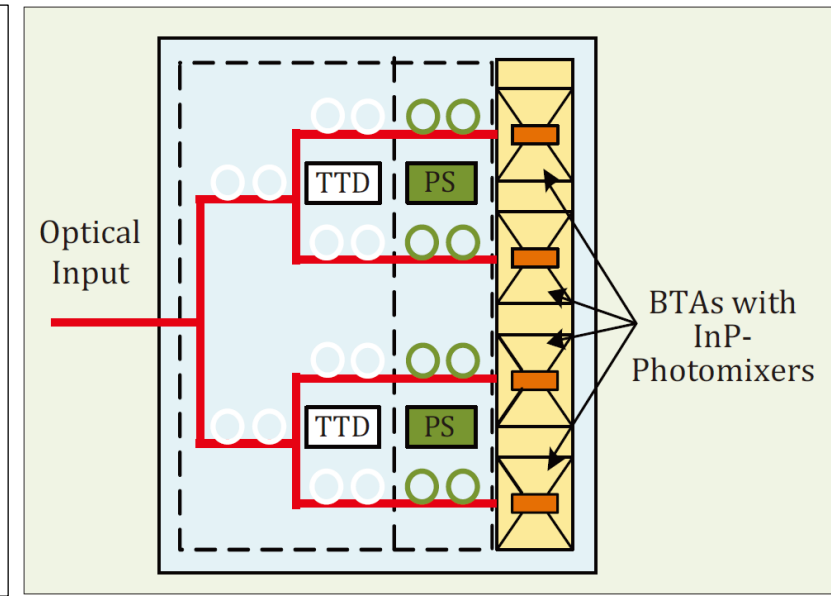
Photonic approaches



Changing the phase difference of two laser beams [a]



Refraction based on the optical lens antennas [b]



The schematic view of an optical TTD-based chip [c]

[a] K.-i. Maki and C. Otani, “**Terahertz Beam Steering and Frequency Tuning by Using the Spatial Dispersion of Ultrafast Laser Pulses,**” *Opt. Express*, vol. 169, July 2008, pp. 10,158–69.

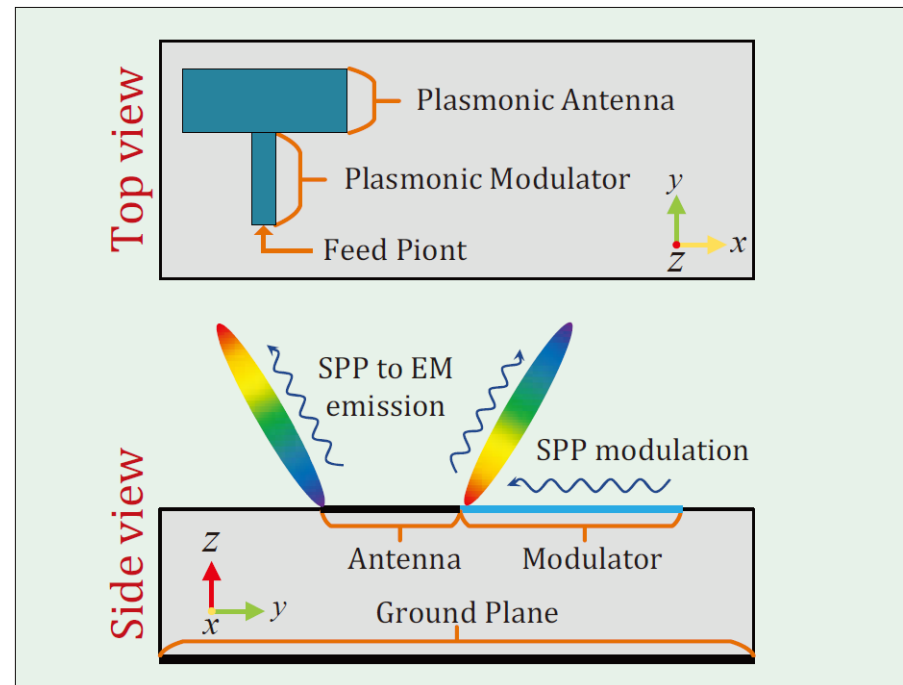
[b] M. Alonso-delPino et al., “**Beam Scanning of Silicon Lens Antennas Using Integrated Piezomotors at Submillimeter Wavelengths,**” *IEEE Trans. THz Sci. Tech.*, vol. 9, no. 1, Nov. 2019, pp. 47–54.

[c] P. Lu et al., “**Photonic Assisted Beam Steering for Millimeter-Wave and THz Antennas,**” *IEEE Conf. Antenna Meas. & Appl.*, Sweden, 2018, pp. 1–4.

New material approaches



- **Graphene**, i.e., a two-dimensional form of graphite, has attracted the attention of the scientific community due to its unique **electronic and optical properties**.

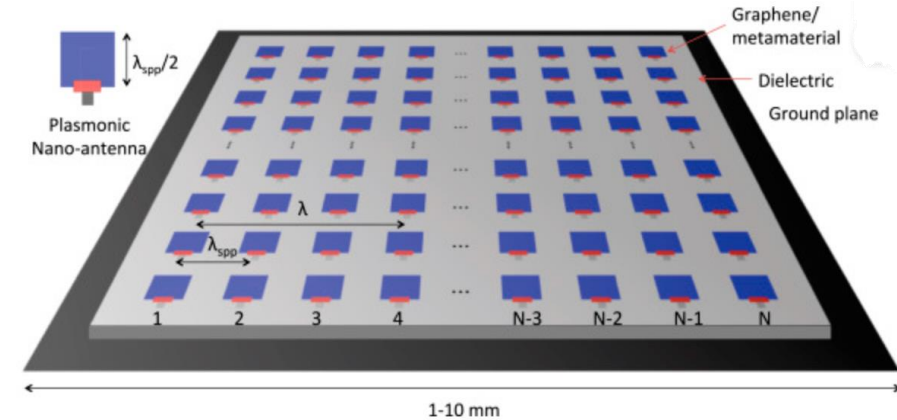


The working principle and design of the THz front end

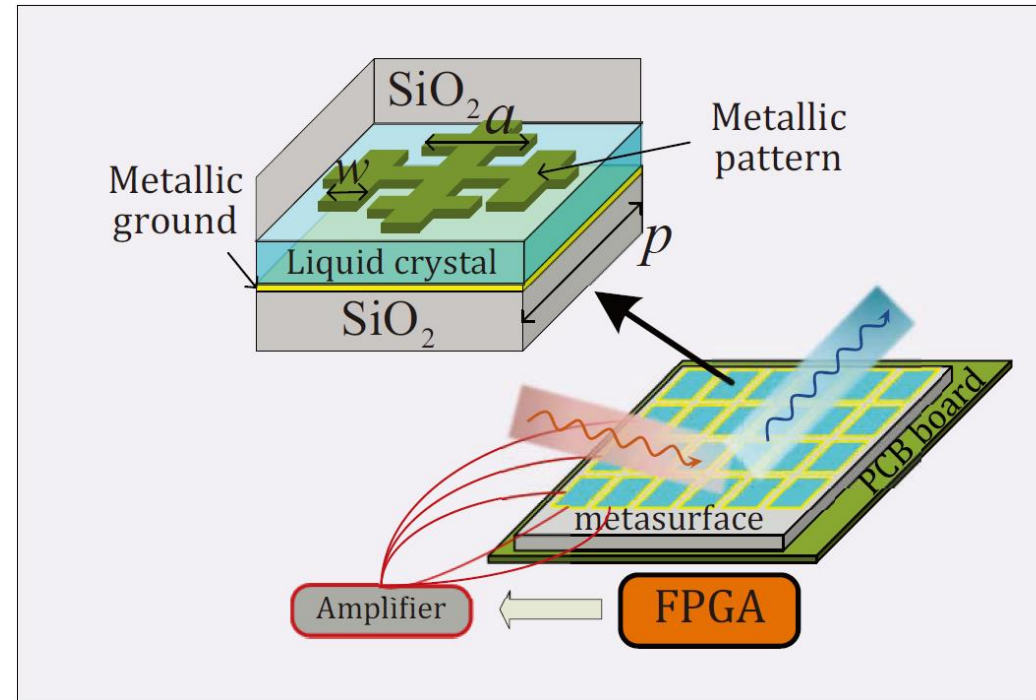
New material approaches



- **Individual** graphene antennas at the THz band
 - with reconfigurable radiation patterns
- **Small-scale** graphene antenna
 - the beam scanning range has not been piratically tested
- **Reconfigurable** MIMO antenna system for THz communications
- The use of graphene to implement UM-MIMO **plasmonic nano-antenna** arrays
 - implement a 1024×1024 UM-MIMO system at 1THz with arrays that occupy just 1 mm^2
- **Liquid crystal** and **graphene** also show application potential in reconfigurable reflect arrays



New material approaches



The LC reflect array at 0.67 THz

This array is made up of :

- a 24 element linear array
- each element is composed of 50 rows and 2 columns of unit cells with meta-insulator metal-resonator structure

New material approaches



- The reported THz antenna arrays with **dynamic beam scanning capability**

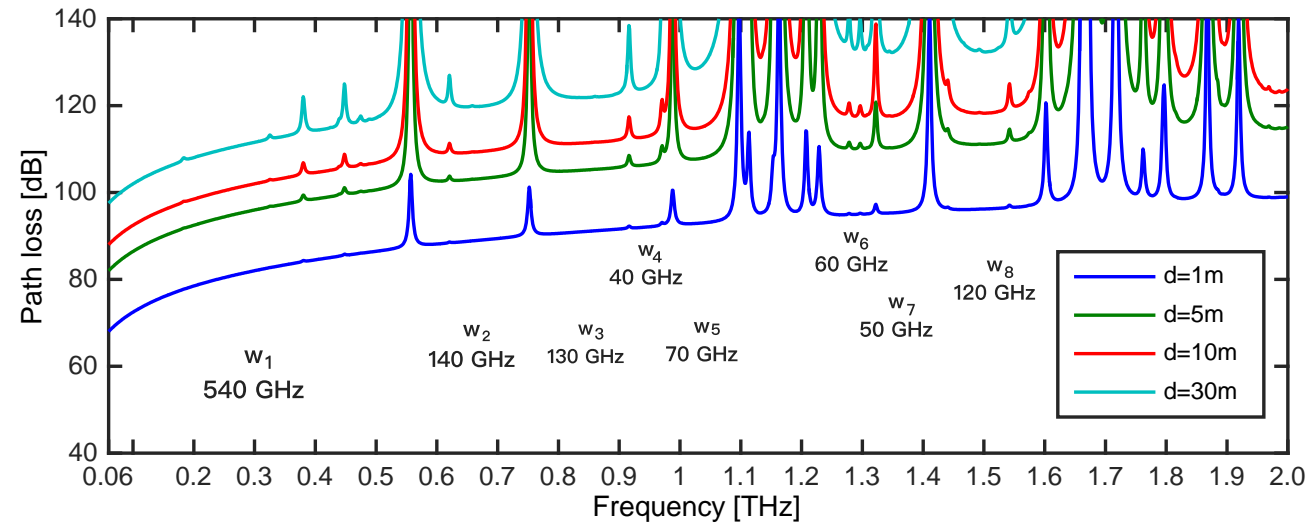
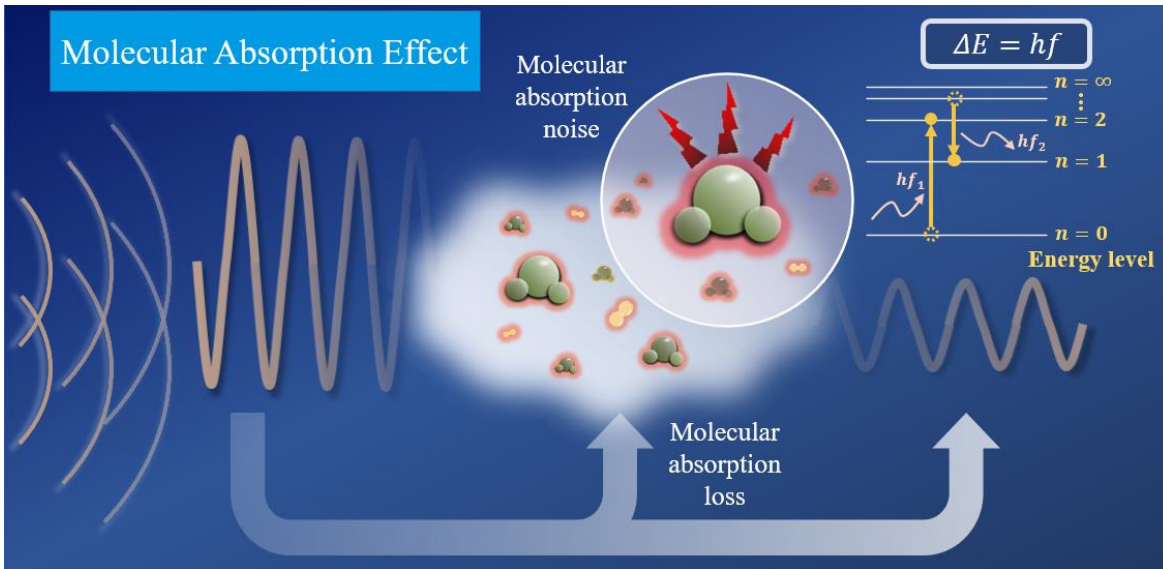
Freq (Hz)	Size	Process	Beam scan	Gain	Antenna type
280 G	4 × 4 arrays	45 nm SOI CMOS	80°/80° ¹	16 dBi	on-chip
140 G	2 × 4 arrays	65 nm CMOS	40°	-	multi-chip
0.53 T	1 × 4 arrays	40 nm CMOS	60°	11.7 dBi	patch
400 G	1 × 8 arrays	45 nm SOI CMOS	75°	12 dBi	patch
0.34 T	2 × 2 arrays	130 nm SiGe BiCMOS	128°/53° ¹	-	patch
320 G	1 × 4 arrays	130 nm SiGe BiCMOS	24°	13 dBi	patch
338 G	4 × 4 arrays	65 nm CMOS	45°/50° ¹	18 dBi	microstrip
317 G	4 × 4 arrays	130 nm SiGe BiCMOS	-	17.3 dBi	return-path gap coupler
280 G	2 × 2 arrays	65 nm CMOS	30°	12.5 dBi	dielectric resonator
300 G	1 × 4 arrays	photonic	90°	10.6 dBi	bow-tie antenna
1.05 T	4 × 4 arrays	graphene	-	13.9 dBi	dipole
1.1 T	2 × 2 arrays	graphene	60°	8.3 dBi	patch
220 – 320 G	600 elements	metallic	48°	28.5 dBi	frequency scanning
0.8 T	2 × 2 arrays	graphene	-	-	photoconductive
1.3 T	25448 elements	graphene	-	29.3 dBi	reflectarray
220 – 320 G	8 × 8 arrays	brass sheets	50°/45° ¹	17 dBi	frequency scanning
100 G	54 × 52 cells	liquid crystals	55°	15 dBi	reflectarray
345 G	-	liquid crystals	20°	35 dBi	reflectarray
100 G	-	VO2	44°/44°	-	metasurfaces
115 G	39 × 39 cells	liquid crystals	20°	16.55 dBi	reflectarray

Device technologies



- Lesson 1: some promising fabrication techniques for implementing UM-MIMO antenna arrays have been developed in the THz range → **we are almost ready**
- Lesson 2: future research may focus on seeking potential solutions for better beam flexibility as well as a larger array size → **we still can do better**
 - **Improve the dynamic beamforming capabilities** of the THz arrays, including adjustment accuracy and scanning range
 - **Increase the size of the antenna array** and pushing it to the level of thousands of elements
 - **Reduce mutual coupling effects** caused by large-scale integration

Molecular Absorption Effect



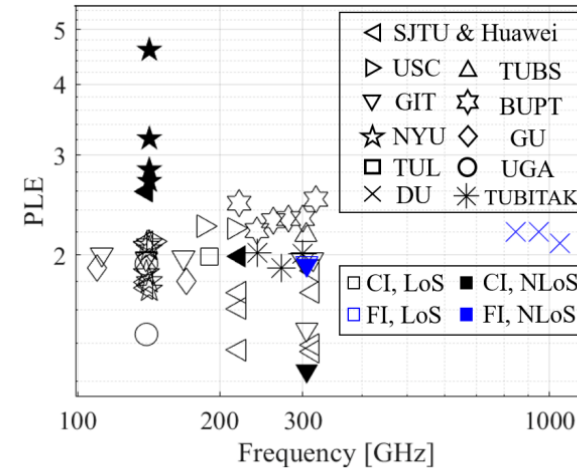
Spectral windows created by molecular absorption effects

Each window has multi-GHz BW, sensitive to f , d , env.

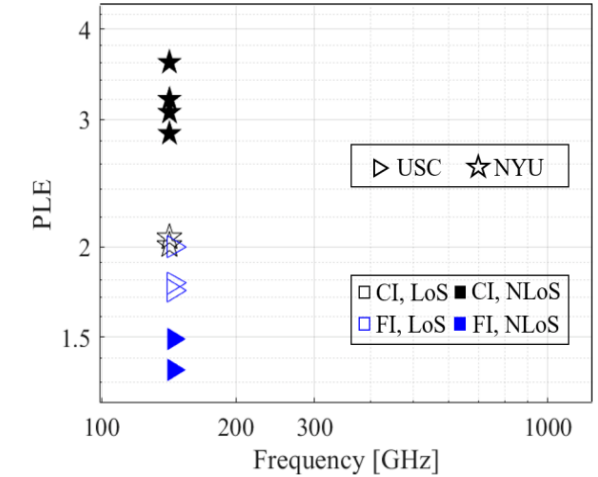
Channel Characteristics



- Path loss exponent (PLE)
 - Larger PLEs in NLoS
 - Mostly close to 2, indicating the dominance of LoS path in the THz band (sparsity)

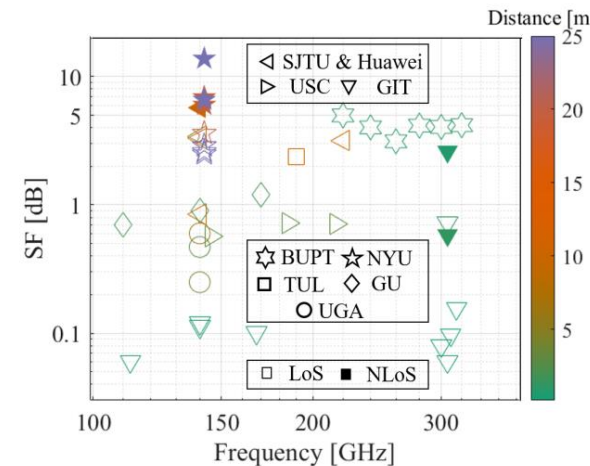


(a) Indoor scenarios

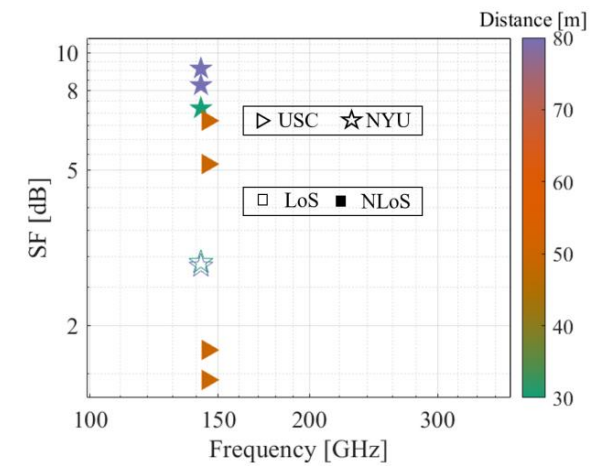


(b) Outdoor scenarios

- Shadow fading (SF): additional loss caused by blockage; mostly calculated as the deviation of path loss to path loss models
 - **Severer shadow fading in NLoS**
 - Mostly lower than 1 in indoor scenarios



(a) Indoor scenarios

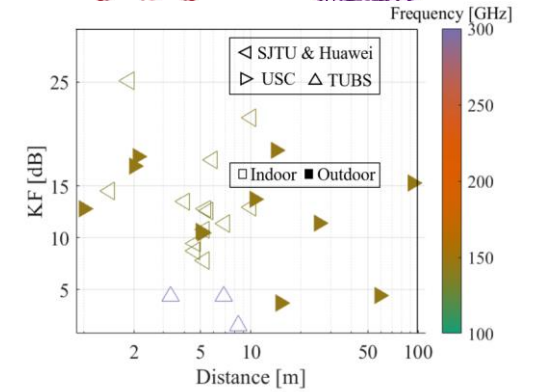


(b) Outdoor scenarios

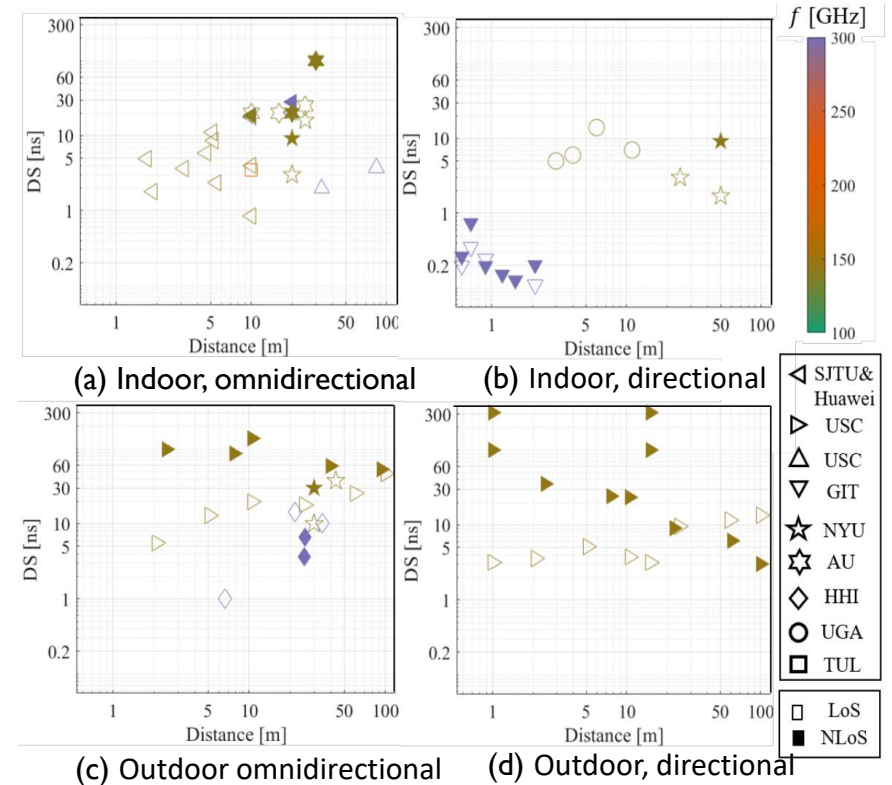
Channel Characteristics



- K-factor (KF): power ratio between the strongest path and other paths
 - Generally larger KF in outdoor scenarios
 - Mostly very large in the THz band (>10 dB), indicating **high sparsity**



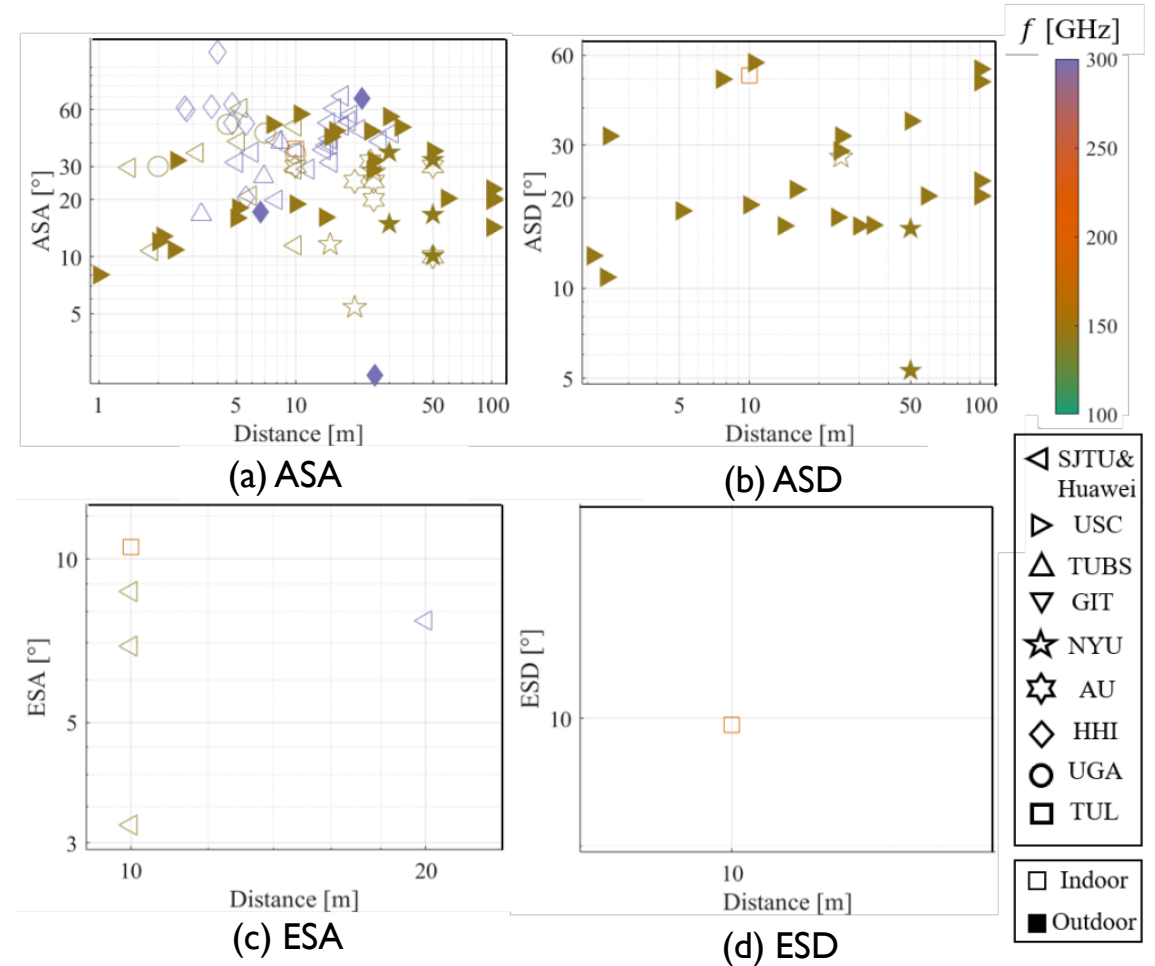
- Delay spread (DS): power dispersion in temporal domain
 - Generally larger DS in outdoor scenarios
 - Smaller DS for higher frequencies
 - Typically around **5~30 ns** in indoor scenarios
 - **5-60 ns** in outdoor scenarios



Channel Characteristic – Angular Spread



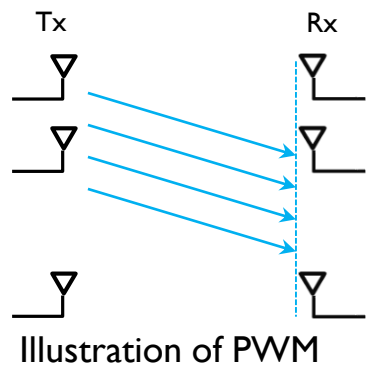
- Angular spread (AS): the power dispersion in the spatial domain
 - Close AS in indoor and outdoor scenarios
 - Typically around 10-60° for ASA and ASD



UM-MIMO Channel Model

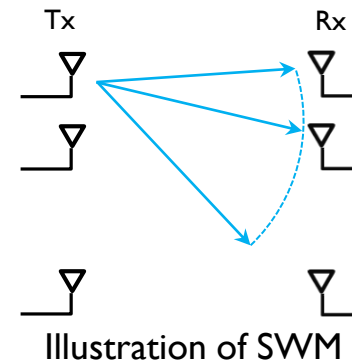


- **Spherical-wave propagation** is the ground truth of electromagnetic wave propagation
 - Individually calculating the channel response of all antennas pairs between Tx and Rx
 - High complexity
- **Planar-wave assumption** is a simplification of spherical-wave propagation
 - Valid in far-field communications
 - Signal transmission is approximated as parallel and the wavefront is analyzed as a plane
 - Low complexity



$$\mathbf{H}_P = \sum_{p=1}^{N_p} \alpha_p \mathbf{a}_{rp} \mathbf{a}_{tp}^H$$

Neglect the non-linear phase from the spherical model

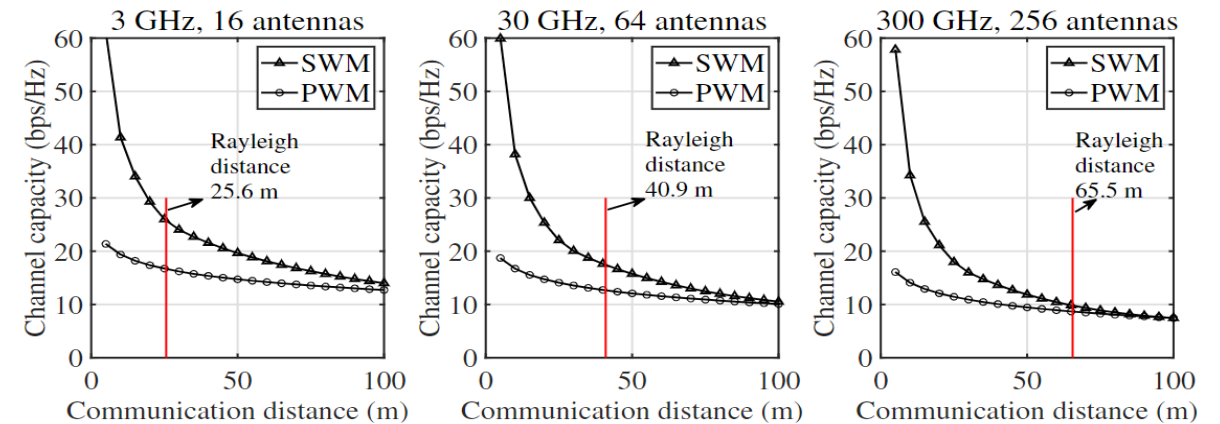
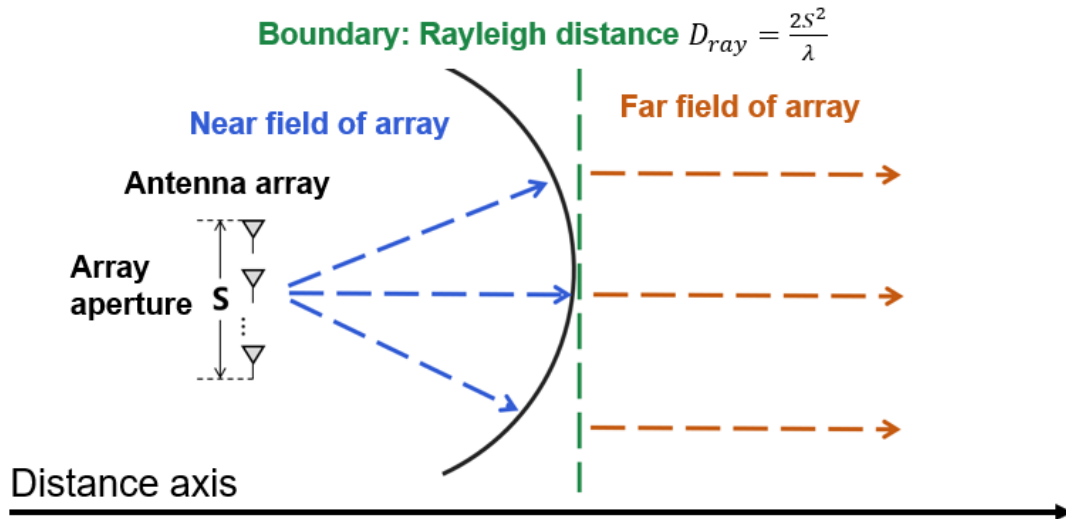


$$\mathbf{H}_S[n_r, n_t] = \sum_{p=1}^{N_p} |\alpha_p^{n_r n_t}| e^{-j \frac{2\pi}{\lambda} D_p^{n_r n_t}}$$

Inaccuracy of Planar-wave Channel Models



- **Rayleigh distance** is the classis boundary between the near-field and far-field, below which **near-field propagation dominates** and the **planar-wave model (PWM)** becomes inaccurate



Channel capacity based on PWM and SWM in different communication distances and frequencies

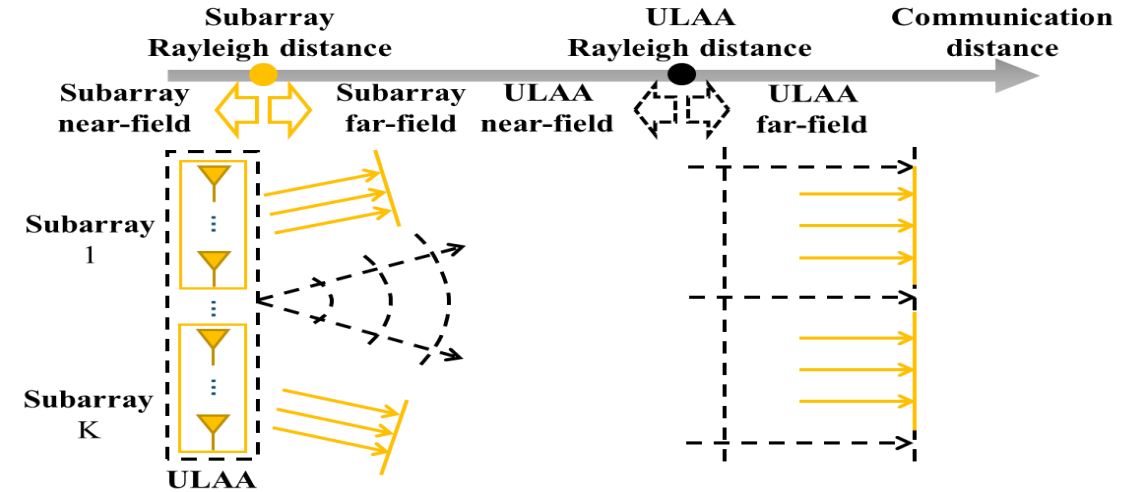
The communication distance $D \gg D_{ray} \rightarrow$ **Planar-wave assumption is valid**

Otherwise, e.g., $D < D_{ray} \rightarrow$ **Spherical-wave propagation needs to be considered**

Hybrid Spherical- and Planar- Wave Model

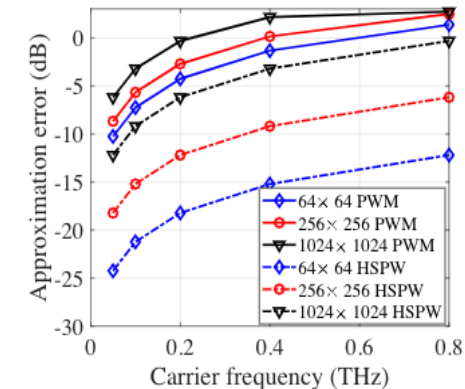
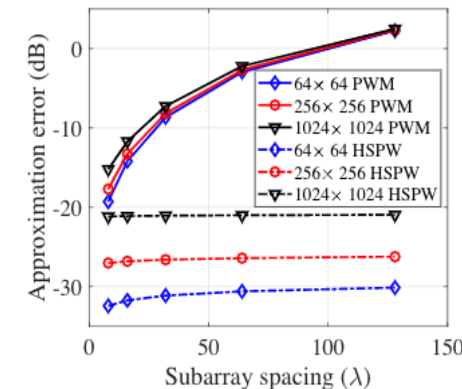
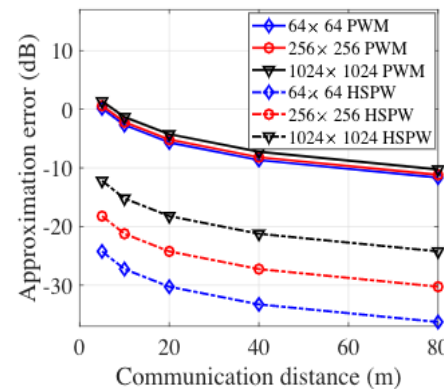


- Consider a generalized THz UM-MIMO system
 - Transmitter and receiver antennas are **divided into several subarrays**
- Employ **PWM within one subarray**
 - Remain precise due to the relatedly small array size
 - Achieve **reduced complexity**
- Employ **SWM among subarrays**
 - **Improved modeling accuracy**



$$\mathbf{H}_{\text{HSPM}} = \sum_{p=1}^{N_p} \begin{bmatrix} \alpha_p^{11} \mathbf{a}_{rp}^{11} (\mathbf{a}_{tp}^{11})^H & \dots & \alpha_p^{11} \mathbf{a}_{rp}^{1K_t} (\mathbf{a}_{tp}^{1K_t})^H \\ \vdots & \ddots & \vdots \\ \alpha_p^{11} \mathbf{a}_{rp}^{K_r 1} (\mathbf{a}_{tp}^{K_r 1})^H & \dots & \alpha_p^{11} \mathbf{a}_{rp}^{K_r K_t} (\mathbf{a}_{tp}^{K_r K_t})^H \end{bmatrix}$$

HSPM channel matrix

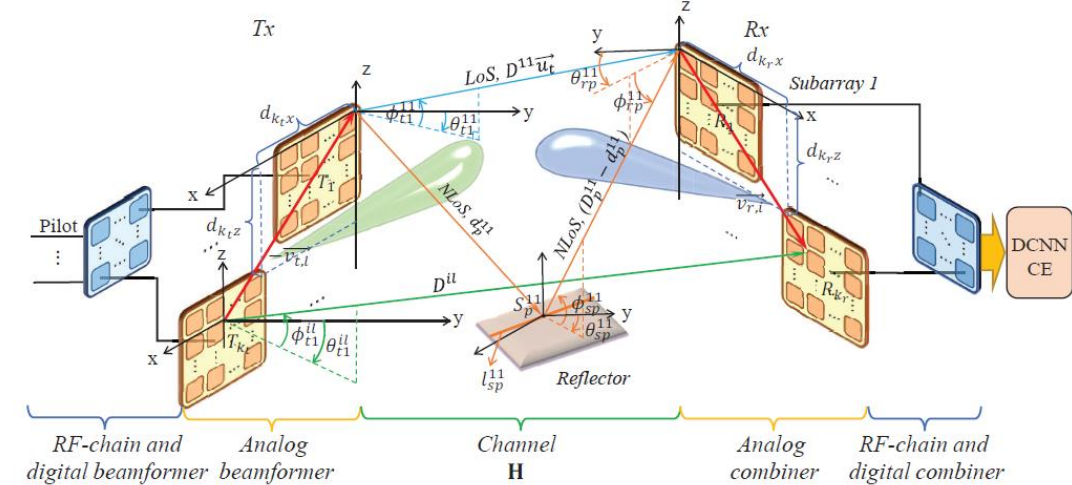


UM-MIMO Channel Estimation

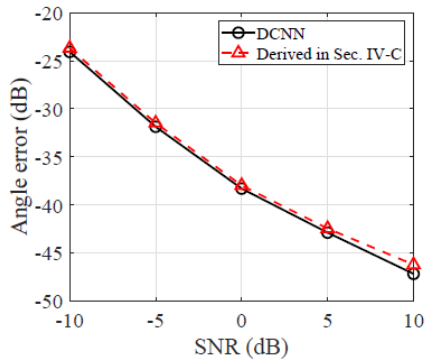


DCNN parameter estimation of reference subarray

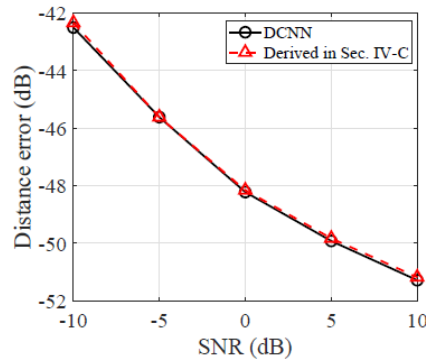
- Fifteen-layer DCNN structure
- Training labels:
 - Spherical-wave channel parameters: Angles, communication distance, amplitude of channel gain
- Loss function: $L_{loss} = \iota_1 L_{angle} + \iota_2 L_{dist} + \iota_3 L_{gain}$



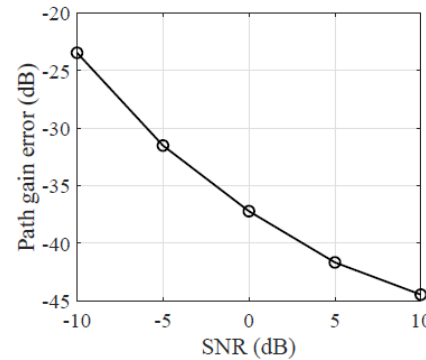
System model and channel estimation block diagram



(a) Estimation error of angle.

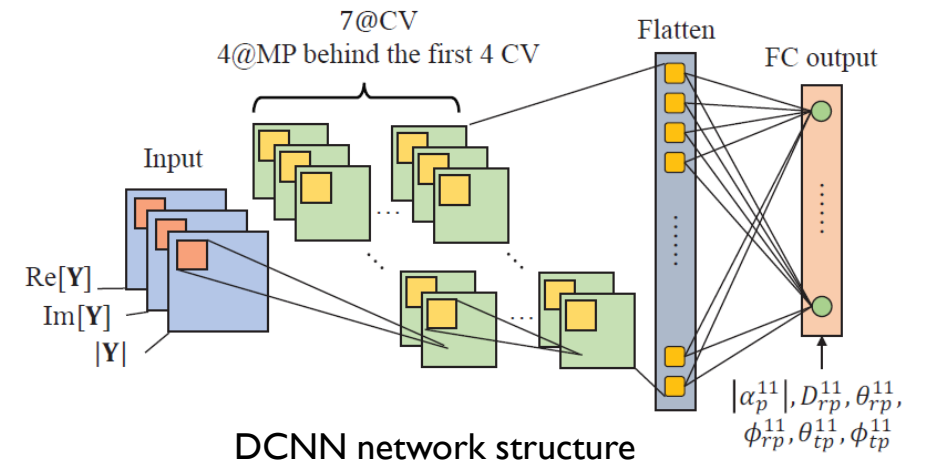


(b) Estimation error of distance.



(c) Estimation error of path gain.

Channel parameter estimation accuracy of DCNN method



DCNN network structure

Geometric-based Hierarchical Channel Recovery



- Instead of estimating for each antenna or each subarray, we propose **geometric-based hierarchical channel recovery**

➤ Employ the geometric relationships between channel parameters among subarrays

$$\theta_t^{k_t k_r} = \arccos\left(\frac{D_{xy}^{11} \cos \theta_t^{11}}{D_{xy}^{k_t k_r}}\right),$$

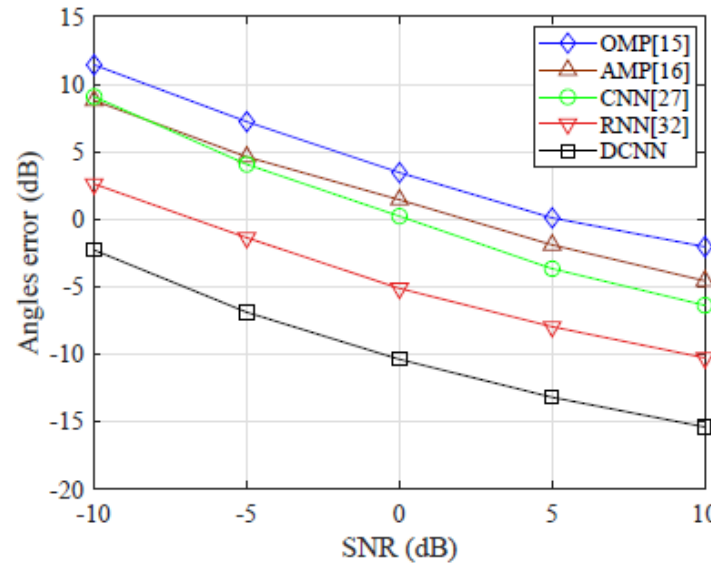
$$\theta_r^{k_t k_r} = \theta_r^{11} + \arcsin\left(\frac{\Delta d_x \cos \theta_t^{11}}{D_{xy}^{k_t k_r}}\right),$$

$$\phi_t^{k_t k_r} = \arccos\left(\frac{D_{yz}^{11} \cos \phi_{t1}^{11}}{D_{yz}^{k_t k_r}}\right),$$

$$\phi_r^{k_t k_r} = -\phi_r^{11} + \arcsin\left(\frac{\Delta d_z \cos \phi_{t1}^{11}}{D_{yz}^{k_t k_r}}\right),$$

$$D^{k_t k_r} = \frac{D_{yz}^{k_t k_r}}{\cos \theta_{t1}^{k_t k_r}} = \frac{D_{xy}^{k_t k_r}}{\cos \phi_{t1}^{k_t k_r}}.$$

Geometric relationship derivation



Estimation NMSE performance comparison

Algorithm 1: DCNN for Channel Estimation

Input: \mathbf{Y}

- Obtain $\{|\alpha_p^{11}|, D_p^{11}, \theta_{rp}^{11}, \phi_{tp}^{11}, \theta_{tp}^{11}, \phi_{tp}^{11}\}$ by DCNN.
- for $k_t = 1, \dots, K_t - 1$
- for $k_r = 1, \dots, K_r - 1$
- Calculate LoS channel parameters by (28).
- Calculate NLoS channel parameters by (31).
- end for
- end for
- Reconstruct \mathbf{H} in (10)

Output: \mathbf{H}

DCNN channel estimation algorithm

Outline

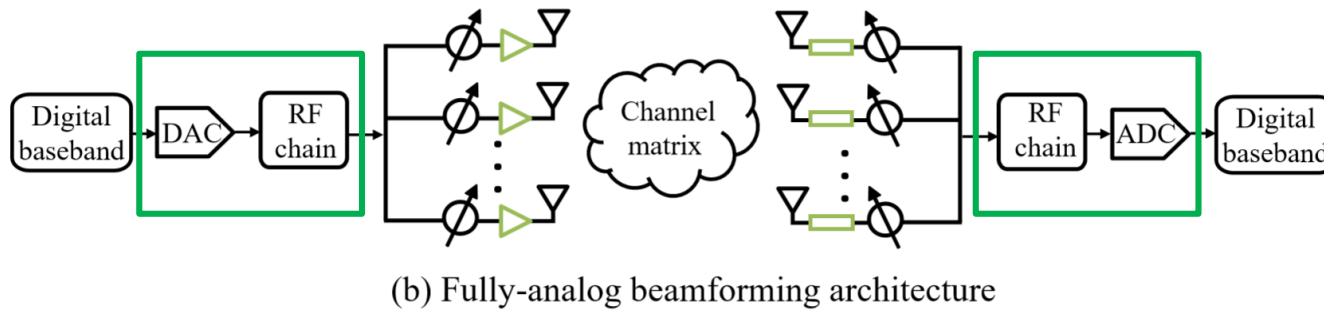


- **Chapter 1: Introduction**
 - i. Evolution to 6G
 - ii. Applications
 - iii. Motivations for THz UM-MIMO
- **Chapter 2: THz UM-MIMO Systems**
 - i. Electronic and photonic approaches
 - ii. New material approaches
 - iii. THz UM-MIMO channel
- **Chapter 3: THz Beamforming Technologies**
 - i. Fundamentals of beamforming
 - ii. State-of-the-art and challenges on beamforming
 - iii. Far-field beamforming
 - iv. Near-field beamforming/beamfocusing
- **Chapter 4: THz Beam Management**
 - i. Fundamentals of beam management
 - ii. State-of-the-art and challenges on beam management
 - iii. Beam estimation/alignment
 - iv. Beam tracking
 - v. Beam-guided medium access
- **Chapter 5: Future Directions**
 - i. Hybrid far- and near-field beamforming
 - ii. IRS-assisted hybrid beamforming
 - iii. Beam management in IRS assisted systems
- **Conclusion**

Beamforming Technologies by Architectures

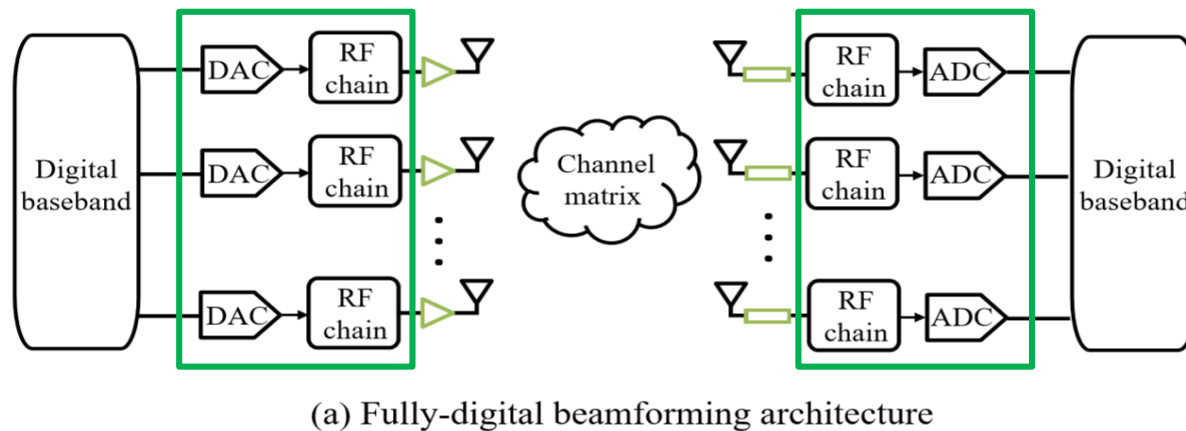


- **Fully-analog beamforming [1960s]:** One RF chain connects to all antennas



- **Pros:** Only one RF chain and DAC/ADC → Low complexity
- **Cons:** Can not support multiple data streams → Poor spectral efficiency

- **Fully-digital beamforming [1980s]:** Each RF chain connects to each antenna



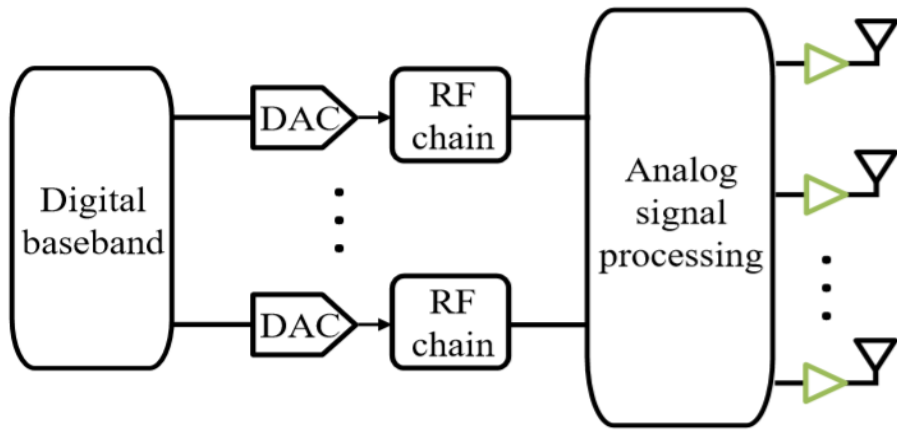
- **Pros:** Optimal spectral efficiency
- **Cons:** Too many RF chains and DAC/ADCs → High hardware complexity and power consumption

R.W. Bickmore, "Adaptive antenna arrays," IEEE Spectrum, vol. 1, no. 8, pp. 78-88, Aug. 1964.

Hybrid Beamforming



- **A more tractable solution: Hybrid beamforming**



- Number of RF chains is much less than the number of antennas
 - **Few high-cost devices**, e.g., RF chains and DAC/ADCs
 - **Large number of low-cost devices**, e.g., phase shifters
- Combine the advantages of both the fully-digital and fully-analog beamforming
 - **Near-optimal** spectral efficiency and **relatively low** hardware complexity and power consumption

Two connection relationships between RF chains and antennas

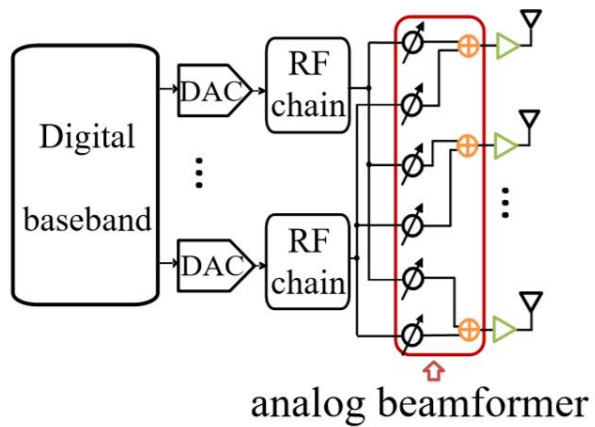
fixed connection

Fixed hybrid beamforming

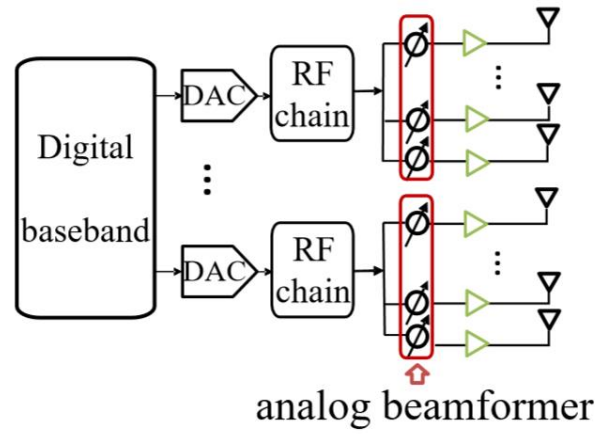
dynamic connection

Dynamic hybrid beamforming

Fixed Hybrid Beamforming



(a) Fully-connected (FC) [2014]



(b) Array-of-subarray (AoSA) [2015]

FC: Each RF chain connects to each antenna through a phase shifter

AoSA: Each RF chain only connects to a subset of antennas through phase shifters

	FC	AoSA
Connection between RF chains and antennas	Full	Partial
Spectral efficiency	High	Low
Power consumption	High	Low

Both the FC and AoSA hybrid beamforming can not balance the spectral efficiency and power consumption

Dynamic architectures are needed!

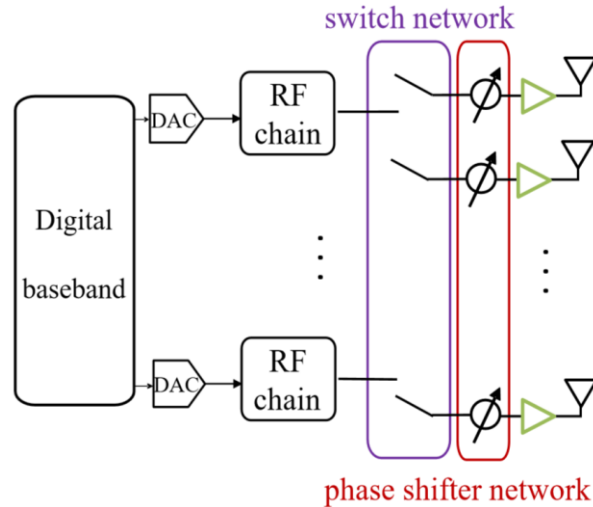
O. E. Ayach, S. Rajagopal, S. Abu-Surra, Z. Pi and R. W. Heath, **"Spatially Sparse Precoding in Millimeter Wave MIMO Systems,"** IEEE Transactions on Wireless Communications, vol. 13, no. 3, pp. 1499-1513, Mar. 2014.

S. Han, C. -I. I, Z. Xu and C. Rowell, **"Large-scale antenna systems with hybrid analog and digital beamforming for millimeter wave 5G,"** IEEE Communications Magazine, vol. 53, no. 1, pp. 186-194, Jan. 2015.

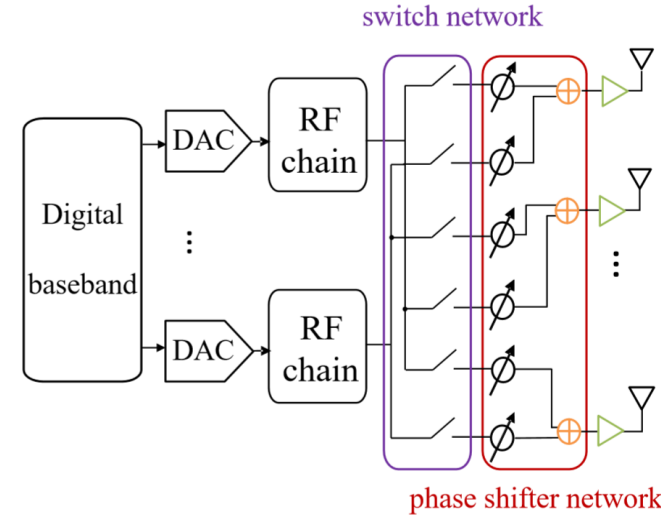
Dynamic Hybrid Beamforming



Key idea: Inserting switches between RF chains and phase shifters to control the connections



(a) Dynamic-subarray (DS) [2017]



(b) Fully-adaptive-connected (FAC) [2020]

- Switch is a **low-cost** device which only has 2 states, i.e., on and off
 - **Switch on** → Closed circuit → Phase shifter is **active** and **contributes to the spectral efficiency**
 - **Switch off** → Open circuit → Phase shifter is **inactive** and **does not consume power**
- **Control the state of switch** to adjust the spectral efficiency and power consumption

S. Park, A. Alkhateeb and R. W. Heath, “**Dynamic Subarrays for Hybrid Precoding in Wideband mmWave MIMO Systems,**” IEEE Transactions on Wireless Communications, vol. 16, no. 5, pp. 2907-2920, May 2017.

X. Xue, Y. Wang, L. Yang, J. Shi and Z. Li, “**Energy-Efficient Hybrid Precoding for Massive MIMO mmWave Systems With a Fully-Adaptive-Connected Structure,**” IEEE Transactions on Communications, vol. 68, no. 6, pp. 3521-3535, Jun. 2020.

Challenges of THz Beamforming



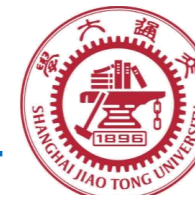
- **Very high path loss**
 - Distance limitation → **Beamforming is critical**
- **Very strong channel sparsity**
 - Limited number of multi-paths → **Limited spatial multiplexing gains**
- **Large multipath K factor**
 - Line-of-sight (LoS) dominance → **Inter-intra-spatial multiplexing and blockage**
- **Very large antenna array**
 - Many antennas, phase shifters, RF chains → **Hardware and energy efficiency**
 - Phase front fluctuation → **Spherical-wave or planar-wave propagation**
 - Wideband over large bandwidth → **Beam squint/split mitigation**

Outline

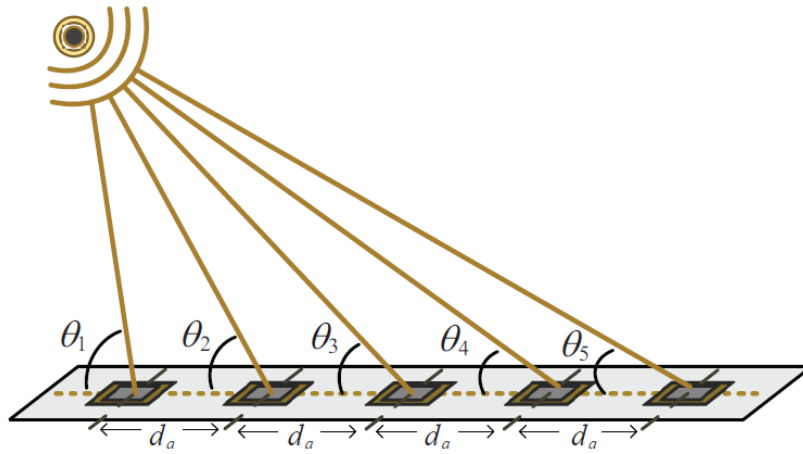


- Chapter 1: Introduction
 - i. Evolution to 6G
 - ii. Applications
 - iii. Motivations for THz UM-MIMO
- Chapter 2: THz UM-MIMO Systems
 - i. Electronic and photonic approaches
 - ii. New material approaches
 - iii. THz UM-MIMO channel
- **Chapter 3: THz Beamforming Technologies**
 - i. Fundamentals of beamforming
 - ii. State-of-the-art and challenges on beamforming
 - iii. Far-field beamforming
 - iv. Near-field beamforming/beamfocusing
- Chapter 4: THz Beam Management
 - i. Fundamentals of beam management
 - ii. State-of-the-art and challenges on beam management
 - iii. Beam estimation/alignment
 - iv. Beam tracking
 - v. Beam-guided medium access
- Chapter 5: Future Directions
 - i. Hybrid far- and near-field beamforming
 - ii. IRS-assisted hybrid beamforming
 - iii. Beam management in IRS assisted systems
- Conclusion

Near-field and Far-field

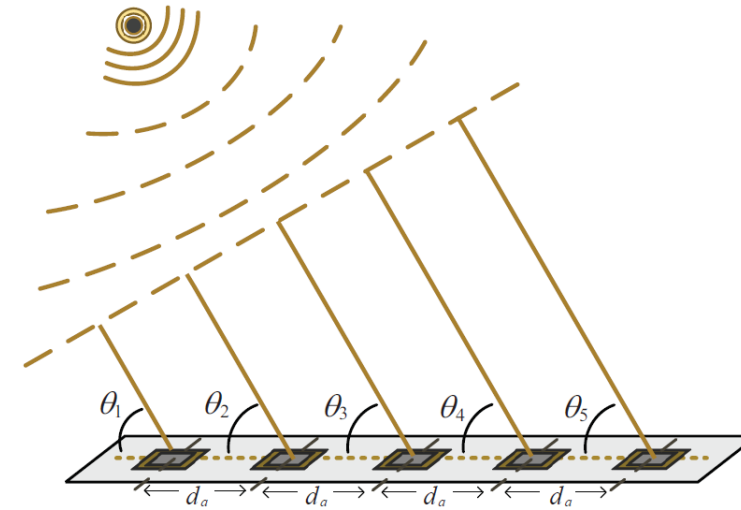


Near RF Source



$$\theta_1 \neq \theta_2 \neq \theta_3 \neq \theta_4 \neq \theta_5$$

Far RF Source



$$\theta_1 = \theta_2 = \theta_3 = \theta_4 = \theta_5 = \theta$$

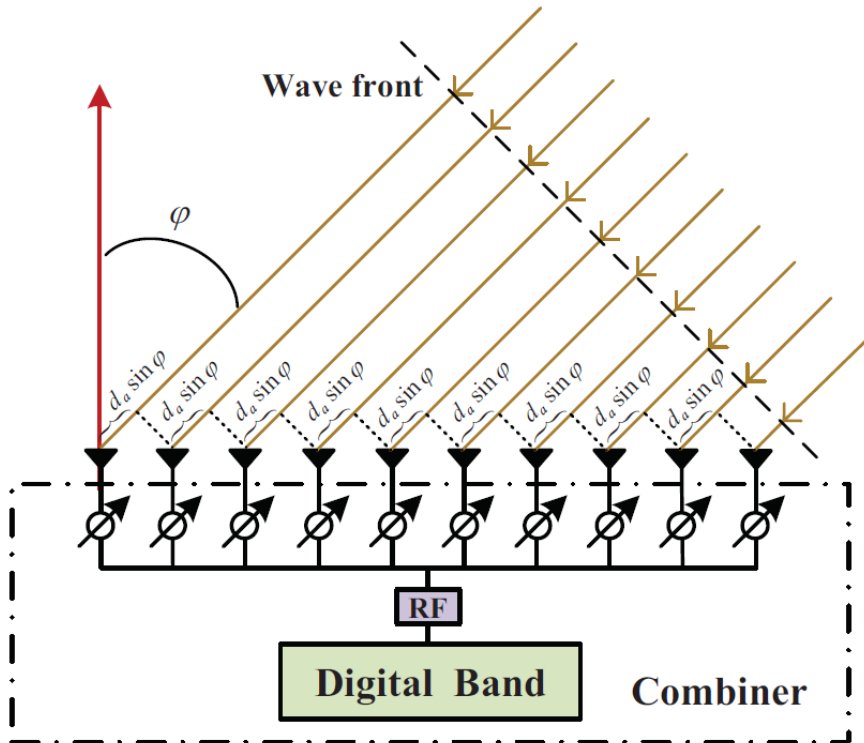
Array Response Vector:

$$\mathbf{a}(\theta_1, \theta_2, \theta_3, \theta_4, \theta_5) = \left[e^{j \frac{2\pi R}{\sin \theta_1 \lambda}}, e^{j \frac{2\pi R}{\sin \theta_2 \lambda}}, \dots, e^{j \frac{2\pi R}{\sin \theta_5 \lambda}} \right]^T$$

$$\mathbf{a}(\theta) = \left[1, e^{j\pi \cos \theta}, \dots, e^{j4\pi \cos \theta} \right]^T$$

The operation complexity of far-field beamforming is low

Far-field Array Response



For far-field beamforming, the phase difference between adjacent antennas is the same, and the array response vector can be written as

$$\mathbf{a}_r(\varphi) = \frac{1}{\sqrt{N_r}} \left[1, e^{-jkd_a \sin \varphi}, \dots, e^{-jkd_a(N_r-1) \sin \varphi} \right]^T$$

The combiner is optimized to maximize the resulting power, i.e.,

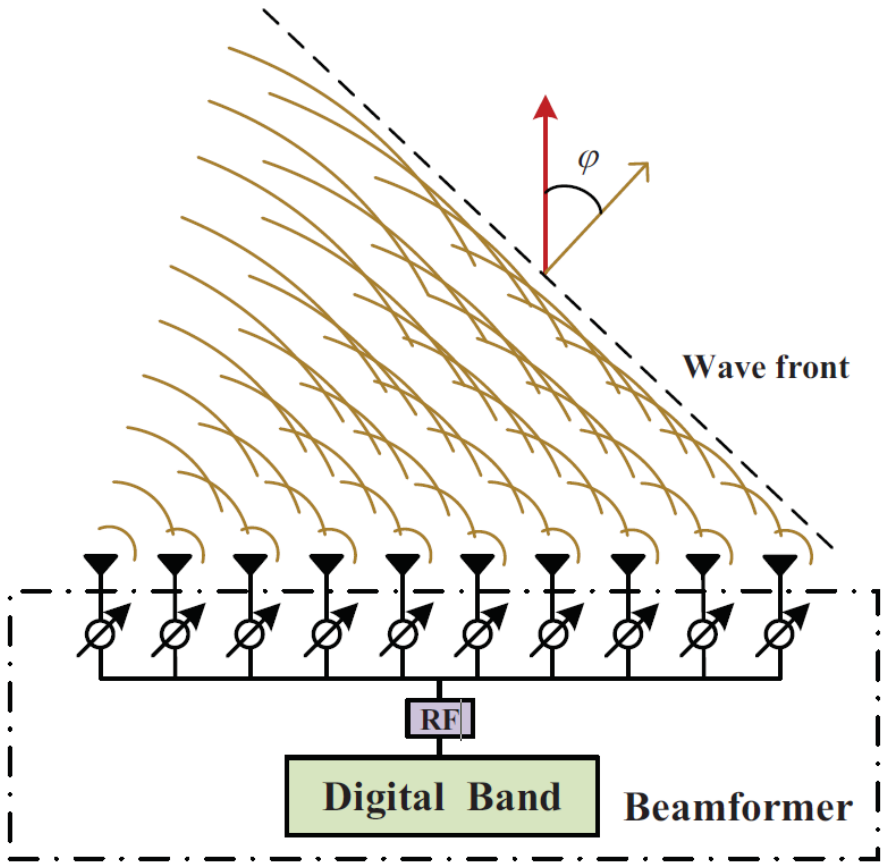
$$\begin{aligned} & \max_{\mathbf{w}} |\mathbf{w}^H \mathbf{a}_r(\varphi)|^2 \\ & \text{s.t. } |\mathbf{w}(i)| = \frac{1}{\sqrt{N_r}}, \quad i = 1, 2, \dots, N_r. \end{aligned}$$

It is easy to verify that an optimal solution is given by

$$\mathbf{w} = \mathbf{a}_r(\varphi),$$

Using array response vector to receive

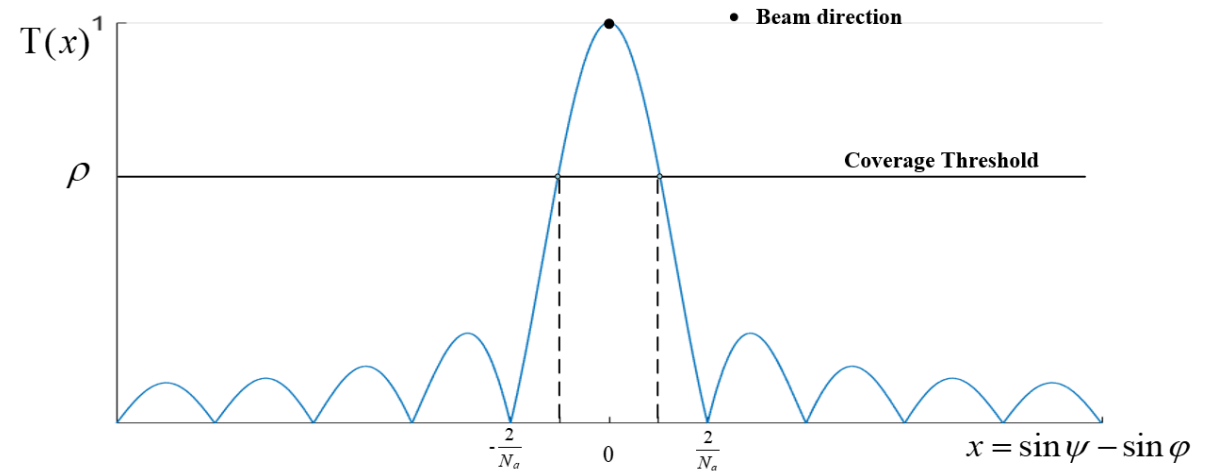
Far-field Beam Pattern



We have known that using **array response vector** as a combiner can maximize the received power with AoA φ .

On the contrary, if we use **array response vector** as a beamformer/precoder, the wavefront moves in the direction of AoD φ .

The radiation beam pattern of array response vector:



Thus, the array response vector can be regarded as **a narrow beam covering a certain zone.**

Using array response vector to transmit

Far-field Codebook



We can **predefine a codebook** that includes many antenna response vectors representing the narrow beams corresponding to different AoAs/AoDs.

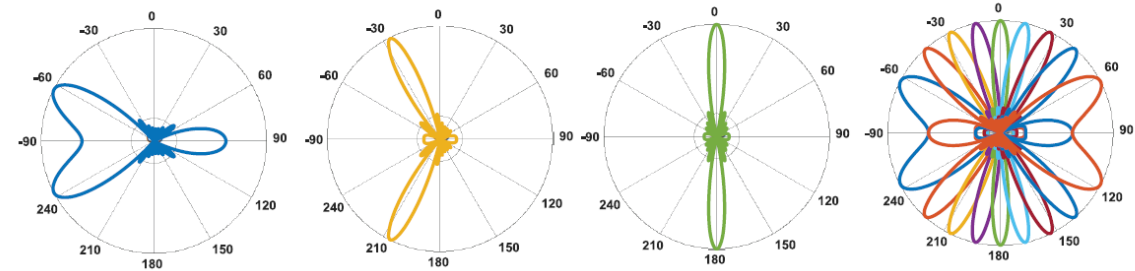
$$\mathcal{F} = \{\mathbf{a}(\varphi_1), \mathbf{a}(\varphi_2), \dots, \mathbf{a}(\varphi_N)\},$$

Some Properties of the narrow beams:

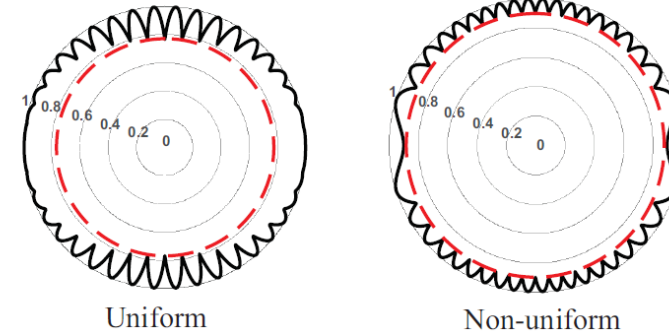
Lemma 1. Beams within $[-\frac{\pi}{2}, \frac{\pi}{2}]$ and beams within $[\frac{\pi}{2}, \frac{3\pi}{2}]$ are isomorphic for ULA. In particular, the narrow beam in direction of φ is equivalent to that in direction of $\pi - \varphi$, i.e.,

$$\mathbf{a}(\varphi) = \mathbf{a}(\pi - \varphi).$$

Moreover, the beam is **narrower** with the AoA/AoD around 0 and is **wider** with the AoA/AoD around $\pm\pi/2$.



(a)

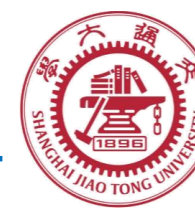


--- Normalized worst-case performance

(b)

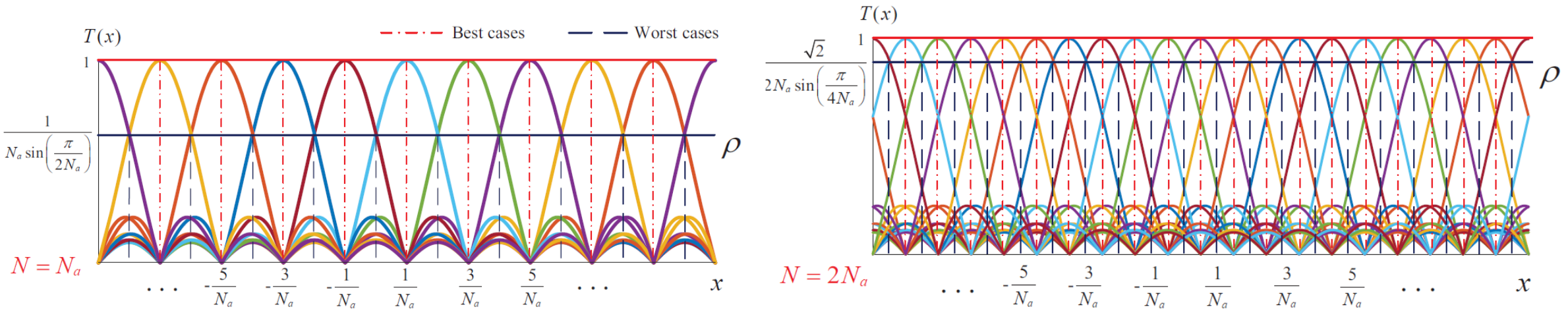
The codebook with **non-uniformly distributed beams** may achieve **a higher worst-case performance** than that with uniformly distributed beams

Far-field Codebook



How many narrow beams we need in a codebook?

Generally, the number of beams N required in the codebook is proportional to the number of array antennas N_a .



The normalized worst-case performance of the above two cases is given by

$$\frac{1}{N_a \sin\left(\frac{\pi}{2N_a}\right)}, \quad N = N_a$$

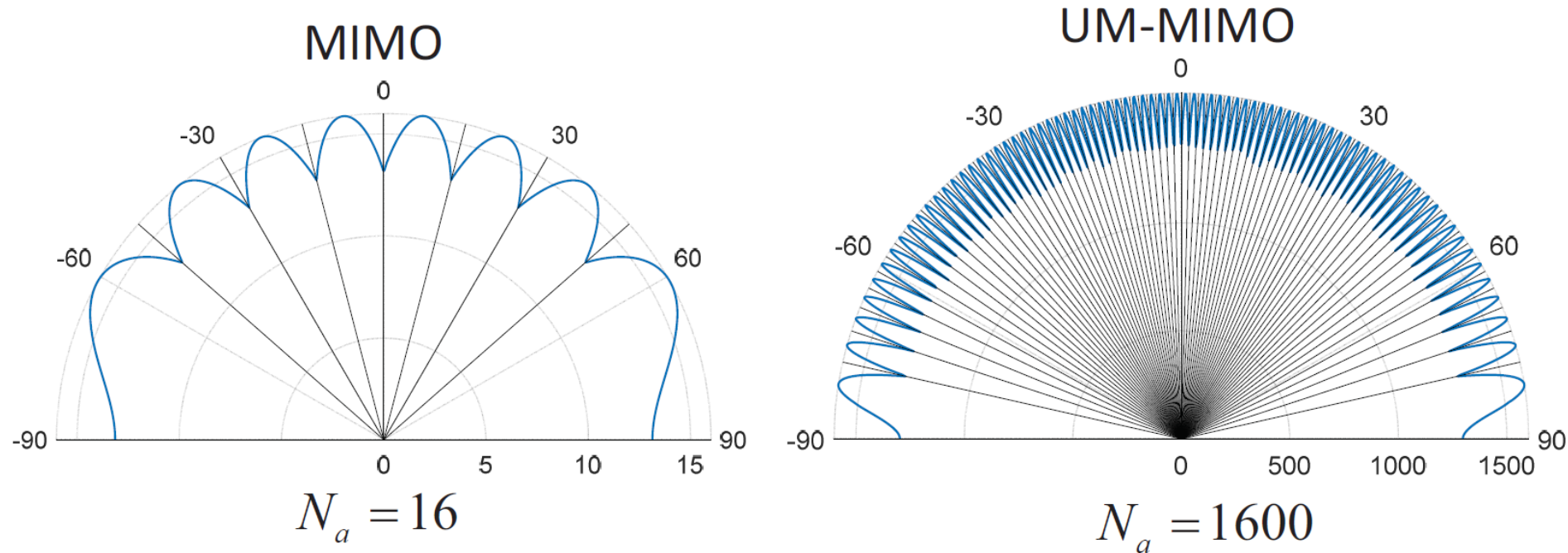
$$\frac{\sqrt{2}}{2N_a \sin\left(\frac{\pi}{4N_a}\right)}, \quad N = 2N_a$$

Far-field Codebook



How many narrow beams we need in a codebook?

Thus, the numbers of narrow beams in the UM-MIMO THz systems **is much larger** than that in conventional MIMO systems, which incurs difficulty in beam alignment and management.

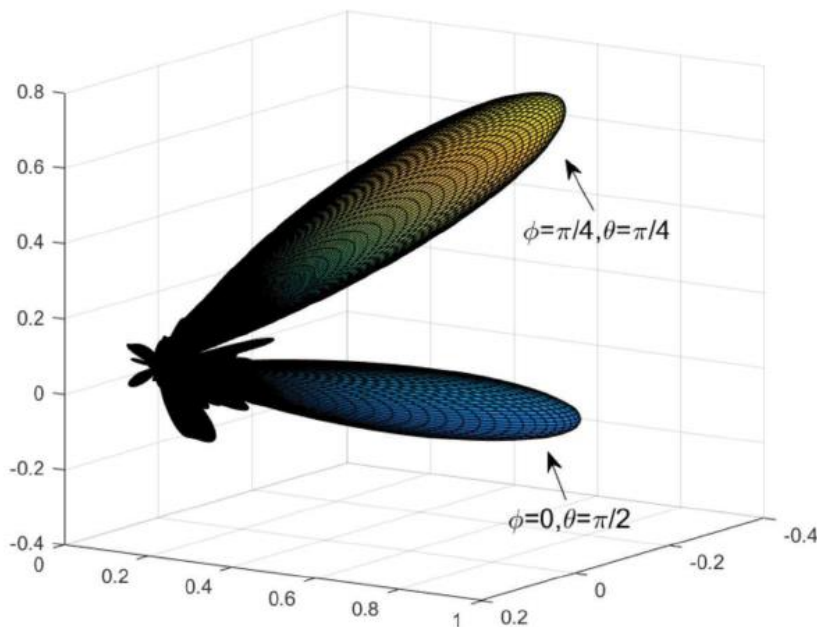


Far-field Beamforming



3D beamforming

3D beamforming allows **higher transmission gain** and **stronger directivity** for THz communication to provide large-capacity and less-interference multiple access.



This feature will help the **connection management** of a large number of air targets (e.g. cellular-connected drones) in the **future air-ground integrated wide-area coverage network**.

Far-field Beamforming

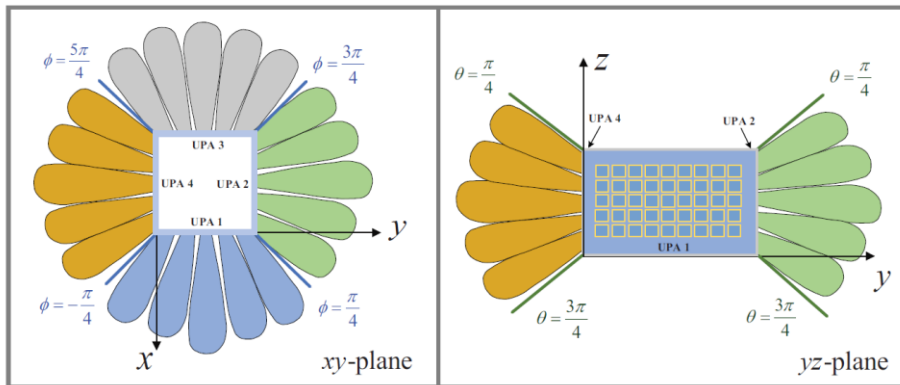
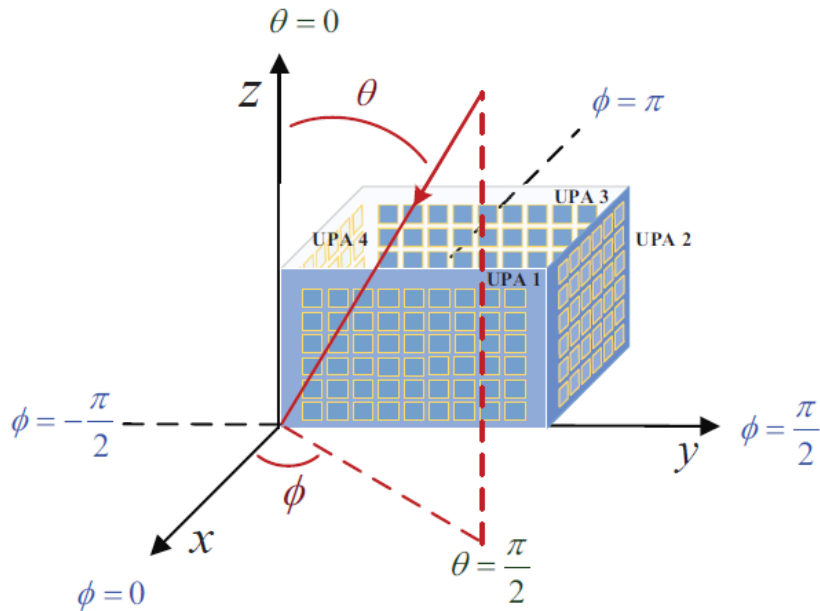


Quadruple-UPA (QUPA) architecture

As THz channel is LoS dominant, the signal coverage by one array is limited, which significantly reduces the flexibility of the beam control.

Merits:

- QUPA architecture can cover omni-direction in the azimuth, which has an **improved signal coverage range**.
- As each UPA only serves a confined range, **higher antenna gain** can be achieved by using the directional antenna element.
- As each UPA in the QUPA has substantially **less angular deflection** and the **beam squint loss can be reduced**.



Far-field Beamforming



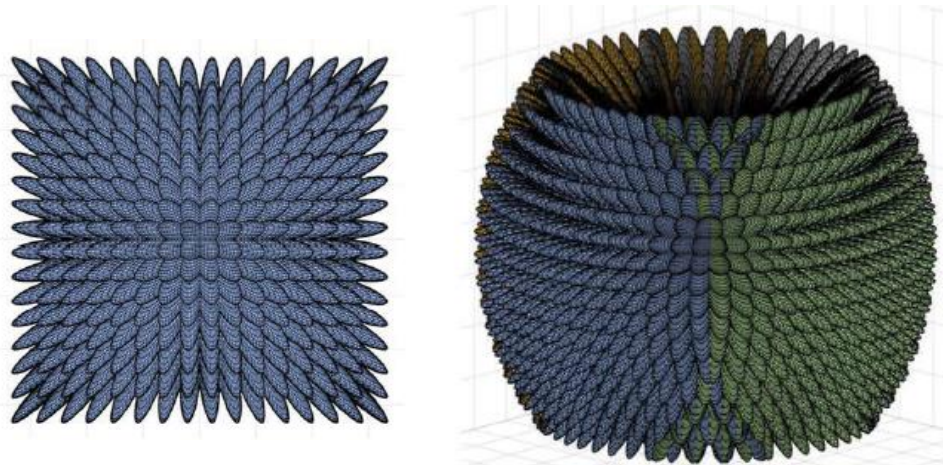
Quadruple-UPA (QUPA) architecture

The Codebook for QUPA should be customized.

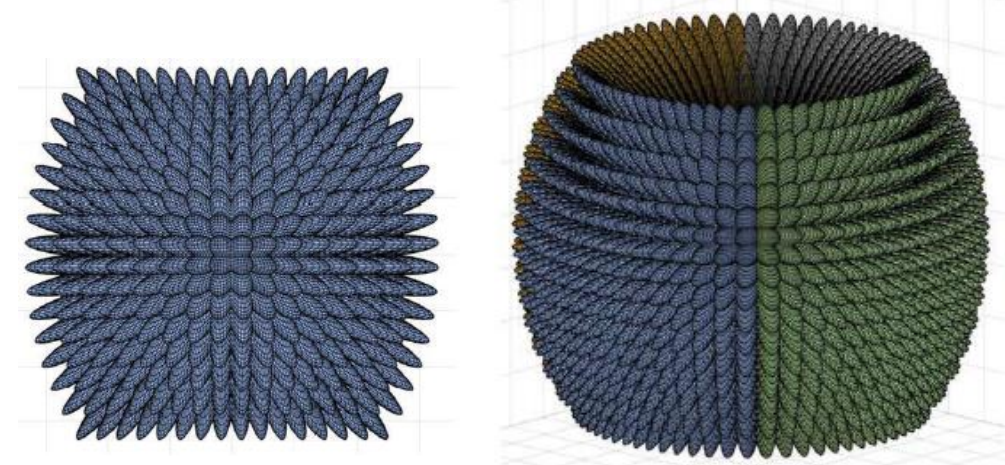
If straightforwardly using the Kronecker product of existing 2D codewords, the azimuth coverage expands when beams are above/below 90 degrees of elevation angle, which makes the total coverage of the QUPA cannot constitute an exact sphere.

The worst-case performance is maximized

$$\eta_{\text{worst}} = \frac{\sin [(\sqrt{2}N_z\pi)/4N] \sin [(\sqrt{2}\beta N_y\pi)/4N]}{N_y N_z \sin [(\sqrt{2}\pi)/4N] \sin [\sqrt{2}\beta\pi/4N]}$$



Kronecker product of 2D codebook



Customized 3D codebook

Hybrid Far-field Beamforming



Recall two typical hybrid beamforming architectures

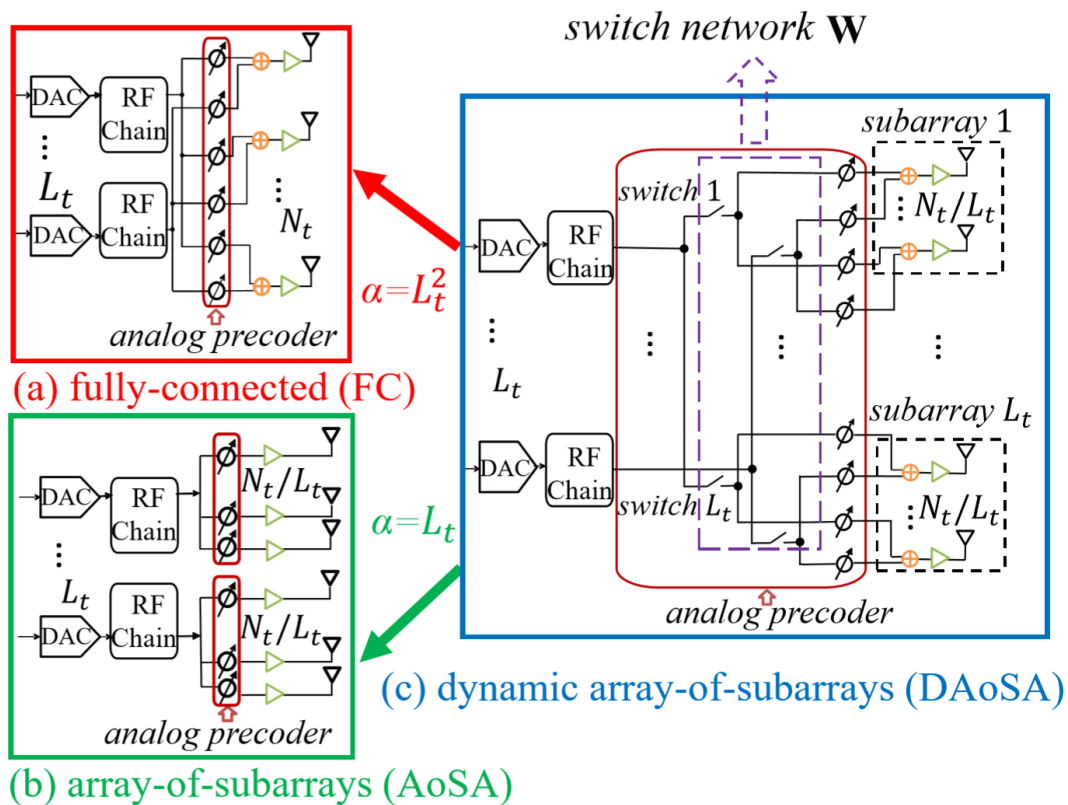
- Fully-connected (FC) and array-of-subarrays (AoSA) architectures:

	Hardware Complexity	Quantity of Devices	Spectral Efficiency
Fully-connected	Higher	Larger	Higher
Array-of-subarrays	Lower	Smaller	Poorer

- Total power = Quantity of devices \times Individual power
 - High operation frequency of THz \rightarrow Large individual device power \rightarrow Power consumption of FC architecture is too high
- Data rate = Spectral efficiency \times Bandwidth
 - Huge bandwidth of THz \rightarrow Large data rate loss of AoSA architecture
- Both FC and AoSA can not achieve low power consumption and high data rate concurrently

A balanced trade-off between FC and AoSA \rightarrow Dynamic array-of-subarrays (DAoSA)

Dynamic Array-of-Subarrays Hybrid Beamforming

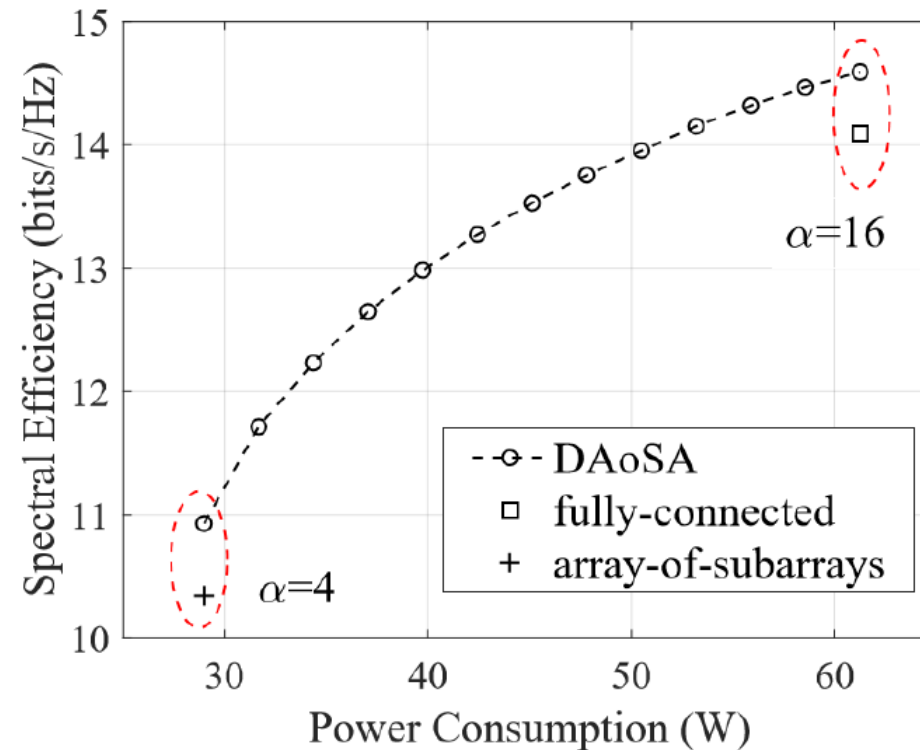


Hybrid beamforming architectures. (a) FC architecture; (b) AoSA architecture; (c) Proposed DAoSA architecture

DAoSA

- Antennas are divided into L_t subarrays
- Insert one switch between each RF chain and each subarray
 - **Switch on** → phase shifters in one subarray are **active** and **contribute to the spectral efficiency**
 - **Switch off** → phase shifters in one subarray are **inactive** and **do not consume power**
- Carefully disconnect some switches to **reduce the power consumption while still achieving high spectral efficiency**
- Denote α as the number of connected switches
 - The FC architecture is a special case with $\alpha = L_t^2$
 - The AoSA architecture is another special case with $\alpha = L_t$

Dynamic Array-of-Subarrays Hybrid Beamforming



Numerical results of 256 antennas at transmitter and receiver, transmitted power is 20 dBm, $L_t = 4$.

- Both the FC and AoSA architectures are special cases when $\alpha = 16$ and 4
- Through intelligently controlling switches, the DAAoSA architecture achieves different levels of spectral efficiency and power consumption

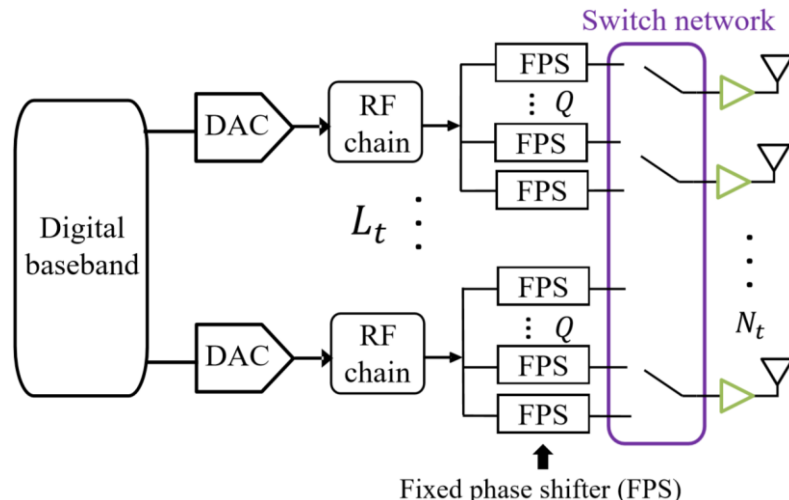
L. Yan, C. Han and J. Yuan, "A dynamic array-of-subarrays architecture and hybrid precoding algorithms for terahertz wireless communications," IEEE JSAC, 2020.

Hybrid Beamforming with Practical Phase Shifters



- With **growing frequency** and **higher resolution**, both the **power consumption** and **hardware complexity** of phase shifters increase
- At the THz band, it is critical to **reduce the resolution** of the phase shifters
- Most architectures use **infinite-resolution-adjustable phase shifter** → ultra-high hardware complexity
- **low-resolution-adjustable phase shifter** → high hardware complexity
- Use **fixed phase shifter** → low hardware complexity

Dynamic-subarray with fixed phase shifter (DS-FPS) hybrid beamforming design



- **Fixed phase shifter (FPS)** only needs to provide a **non-adjustable and fixed phase**, which is **low-cost**
- To compensate the performance loss caused by the non-adjustable phase of FPSs, we insert a **switch network** to make each antenna select one proper FPS to connect with
- Both FPS and switch are low-cost devices → DS-FPS is an **energy- and hardware-efficient solution**

Hybrid Beamforming Under Partial CSI



- **Typical representation** of channel state information (CSI) for MIMO system at k-th subcarrier

$$\mathbf{H}[k] = \begin{bmatrix} H[k]_{11} & \cdots & H[k]_{1N_t} \\ \vdots & \ddots & \vdots \\ H[k]_{N_r1} & \cdots & H[k]_{N_rN_t} \end{bmatrix}$$

The MIMO channel matrix is composed by $N_r N_t$ channel responses

- The CSI is proportional to the **square of number of antennas**
- Full CSI is hard to acquire for **THz UM-MIMO system**

- **Angular representation** of CSI for MIMO system

$$\mathbf{H}[k] = \sum_{i=1}^{N_p} \alpha_i[k] \mathbf{a}_{r_i}[k] \mathbf{a}_{t_i}[k]^H$$
$$\mathbf{a}_{r_i}[k] = [1, \dots, e^{j \frac{2\pi}{\lambda_k} d(L-1) \sin(\phi_{r_i}) \sin(\theta_{r_i})}]^T \otimes [1, \dots, e^{j \frac{2\pi}{\lambda_k} d(W-1) \cos(\theta_{r_i})}]^T$$

The MIMO channel matrix is composed by N_p multipath components

- The CSI is linearly related to the **number of multipath**, which is small in **sparse** THz channel
- **Much fewer information** than the typical representation

Can we further simplify the CSI we needed? Of course yes!

Hybrid Beamforming Under Partial CSI



Simplified partial CSI:

- **Tx** knows the **DoD** and **amplitude of path gain** of each multipath
- **Rx** knows the **DoA** and **amplitude of path gain** of each multipath

$$\begin{aligned}\mathbf{H}[k] &= \sum_{i=1}^{N_p} \alpha_i[k] \mathbf{a}_{ri}[k] \mathbf{a}_{ti}[k]^H \\ &= \mathbf{A}_r[k] \mathbf{\Lambda}[k] \mathbf{A}_t[k]^H \\ &= \mathbf{A}_r[k] \left(\bar{\mathbf{\Lambda}}[k] \odot e^{j * \mathbf{\Lambda}[k]} \right) \mathbf{A}_t[k]^H\end{aligned}$$

DoA Amplitude of path gain DoD

Reduce the CSI feedback overhead by 50%

Partial CSI at Rx

Partial CSI at Tx

How to utilize this partial CSI to design the THz hybrid beamforming?

Hybrid Beamforming Under Partial CSI



In THz UM-MIMO systems with **ultra-massive antennas** & **sparse multipath components**, the assumption holds that the **array response vectors of different multipath are orthogonal**

$$\mathbf{A}_r[k]^H \mathbf{A}_r[k] \approx N_r \mathbf{I}_{N_p}$$

$$\frac{1}{N_r} \mathbf{a}_{ri}[k]^H \mathbf{a}_{rl}[k] \approx \mathbb{1}(i=l)$$

Spectral efficiency:

$$\frac{1}{K} \sum_{k=1}^K \log_2 \left(\left| \mathbf{I}_{N_r} + (1/\sigma_k^2) \mathbf{H}[k] \mathbf{P}[k] \mathbf{P}[k]^H \mathbf{H}[k]^H \right| \right)$$

$$\approx \frac{1}{K} \sum_{k=1}^K \log_2 \left(\left| \mathbf{I}_{N_p} + (N_r/\sigma_k^2) \underline{\Lambda}[k]^2 \mathbf{A}_t[k]^H \mathbf{P}[k] \mathbf{P}[k]^H \mathbf{A}_t[k] \right| \right)$$

Amplitude of path gain

DoD

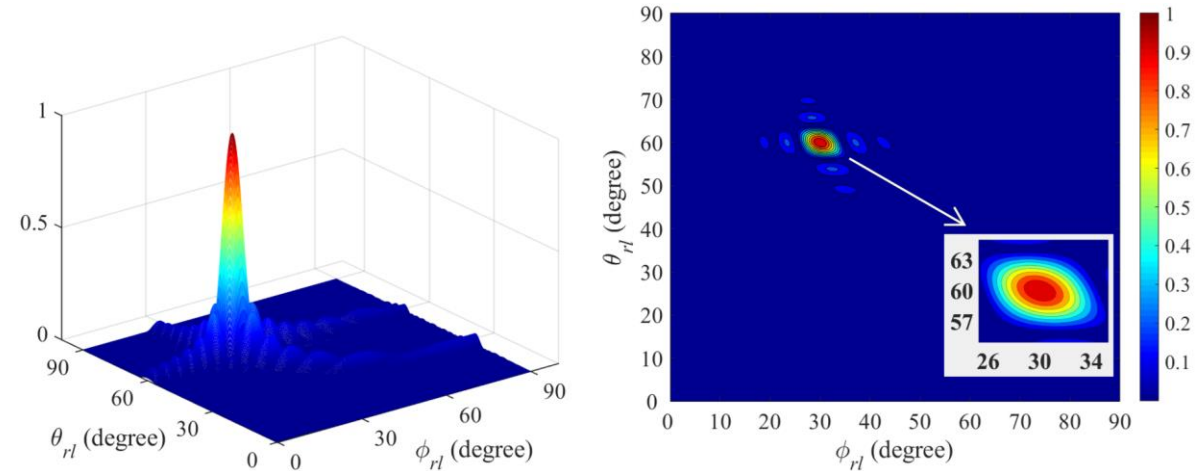


Illustration of the orthogonality of array response vectors

- For most angles of ϕ_{rl} and θ_{rl} , which locate in the blue region, $\frac{1}{N_r} |\mathbf{a}_{ri}[k]^H \mathbf{a}_{rl}[k]| \approx 0$

Only DoD information and amplitude of path gain is needed to design hybrid beamformer.

Error of Partial CSI



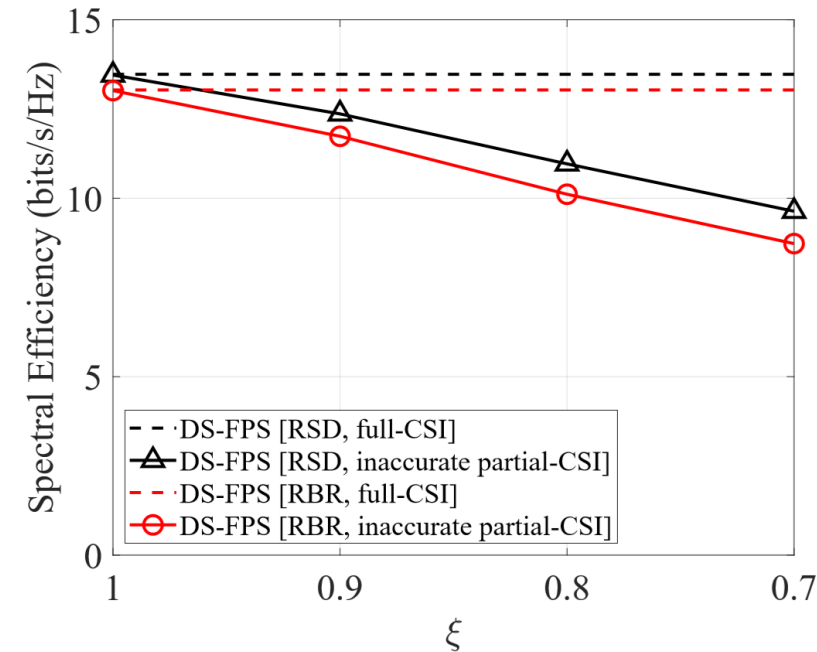
Row-successive-decomposition (RSD) algorithm

- Design the digital beamforming matrix via **SVD method** to maximize SE
- Design **each row** of the analog matrix **successively**

Row-by-row (RBR) algorithm

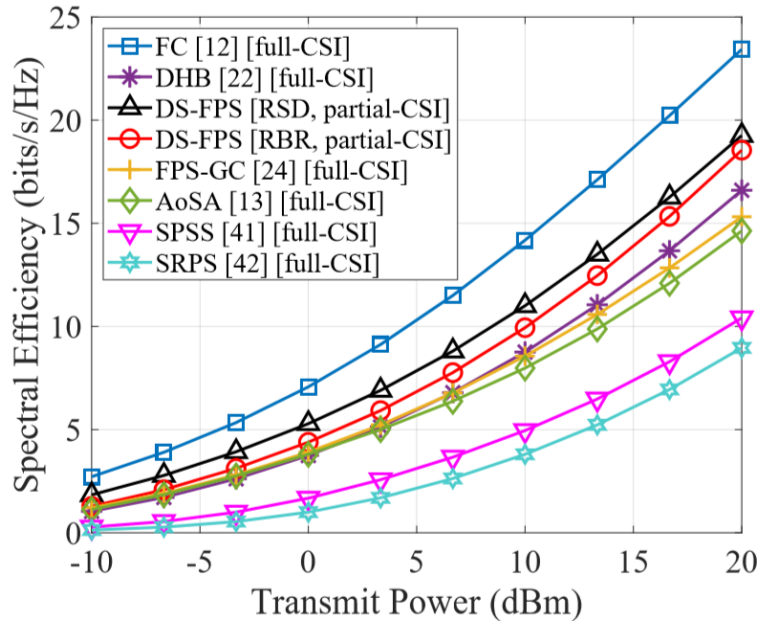
- Transform the SE maximization into Euclidean distance minimization
- Alternatively solve digital and analog beamforming matrices.
- Design **each row** of the analog matrix **in parallel**

- With accurate partial-CSI, both **the two algorithms achieve similar spectral efficiency** with the case of accurate full-CSI
- As the error of partial CSI increases, both the two algorithms achieves decreasing spectral efficiency



- ξ represents the error of partial CSI
- The case $\xi = 1$ denotes that the partial CSI is accurate
- Full-CSI is considered as accurate and unrelated with ξ

Spectral Efficiency



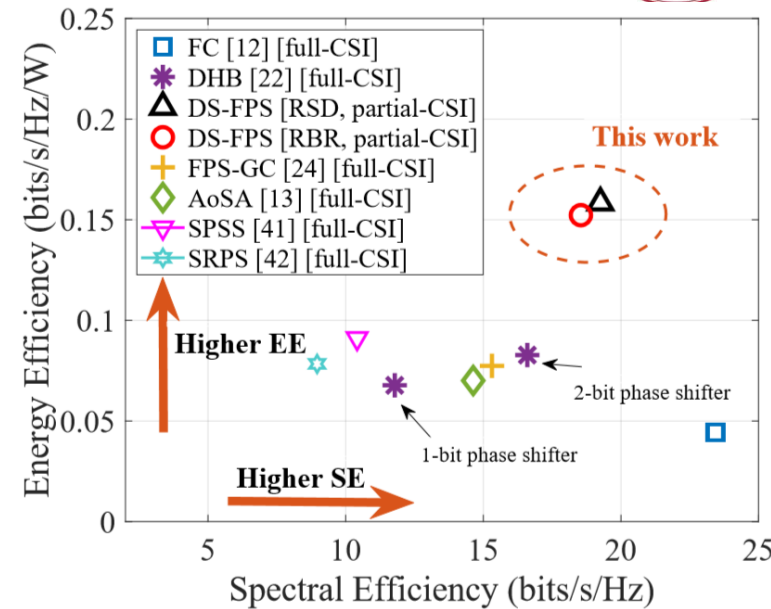
Spectral efficiency versus the transmit power ρ of DS-FPS architecture. $N_t = N_r = 1024$, $D = 40\text{m}$. Number of FPSs is 32.

Left figure:

- The **spectral efficiency** of DS-FPS is lower than FC and **higher** than the other architectures
- The RSD algorithm achieves higher spectral efficiency than the RBR, with higher computational complexity

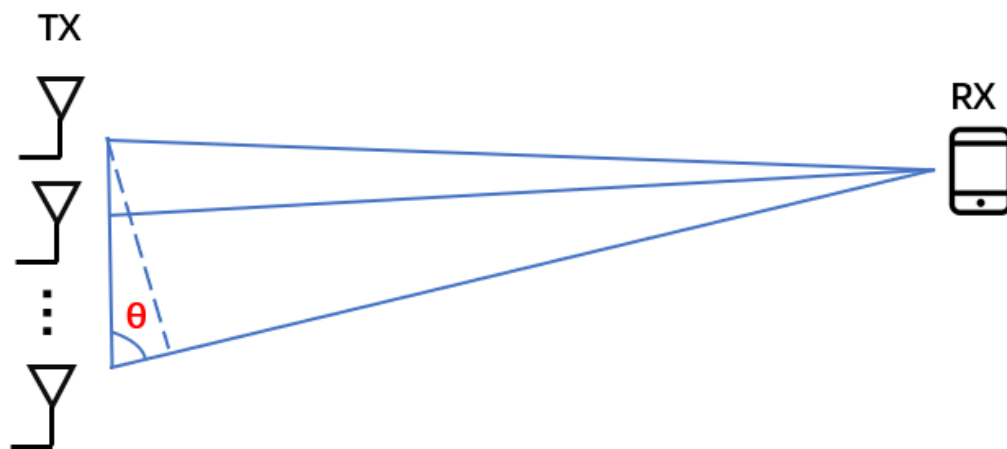
Right figure:

- The **energy efficiency** of the DS-FPS architecture is **substantially higher** than the other existing schemes



Energy efficiency versus spectral efficiency of the DS-FPS architecture. $N_t = N_r = 1024$, $D = 40\text{m}$, $\rho = 20\text{ dBm}$. Number of FPSs is 32.

Beam Squint Problem with Phase Shifters

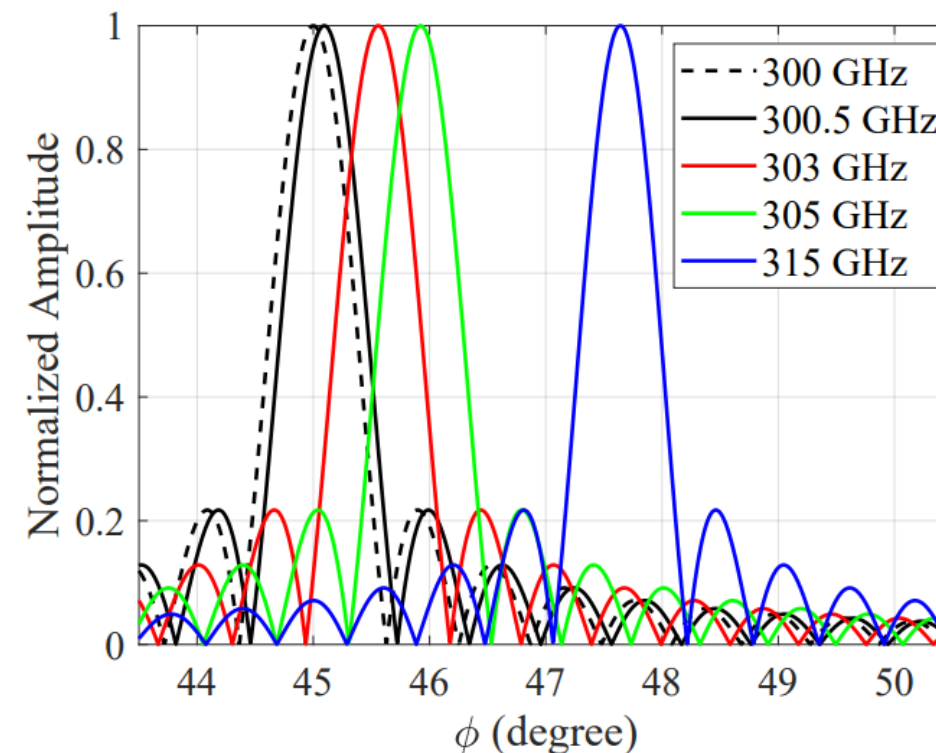


For wideband multi-carrier systems, the beamforming weight of the n^{th} antenna at the m^{th} carrier should be

$$\frac{2\pi f_m}{c} (n - 1)d \cos(\theta)$$

However, due to the **frequency-flat** property of phase shifter, the beamforming weight is usually designed for **central frequency** f_c and is the same for all carriers.

$$\frac{2\pi f_c}{c} (n - 1)d \cos(\theta)$$



0.3 THz central frequency, 256 antennas.

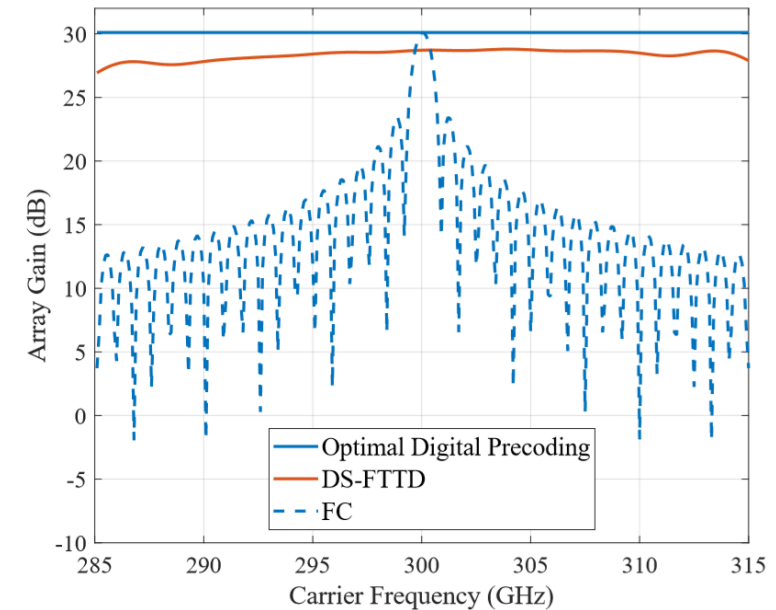
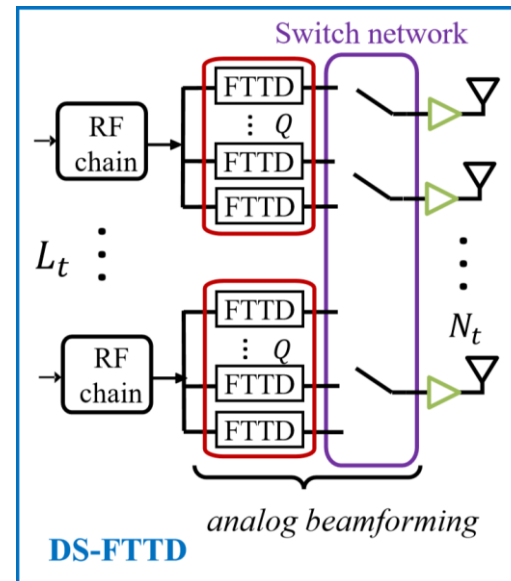
With the frequency deviating from f_c , the **beam direction is misaligned and the array gain is reduced.**

Dynamic Subarray with Fixed True Time Delay



- Ultra-wideband require beamforming weights are proportional to carrier frequency
 - Existing architectures use phase shifter → generate same weight for all carrier frequencies
 - Beam squint problem: error beamforming weights → reduce array gain substantially

- True-time-delay (TTD) can generate frequency-proportional beamforming weights
- However, adjustable TTD is hard to produce in THz band

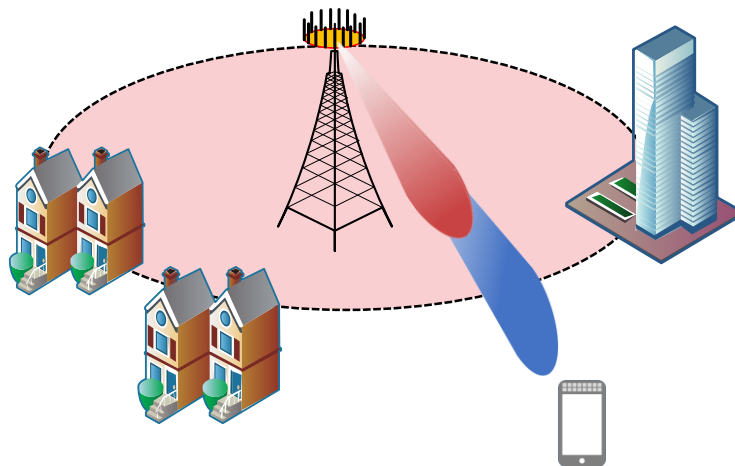


- We propose fixed TTD, with dynamic subarray architecture
 - Array gain outperforms FC substantially and approaches to optimal digital precoding
 - Substantially low hardware complexity

Far-Field Beam Split Effect



- Beam split effect in wideband UM-MIMO systems
 - Beamforming is usually **frequency-independent**, which is accomplished by phased array
 - In wideband systems, the beams at different frequencies will split towards different **angles**



Far-field beam split

System parameters	Beam width	Beam split	Relative split
Carrier 30 GHz, bandwidth 2 GHz, Antenna array 16×16	11.25°	3°	26%
Carrier 30 GHz, bandwidth 2 GHz, Antenna array 60×60	3°	3°	100%
Carrier 100 GHz, bandwidth 20 GHz, antenna array 16×16	11.25°	9°	80%
Carrier 100 GHz, bandwidth 20 GHz, antenna array 60×60	3°	9°	300%

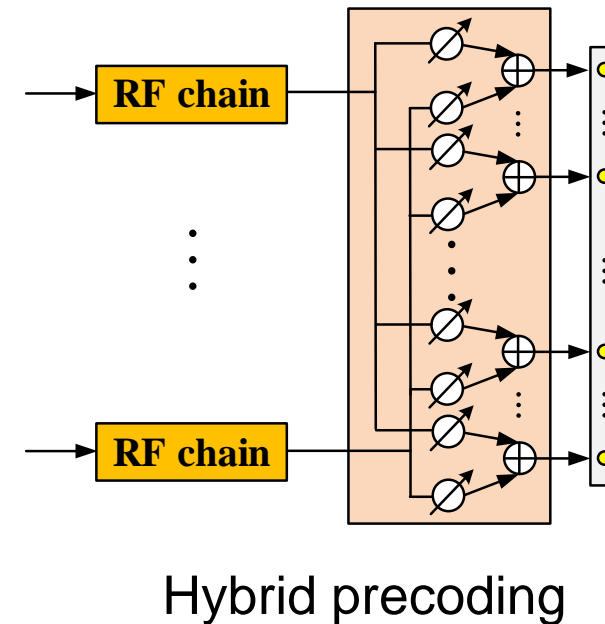
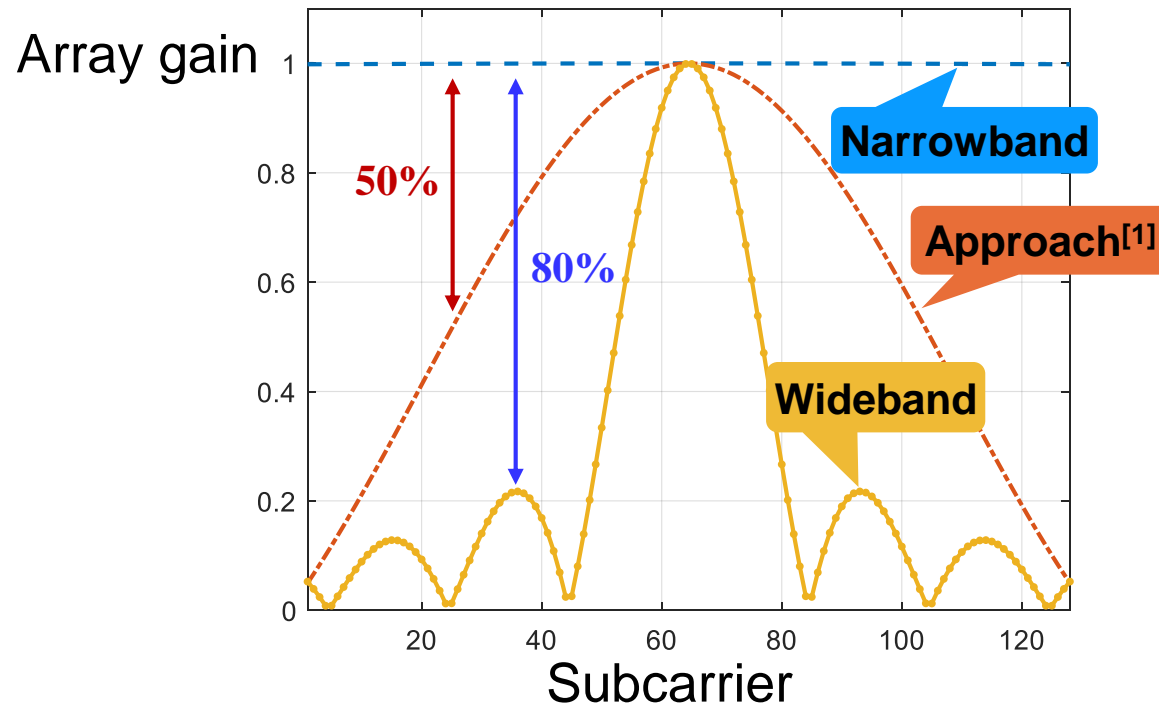
J. Tan and L. Dai, “**Delay-phase precoding for THz massive MIMO with beam split,**” in Proc. IEEE GLOBECOM’19, Hawaii, USA, Dec. 2019.

L. Dai, J. Tan, Z. Chen, and H. Vincent Poor, “**Delay-phase precoding for wideband THz massive MIMO,**” IEEE Trans. Wireless Commun., vol. 21, no. 9, pp. 7271-7286, Sep. 2022.

Negative Influence of Beam Split



- Unacceptable array gain loss
 - Narrowband scheme: more than 80% array gain loss
 - Sum-rate maximization scheme: more than 50% array gain loss



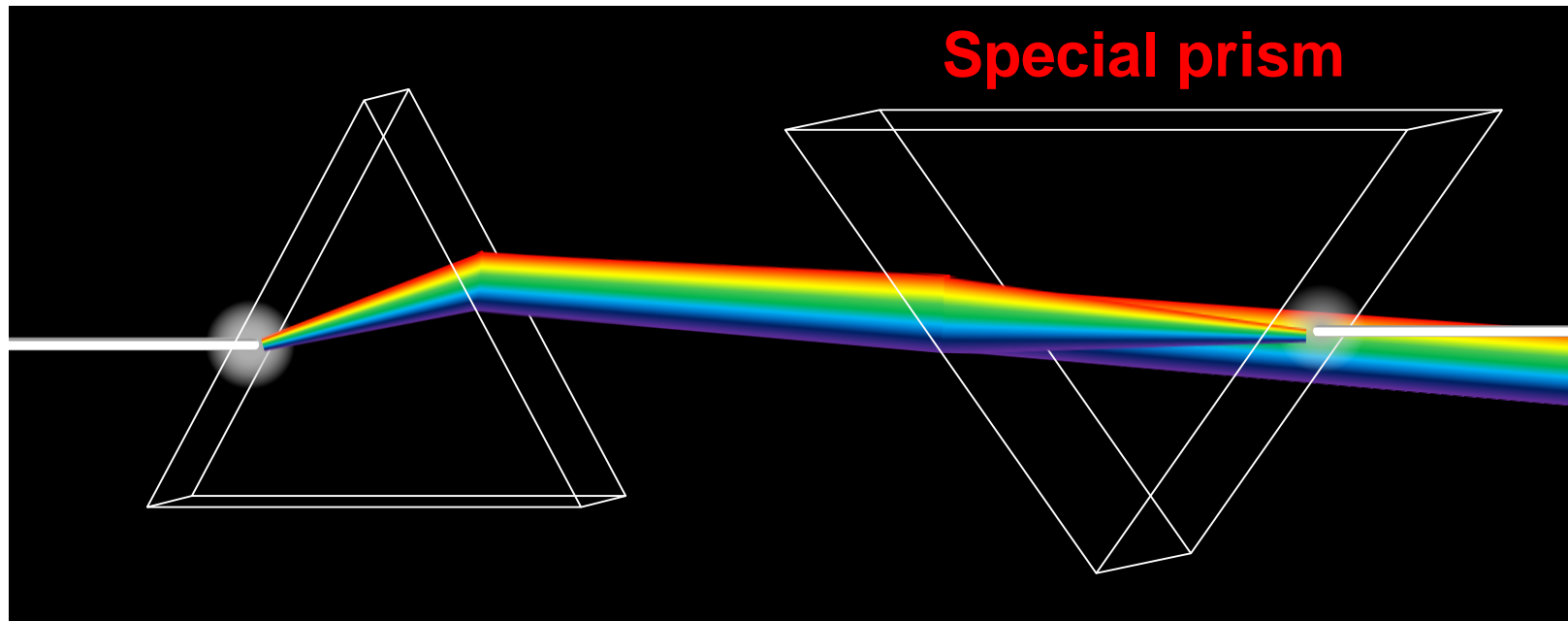
Classical hybrid precoding cannot mitigate the array gain loss caused by beam split

Idea Inspiration



- Technical problem

- THz beam split severely aggravate the communication performance
- Problem analogy: How to eliminate the dispersion of light?

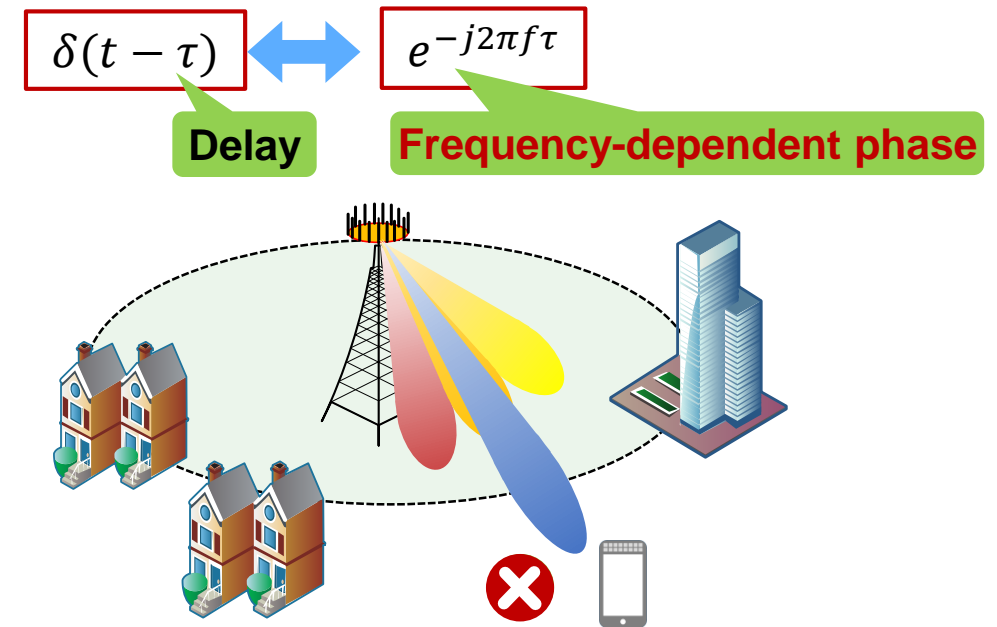
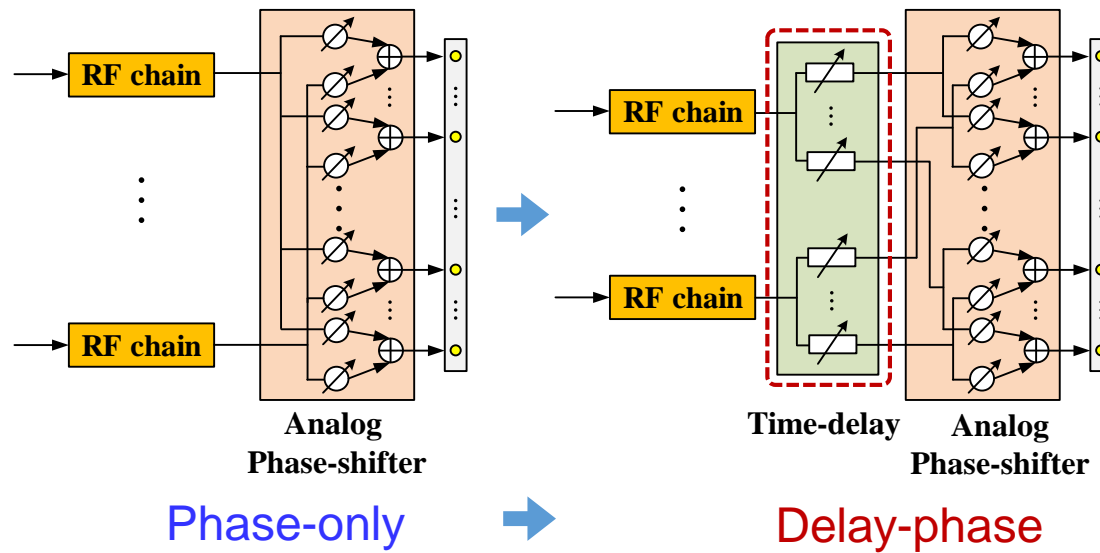


The dispersion of light can be eliminated via a special prism

Delay-Phase Precoding



- Propose the **delay phase precoding (DPP)** architecture
- Introduce the time-delay module to realize **frequency-dependent** phase shift

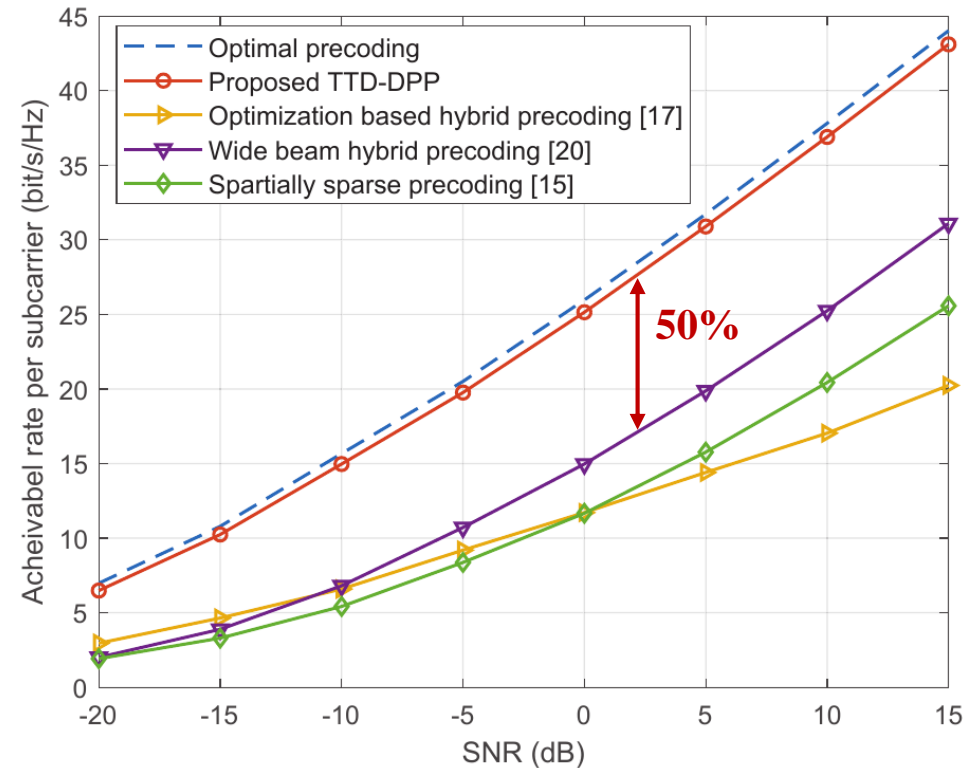
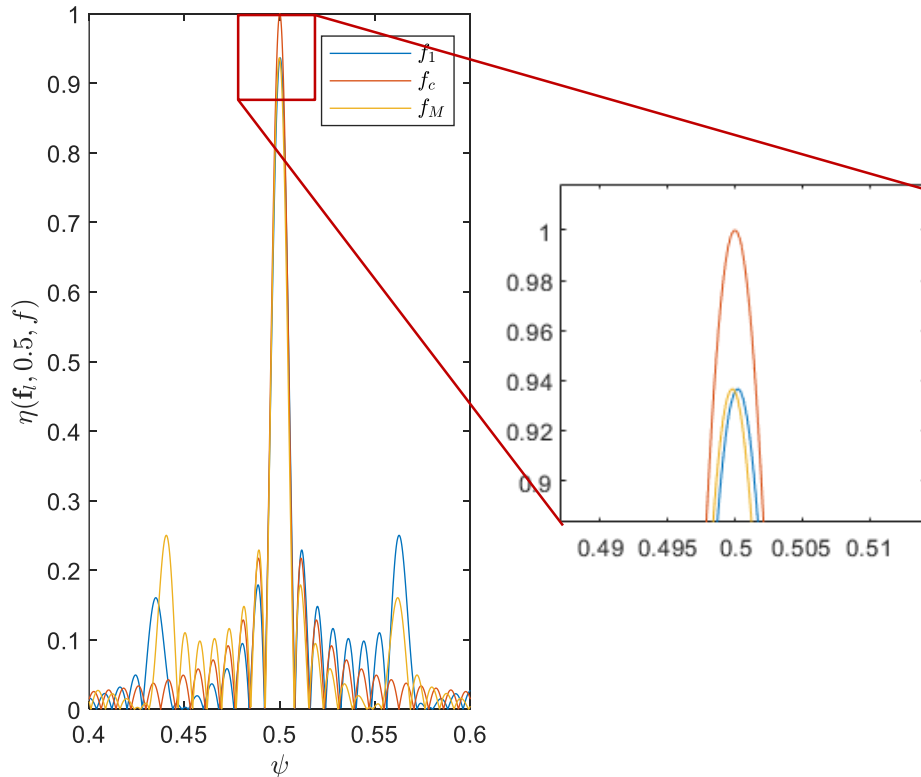


Simulation Result



- Precoding performance

- Parameters: 256 antennas, 0.1 THz carrier frequency, 5 GHz bandwidth



DPP could achieve **near-optimal transmission rate** on all considered subcarriers

Outline

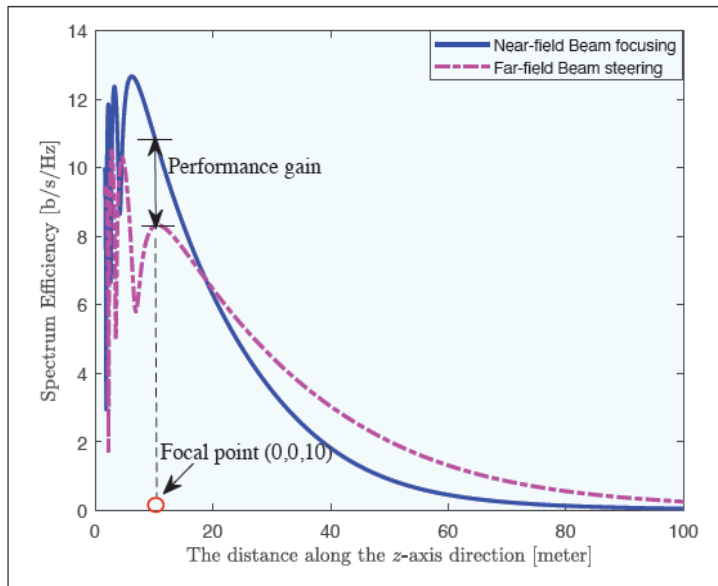


- **Chapter 1: Introduction**
 - i. Evolution to 6G
 - ii. Applications
 - iii. Motivations for THz UM-MIMO
- **Chapter 2: THz UM-MIMO Systems**
 - i. Electronic and photonic approaches
 - ii. New material approaches
 - iii. THz UM-MIMO channel
- **Chapter 3: THz Beamforming Technologies**
 - i. Fundamentals of beamforming
 - ii. State-of-the-art and challenges on beamforming
 - iii. Far-field beamforming
 - iv. Near-field beamforming/beamfocusing
- **Chapter 4: THz Beam Management**
 - i. Fundamentals of beam management
 - ii. State-of-the-art and challenges on beam management
 - iii. Beam estimation/alignment
 - iv. Beam tracking
 - v. Beam-guided medium access
- **Chapter 5: Future Directions**
 - i. Cross far- and near-field beamforming
 - ii. IRS-assisted hybrid beamforming
 - iii. Beam management in IRS assisted systems
- **Conclusion**

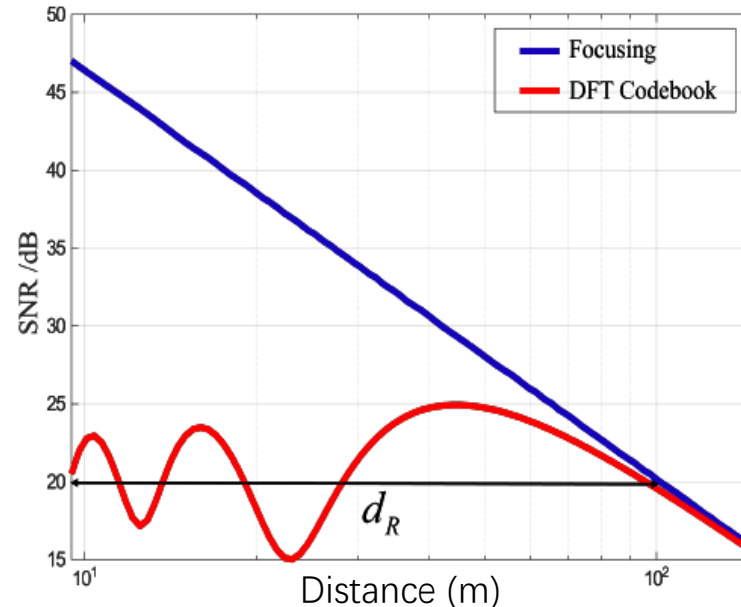
From Far-field to Near-field



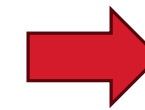
- Can we still use far-field beamforming algorithm in the near-field?
- Far-field channel model: $\mathbf{H}_P = \sum_{p=1}^{N_p} |\alpha_p^{11}| e^{-j\frac{2\pi}{\lambda} D_p^{11}} \mathbf{a}_{rp}(\theta_{rp}^{11}, \phi_{rp}^{11}) \mathbf{a}_{tp}^H(\theta_{tp}^{11}, \phi_{tp}^{11}) \rightarrow$ linear phase
- Near-field channel model: $\mathbf{H}_S[i, l] = \sum_{p=1}^{N_p} |\alpha_p^{il}| e^{-j\frac{2\pi}{\lambda} D_p^{il}} \rightarrow$ non-linear phase



Near-field focusing and far-field beam steering



DFT codebook-based beamforming



Large performance gap

Far-field beamforming, e.g., beam steering & DFT codebook, cannot be used in near-field

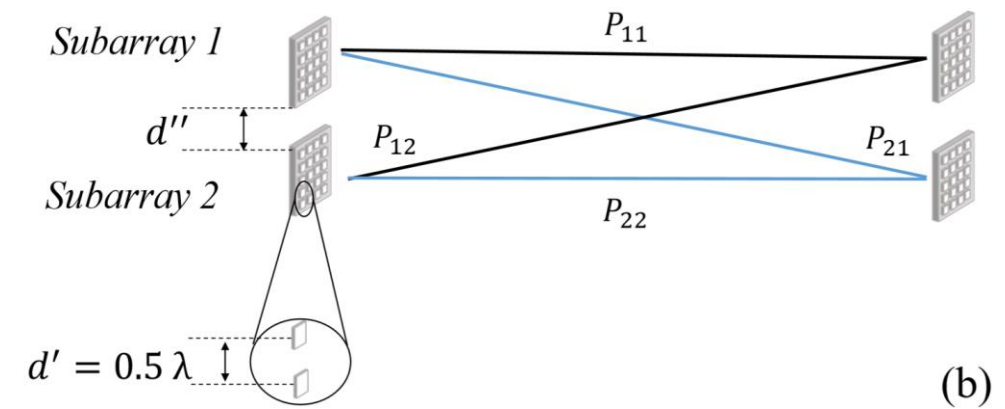
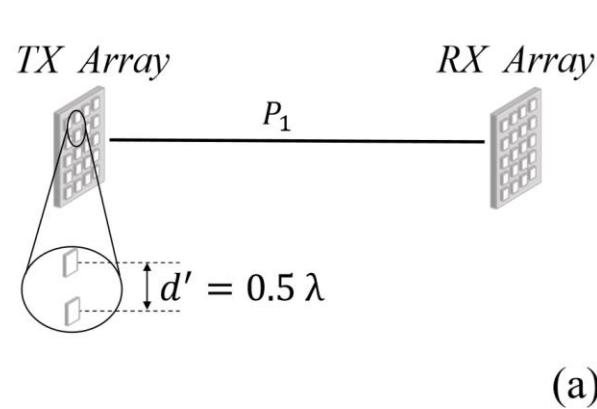
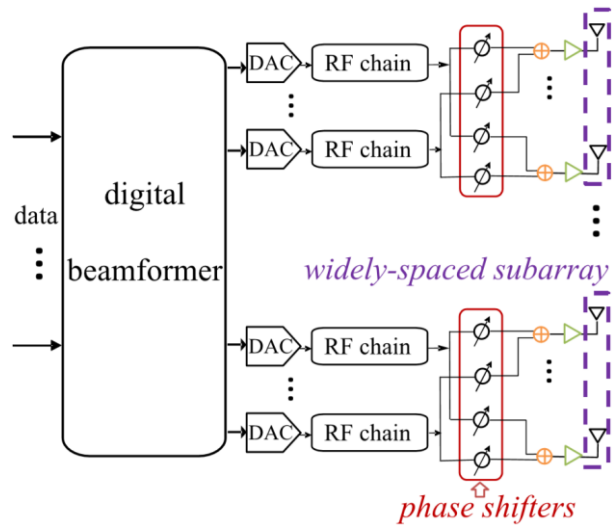
F. Wang et al., "Ring-type Codebook Design for Reconfigurable Intelligent Surface Near-field Beamforming," 2022 IEEE 33rd Annual International Symposium on Personal, Indoor and Mobile Radio Communications (PIMRC), Kyoto, Japan, 2022, pp. 391-396.

H. Zhang, N. Shlezinger, F. Guidi, D. Dardari and Y. C. Eldar, "6G Wireless Communications: From Far-Field Beam Steering to Near-Field Beam Focusing," in IEEE Communications Magazine, vol. 61, no. 4, pp. 72-77, April 2023.

Spatial Multiplexing under Extreme Sparsity



- Do we really “hate” near-field?
- THz channel: extreme sparse (LoS only) → poor inter-path multiplexing → limited data rate



Widely-spaced multi-subarray (WSMS) architecture

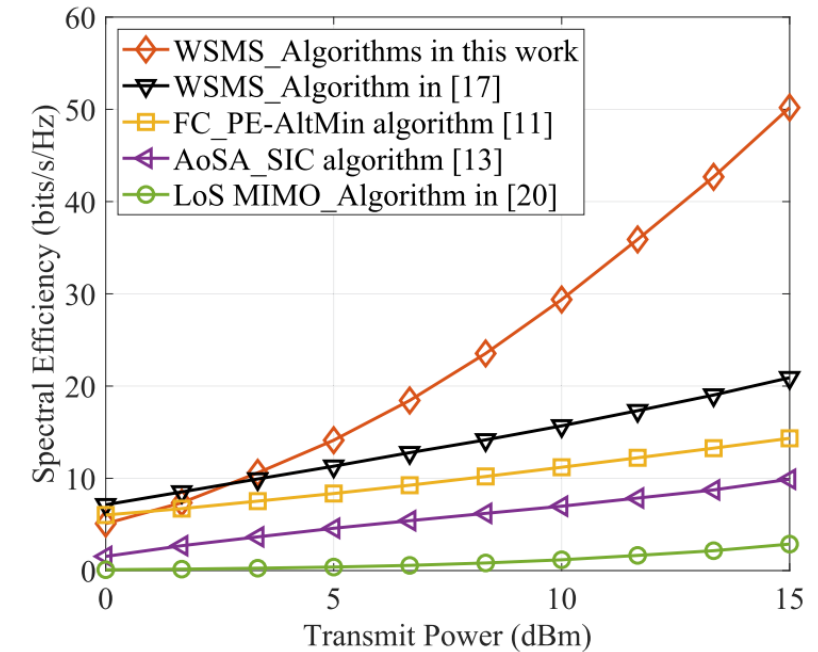
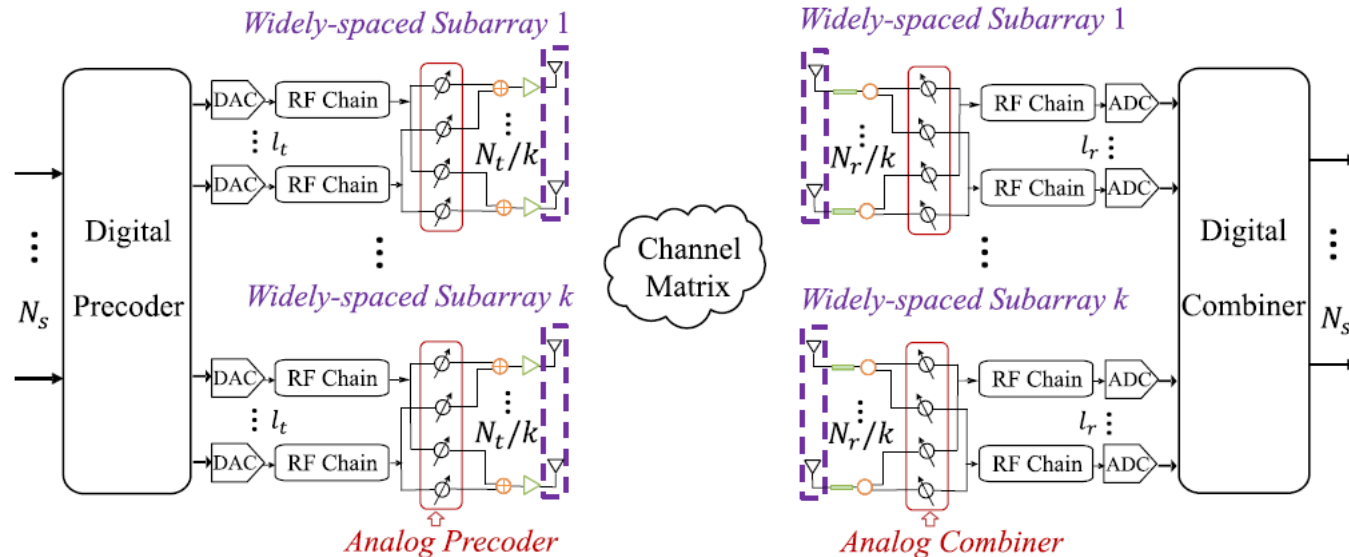
- Widely-spaced subarrays
 - The utilization of the widely-spaced subarrays at Tx **enlarges the range of near-field**
 - Near-field propagation → spherical-wave model → intra-path multiplexing
- Half wavelength antenna in subarray → far-field propagation → planar-wave propagation → inter-path multiplexing

Beamforming for Single-user WSMS System



Single-user Architecture

- Tx & Rx: k widely-spaced compact subarrays



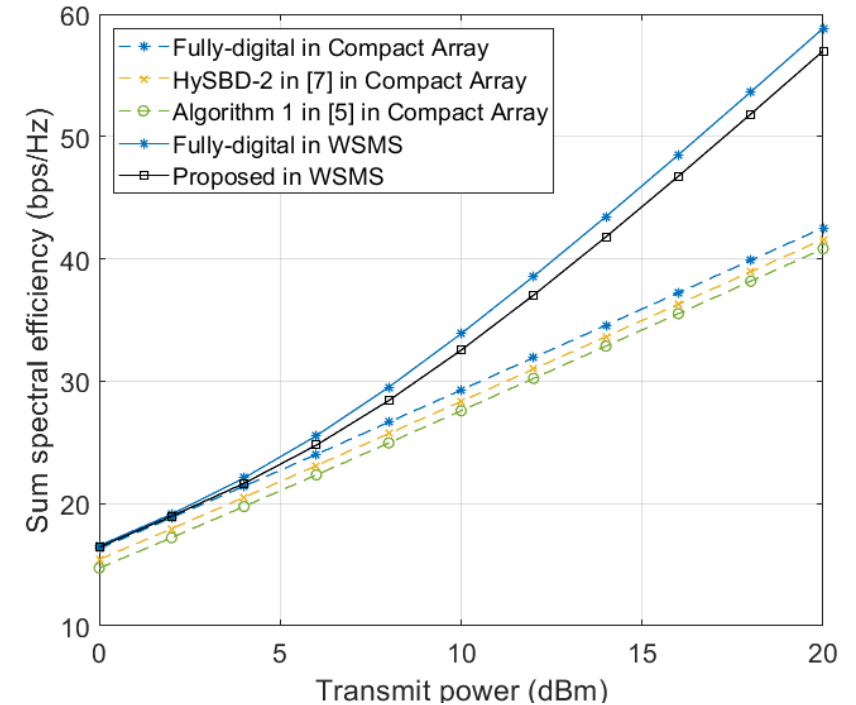
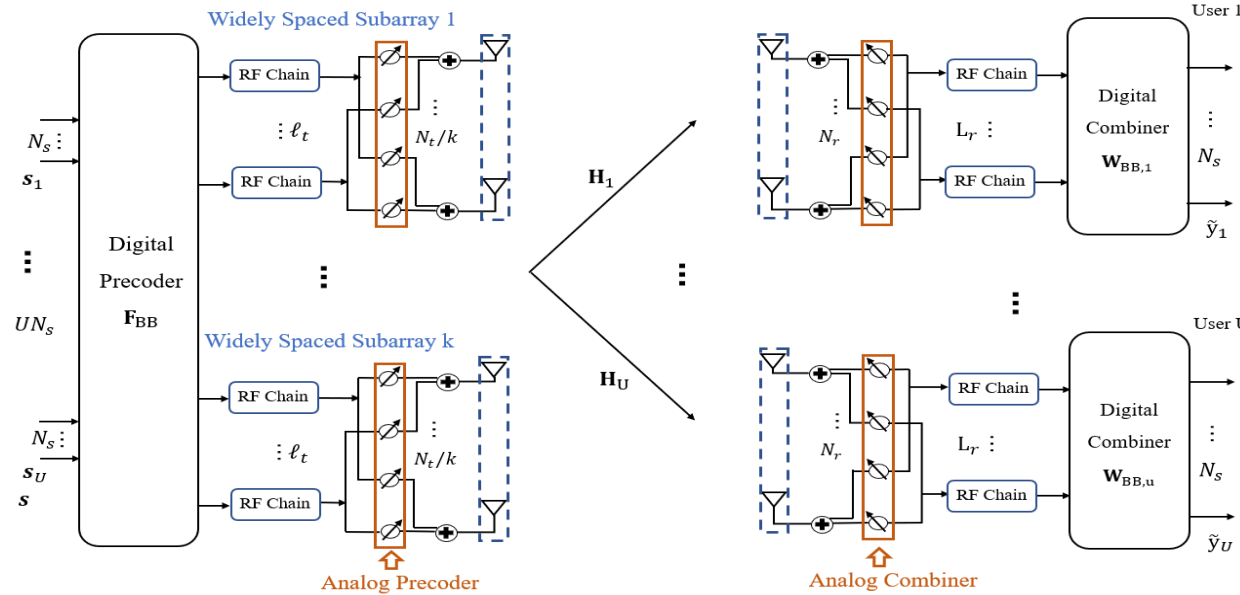
- WSMS architecture achieves 35 bits/s/Hz and 40 bits/s/Hz higher spectral efficiency than FC and AoSA
- The spatial multiplexing gain of WSMS is substantially improved to k times!
- Using **spherical-wave propagation** to exploit **intra-path multiplexing**, in addition to **inter-path multiplexing**

Beamforming for Multi-user WSMS System



Multi-user Architecture

- Base station (BS): k widely-spaced compact subarrays
- Each user: a compact array



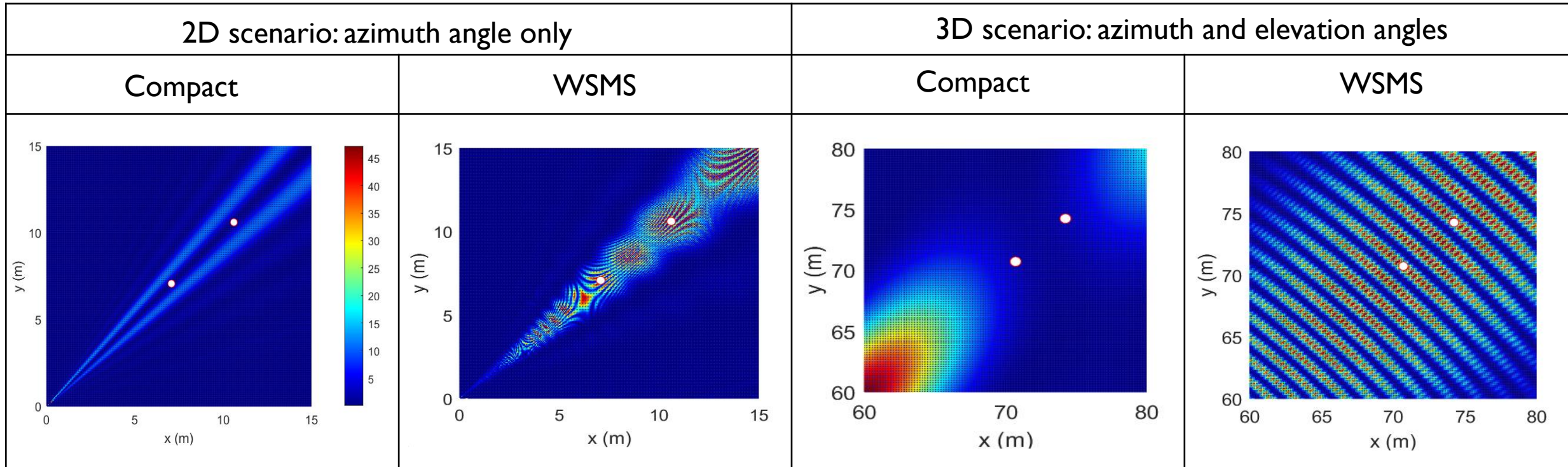
- Proposed algorithm in **multi-user WSMS architecture** achieves enhanced sum spectral efficiency compared to the compact array architectures

H.-Y. Shen, L. Yan, C. Han, and H. Liu (NokiaBell), **“Alternating Optimization Based Hybrid Beamforming in Terahertz Widely-spaced Multi-subarray Systems”**, in Proc. of IEEE GLOBECOM Workshop on Terahertz Communications, 2022.

Near-field Beamforming for MU-WSMS System



- UPA with 1024 antenna (0.3 THz): $d_R \approx 1 \text{ m}$ \rightarrow mostly far field \rightarrow only angle domain
- WSMS with 0.5 m array size: d_R over 180 m \rightarrow enlarged near field \rightarrow additional distance domain

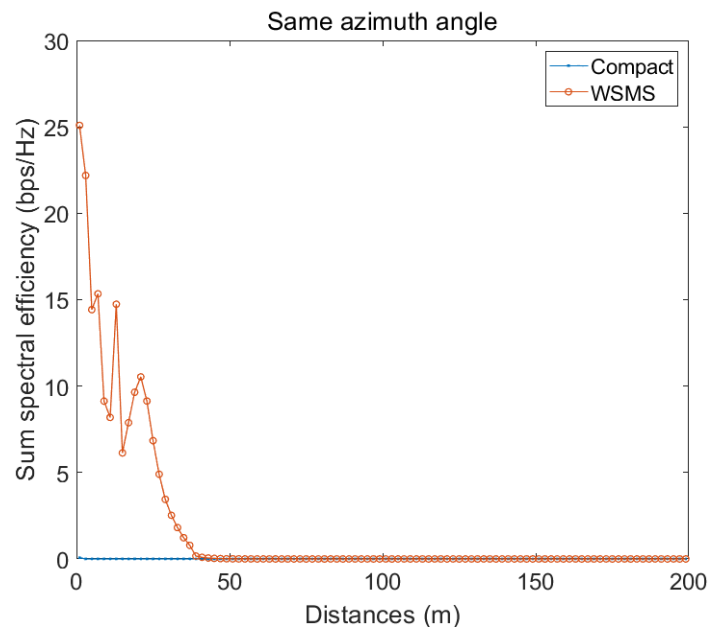


Beamforming algorithm based on user interference cancellation

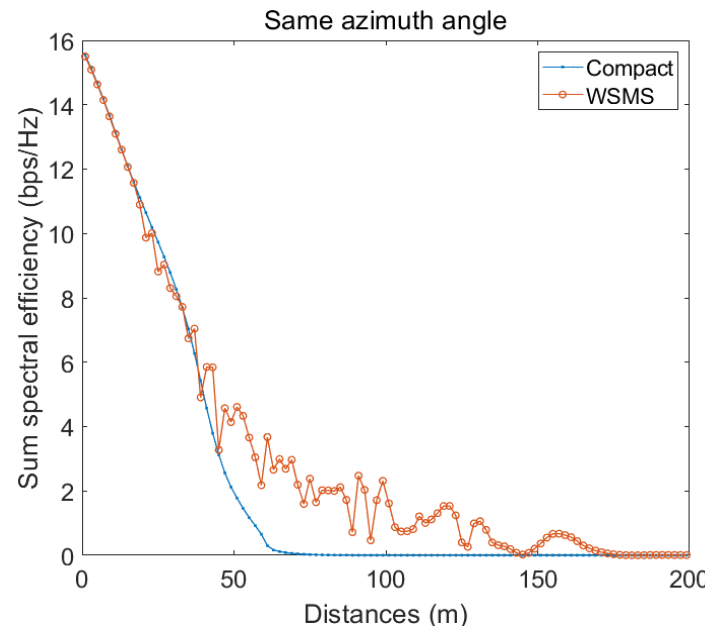
From Far-field to Near-field



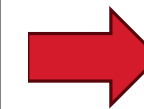
- UPA with 1024 antenna (0.3 THz): $d_R \approx 1 \text{ m}$ \rightarrow mostly far field \rightarrow only angle domain
- WSMS with 0.5 m array size: d_R over 180 m \rightarrow enlarged near field \rightarrow additional distance domain



2D scenario for users at the same azimuth angle



3D scenario for users at the same azimuth angle



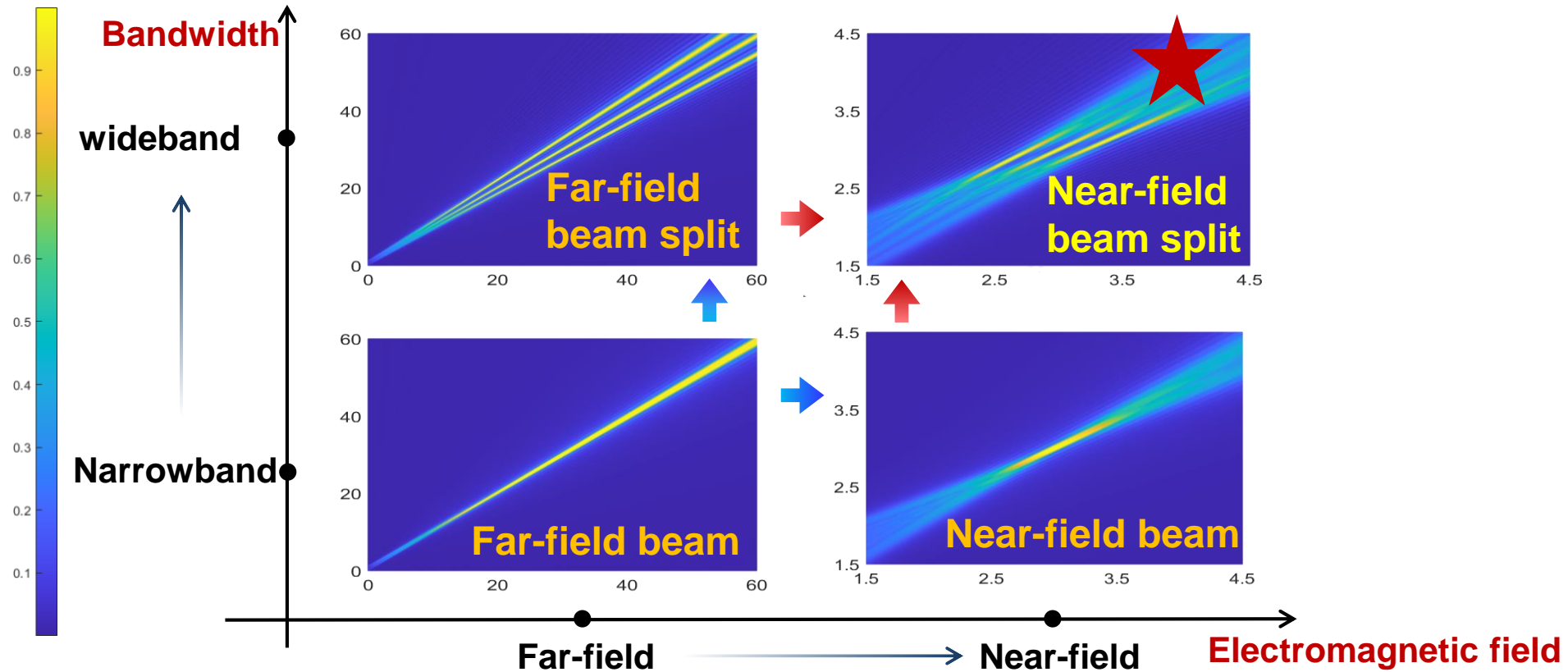
Large performance gap

Neglecting **near-field** effect in multi-user causes noticeable performance **degradation**

Near-Field Beam Split Effect



- **Far-field** beam split: beams at different frequencies be steered to different **angles**
- **Near-field** beam split: beams at different frequencies be focused on different **locations**

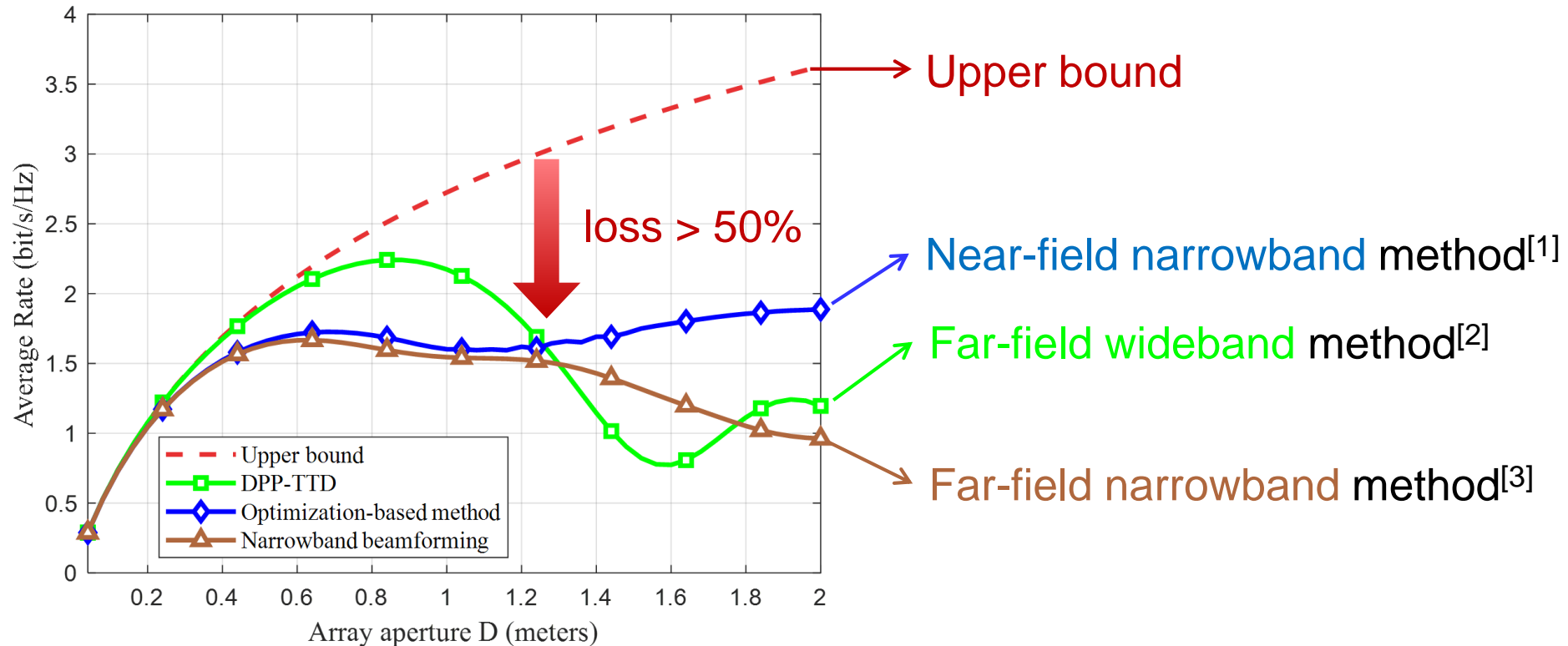


The near-field beam split effect has not been well studied

Challenge in Near-Field Wideband Systems



- Existing beamforming technologies suffer from a severe performance loss due to the near-field beam split effect



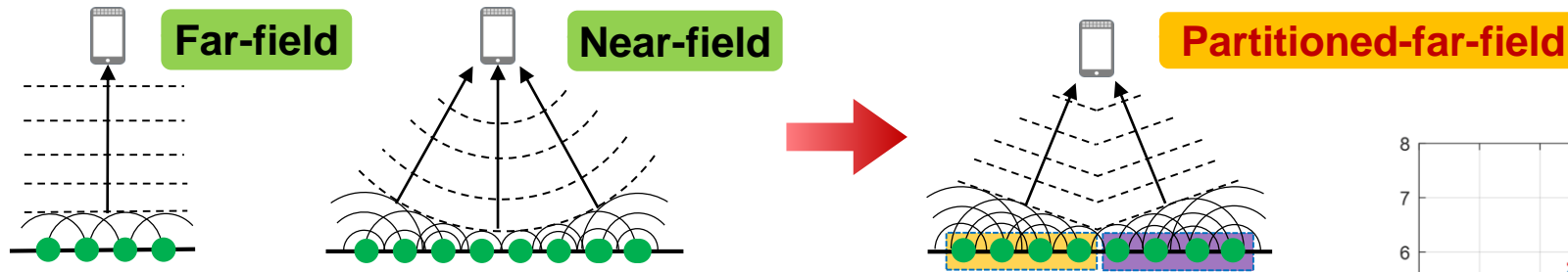
- [1] N. J. Myers and R. W. Heath, "InFocus: A spatial coding technique to mitigate misfocus in near-field LoS beamforming," IEEE Trans. Wireless Commun., vol. 21, no. 4, pp. 2193-2209, Apr. 2022.
- [2] L. Dai, J. Tan, Z. Chen, and H. Vincent Poor, "Delay-phase precoding for wideband THz massive MIMO," IEEE Trans. Wireless Commun., vol. 21, no. 9, pp. 7271-7286, Sep. 2022.
- [3] X. Yu, J. Shen, J. Zhang, and K. B. Letaief, "Alternating minimization algorithms for hybrid precoding in millimeter wave MIMO systems," IEEE J. Sel. Topics Signal Process., vol. 10, no. 3, pp. 485-500, Mar. 2016.

Partitioned-Far-Field Model



- The **partitioned-far-field** approximation of the near-field channel

- Partition the entire large array into Q small sub-arrays



- The user is located in the far-field region of each small subarray

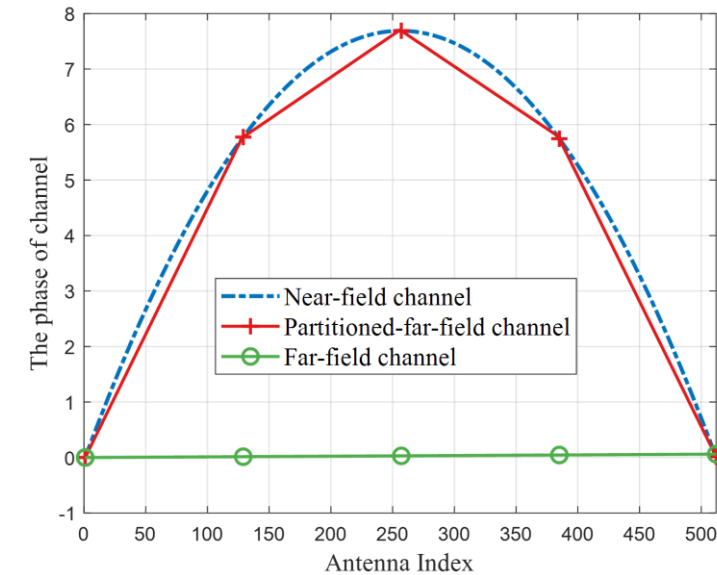
- ✓ For the p -th antenna of the q -th subarray

Distance: $r_q^{(p)} \approx r_q + pd\theta_q$

Phase: $\phi_q^{(p)} = \frac{2\pi}{\lambda} r_q^{(p)} = \frac{2\pi}{\lambda} r_q + \frac{2\pi}{\lambda} pd\theta_q$

Subarray-wise near-field phase

Antenna-wise far-field phase

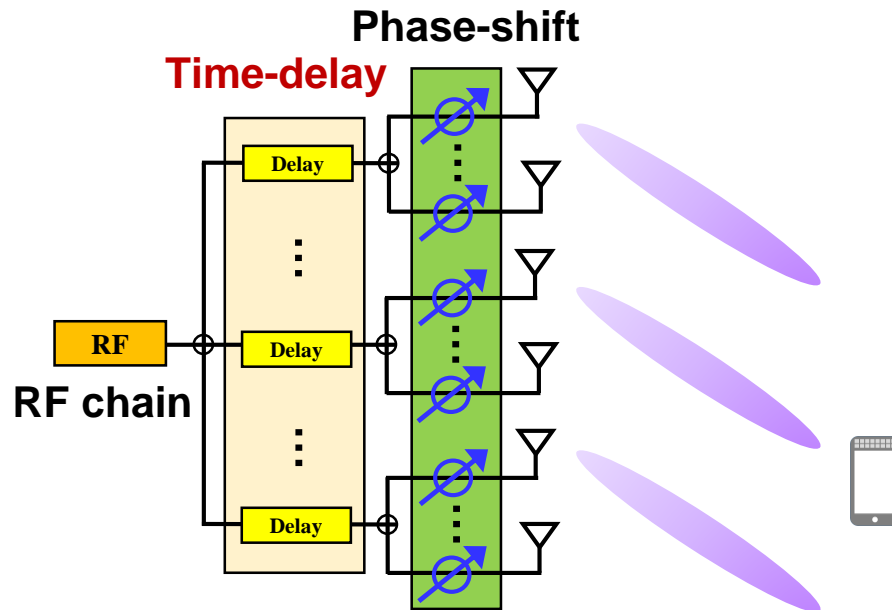


The near-field channel is **decoupled** to multiple far-field channels across different subarrays

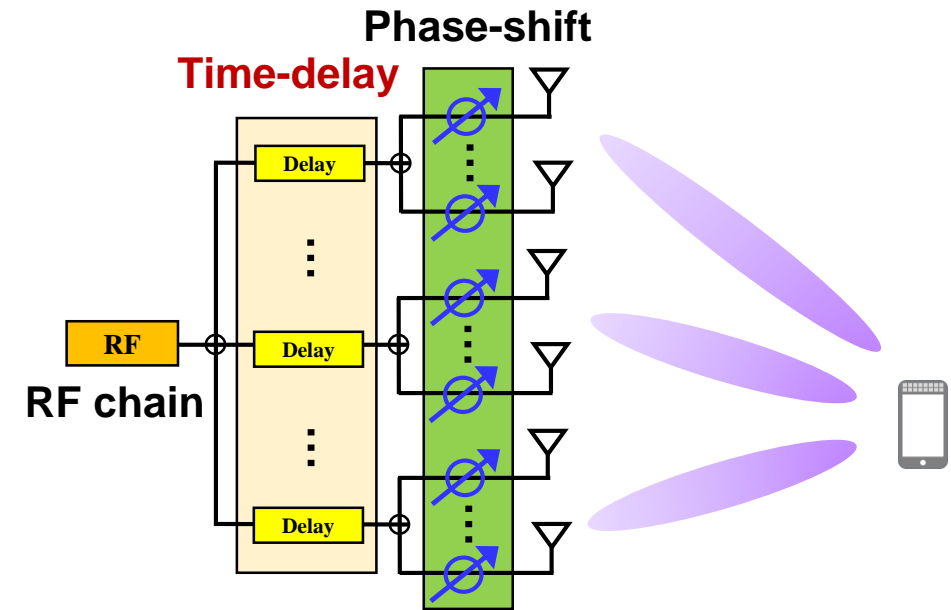
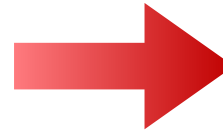
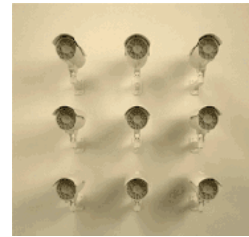
Phase-Delay Focusing (PDF)



- Steer beams from different sub-array towards different directions by **phase shifters**
- Compensate for the subarray-wise near-field phase discrepancies by **time delayers**



(a) Far-field beam split solution



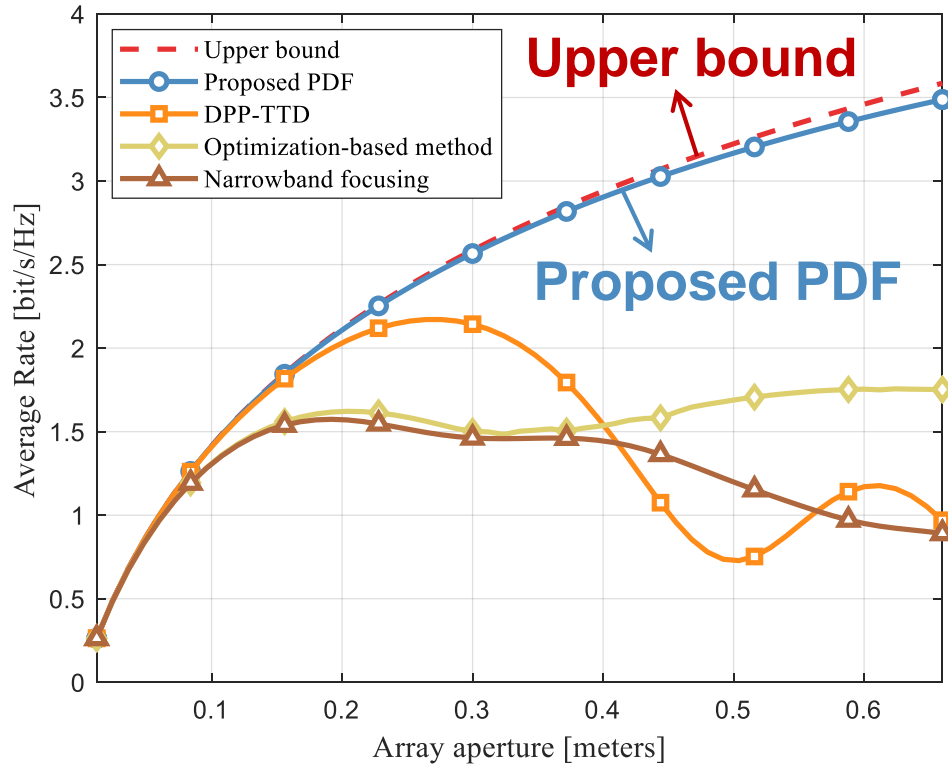
(b) Proposed phase-delay focusing (PDF)

The proposed PDF can **overcome** the near-field beam split effect

Simulation Results



- Achievable average rate vs. array aperture



Parameter	Value
Carrier	100 GHz
Bandwidth	5 GHz
Number of subcarriers	1024
Number of antennas	512
SNR	10 dB

Phase-delay focusing (PDF) can achieve more than 95% of the optimal rate

Outline

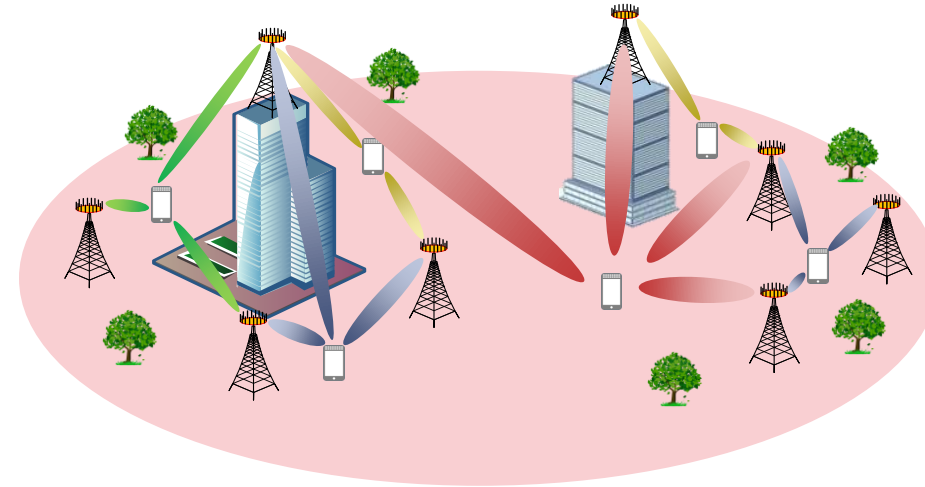


- **Chapter 1: Introduction**
 - i. Evolution to 6G
 - ii. Applications
 - iii. Motivations for THz UM-MIMO
- **Chapter 2: THz UM-MIMO Systems**
 - i. Electronic and photonic approaches
 - ii. New material approaches
 - iii. THz UM-MIMO channel
- **Chapter 3: THz Beamforming Technologies**
 - i. Fundamentals of beamforming
 - ii. State-of-the-art and challenges on beamforming
 - iii. Far-field beamforming
 - iv. Near-field beamforming/beamfocusing
- **Chapter 4: THz Beam Management**
 - i. Fundamentals of beam management
 - ii. State-of-the-art and challenges on beam management
 - iii. Beam estimation/alignment
 - iv. Beam tracking
 - v. Beam-guided medium access
- **Chapter 5: Future Directions**
 - i. Cross far- and near-field beamforming
 - ii. IRS-assisted hybrid beamforming
 - iii. Beam management in IRS assisted systems
- **Conclusion**

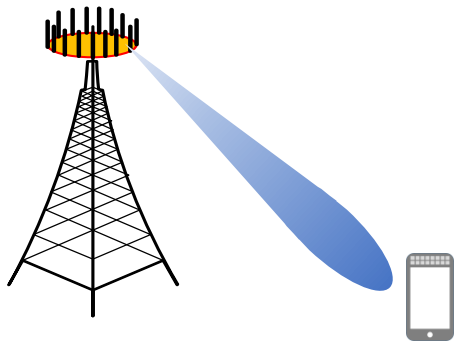
Beam Management



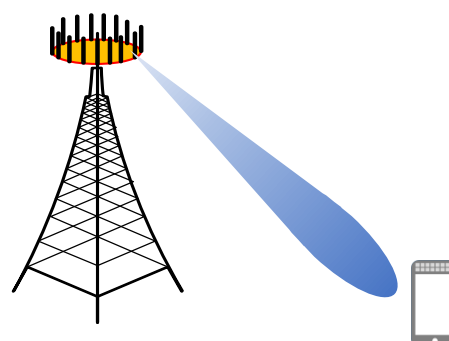
- Beam training/alignment
 - Align the beam with a certain user
- Beam tracking
 - Keep track of the **mobile** user
- Beam-guided medium access
 - Serve **multiple** users



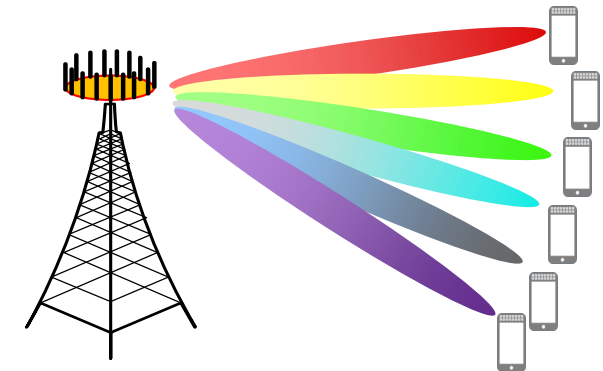
Beam alignment



Beam tracking



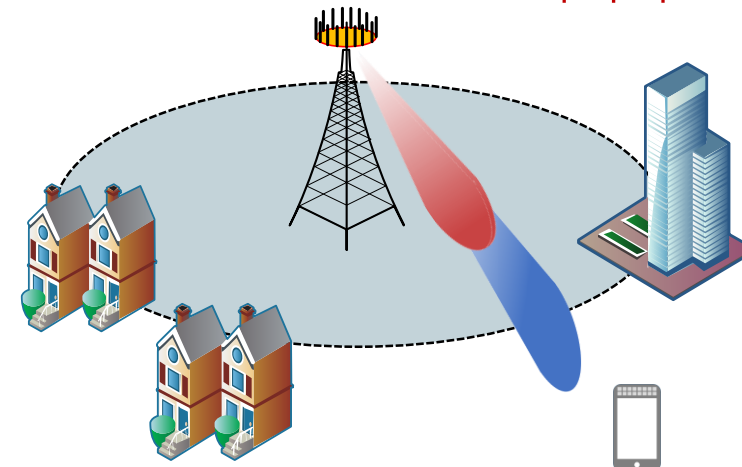
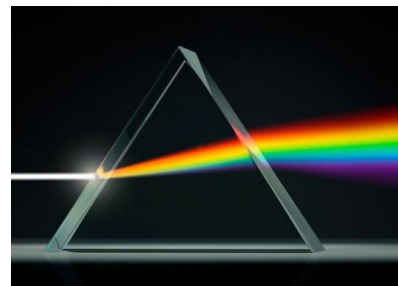
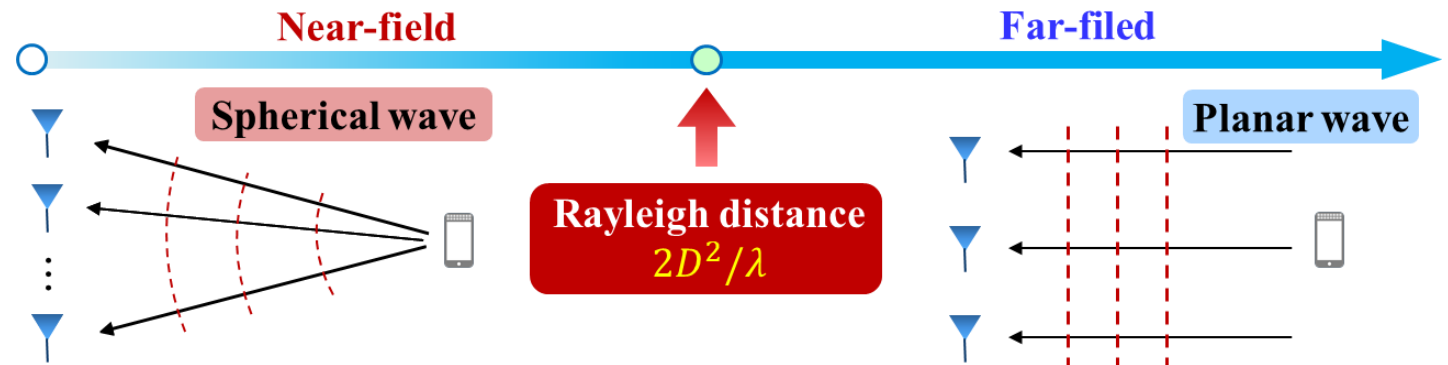
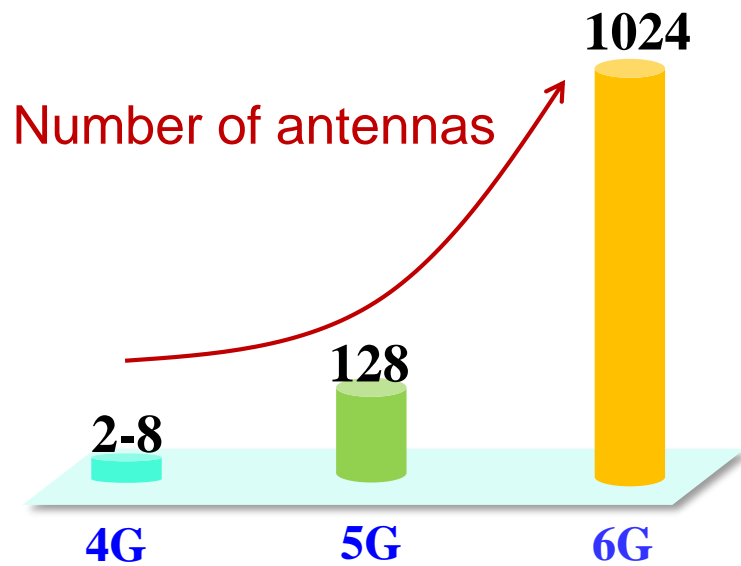
Beam-guided medium access



Challenges on Beam Management



- The cost of beam management is **high** due to the large number of antennas
- The electromagnetic field structure **changes fundamentally** due to the near field communication
- The array gain **decreases** due to the beam split effect caused by large bandwidth



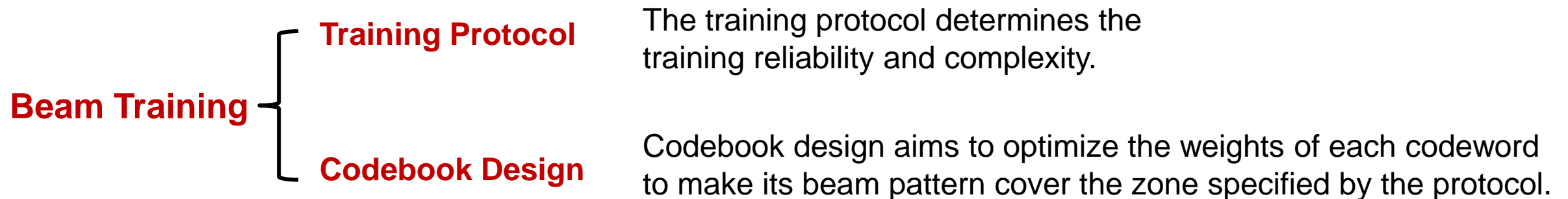
Beam Training



What is beam training?

$$\{\mathbf{w}^{\text{opt}}, \mathbf{f}^{\text{opt}}\} = \arg \max |\mathbf{w}^H \mathbf{a}_r \mathbf{a}_t^H \mathbf{f}|^2, \quad \mathbf{a}_t \text{ and } \mathbf{a}_r \text{ are unknown}$$

Beam training is the process of **seeking the solutions** of the beamformer and combiner, by **testing beam pairs**, without requiring any CSI.



Beam Training Protocol



- ◆ **Exhaustive search** is the simplest protocol, that is, exhaustively testing the narrow beam pairs of the transmitter and the receiver.
- ◆ Compared to the exhaustive search, some **other training protocols** are more appealing owing to their lower training complexity.

TABLE IX
COMPARISON OF THE BEAM TRAINING PROTOCOLS.

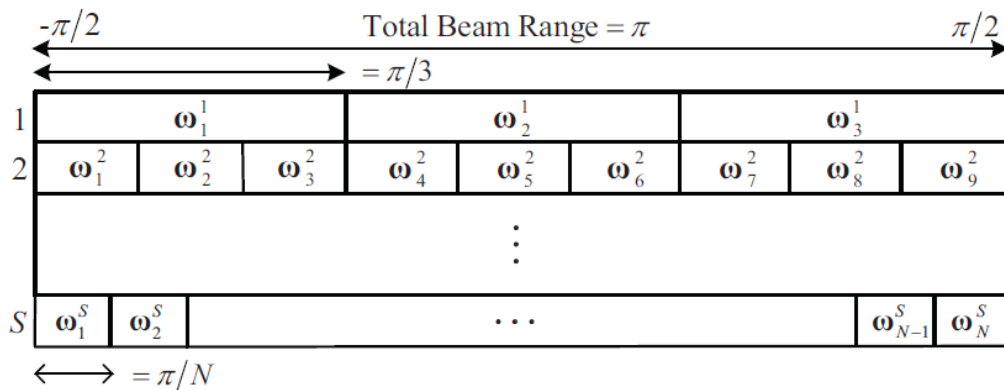
Training Protocol	Training complexity
Exhaustive search	N^2
One-side search	$2N$
Adaptive search	$4 \log_2 N$
Parallel search	N^2 / N_{RF}
Two-stage search	$N^2 / Q + Q$
One-side M -Tree search	$2M \log_M N$
Both-side M -Tree search	$M^2 \log_M N$

Beam Training Protocol

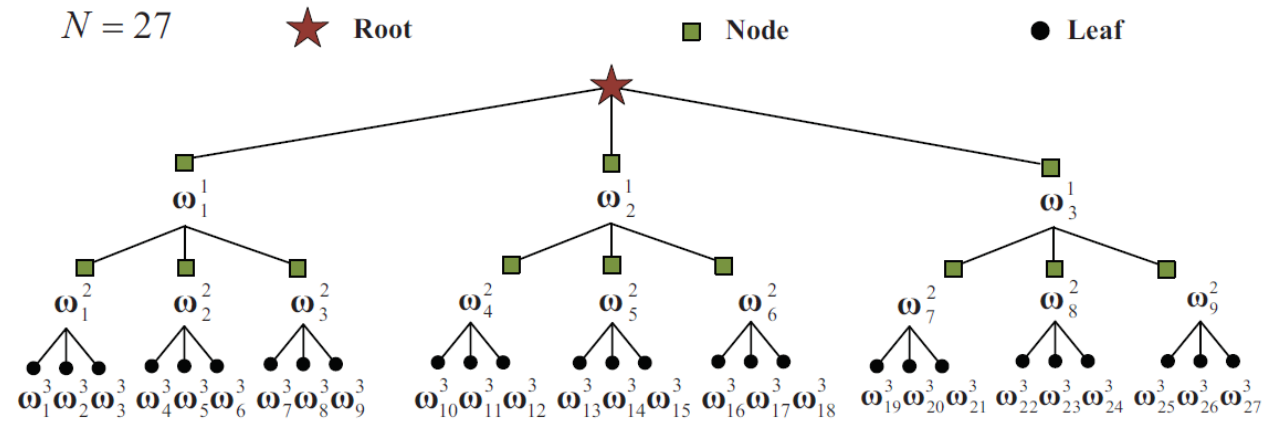


Hierarchical Search

The most efficient protocol is **M-tree search**, which is a multi-stage hierarchical protocol.



Zone Division



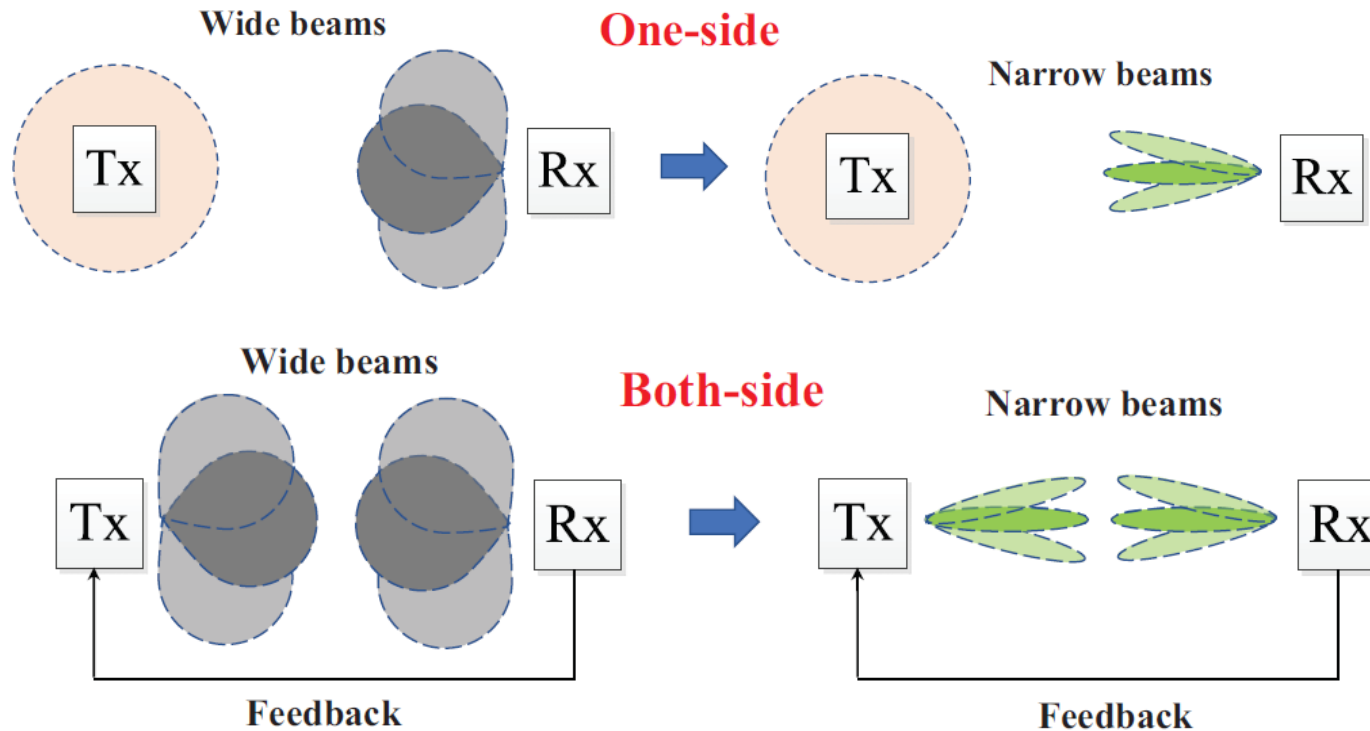
Search Manner

We start with using an omnidirectional beam (root) for initial detection. Then, in each stage of the M-tree search, we find and follow the best beam (node) for the next stage search, until the best narrow beam (leaf) is found.

Beam Training Protocol



M-tree search can be classified as **one-side** M-tree search and **both-side** M-tree search.



The training complexity is given by

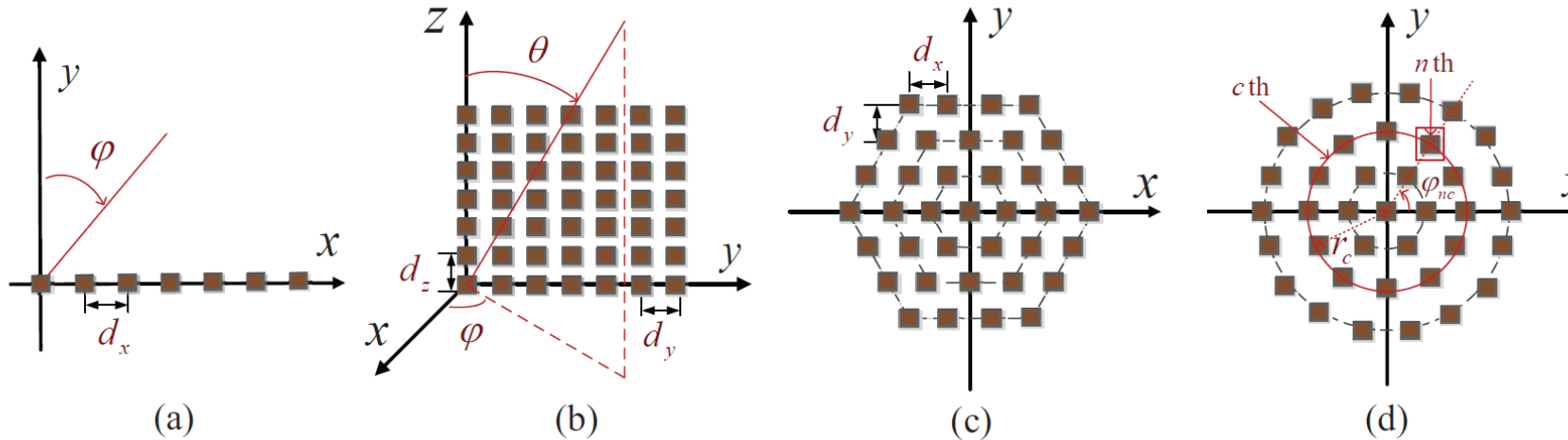
$$T_{\text{one}} = 2M \log_M N.$$

$$T_{\text{both}} = M^2 \log_M N.$$

Beam Training Protocol



- Training Protocol Design is an **open problem**, which is quite different for different scenarios.
- Training Protocol Design includes the **zone division** (for each beam) and the **search manner**.
- Training Protocol Design is related to the **antenna geometries**, **serving range**, and **power constraint**.



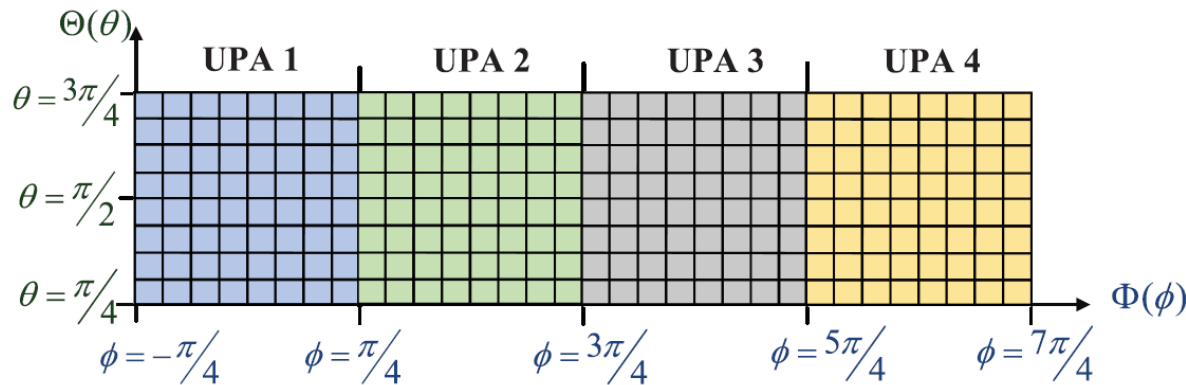
Beam Training Protocol



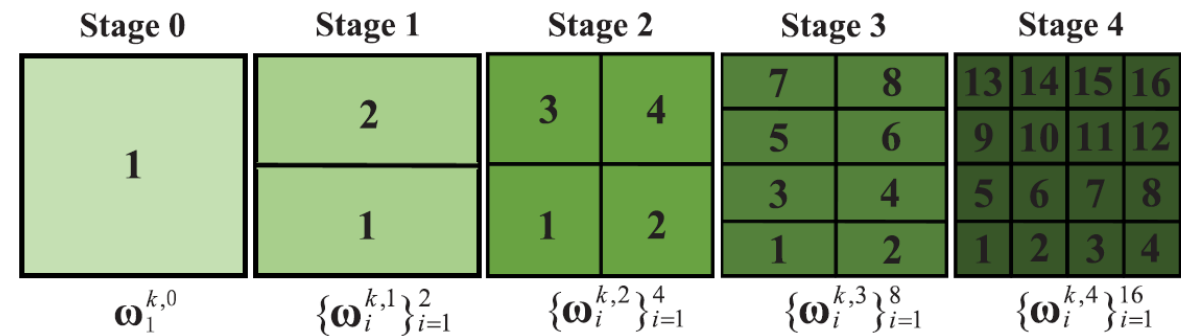
Protocol for 3D Beams

- For THz UM-MIMO system with QUPA architecture, we proposed a grid-based (GB) training protocol.

Define $\Theta(\theta) = -\cos \theta$ and $\Phi(\phi) = \sin(\phi - \frac{\pi(k-1)}{2}) + \sqrt{2}(k-1)$.

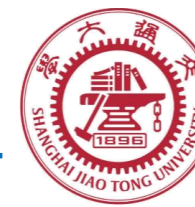


Narrow Beams



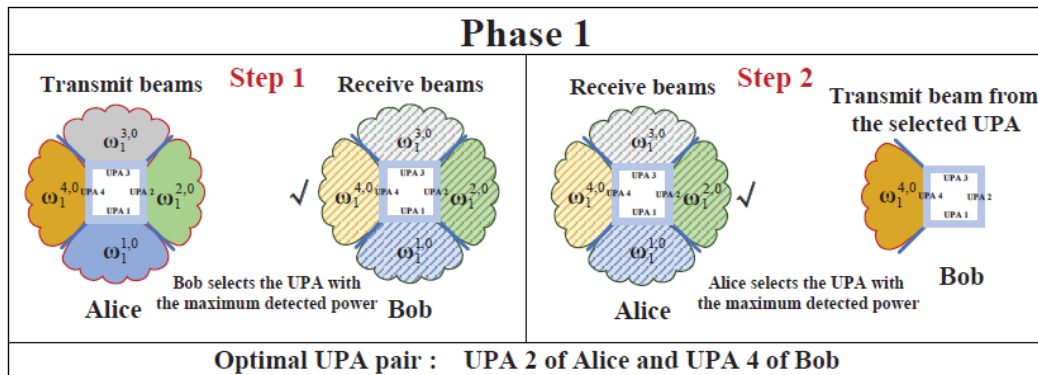
Wide Beams

Beam Training



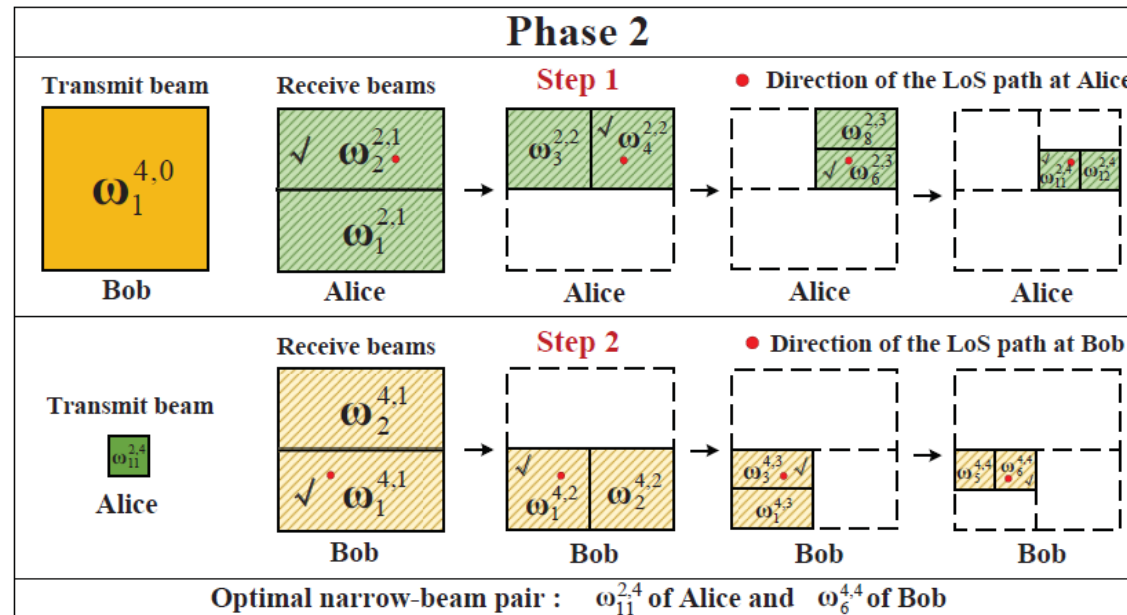
Protocol for 3D Beams

- For THz UM-MIMO system with QUPA architecture, we proposed a grid-based (GB) training protocol.



Phase 1: Find the optimal array pair

The proposed beam training has a time complexity of $4\log_2 N^2 + 4$.



Phase 2: Find the optimal narrow beam pair

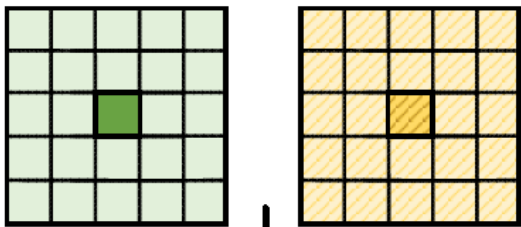
Beam Tracking Protocol



Beam Training and Tracking

After a successful beam alignment by training protocol, we can apply the **tracking protocol** by leveraging the **prior information** of aligned beams, which helps to **reduce the training overhead**.

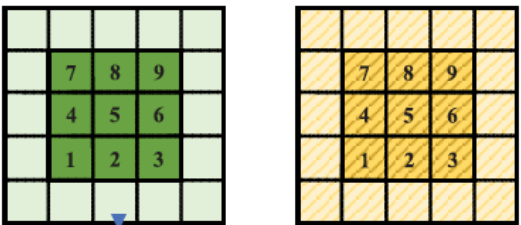
Adopted narrow-beam pair in the last interval



Alice

Bob

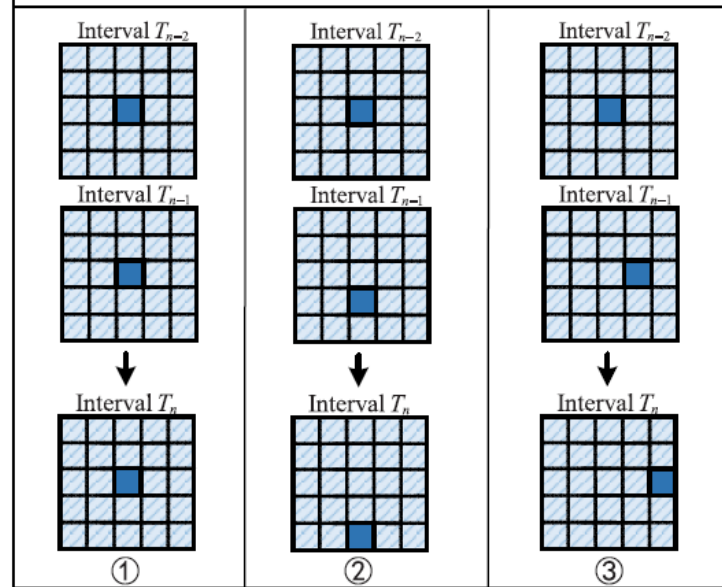
Possible narrow-beam pairs in the new interval



Alice

Bob

Tracking Mode 1



①

②

③

Tracking Mode 2

Mode 1: Only know the last beam pair

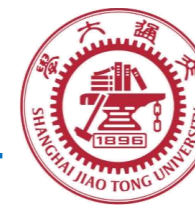
We need **12 beam tests** to find the beam pair in the 9x9 pairs.

Mode 2: know the last two beam pairs

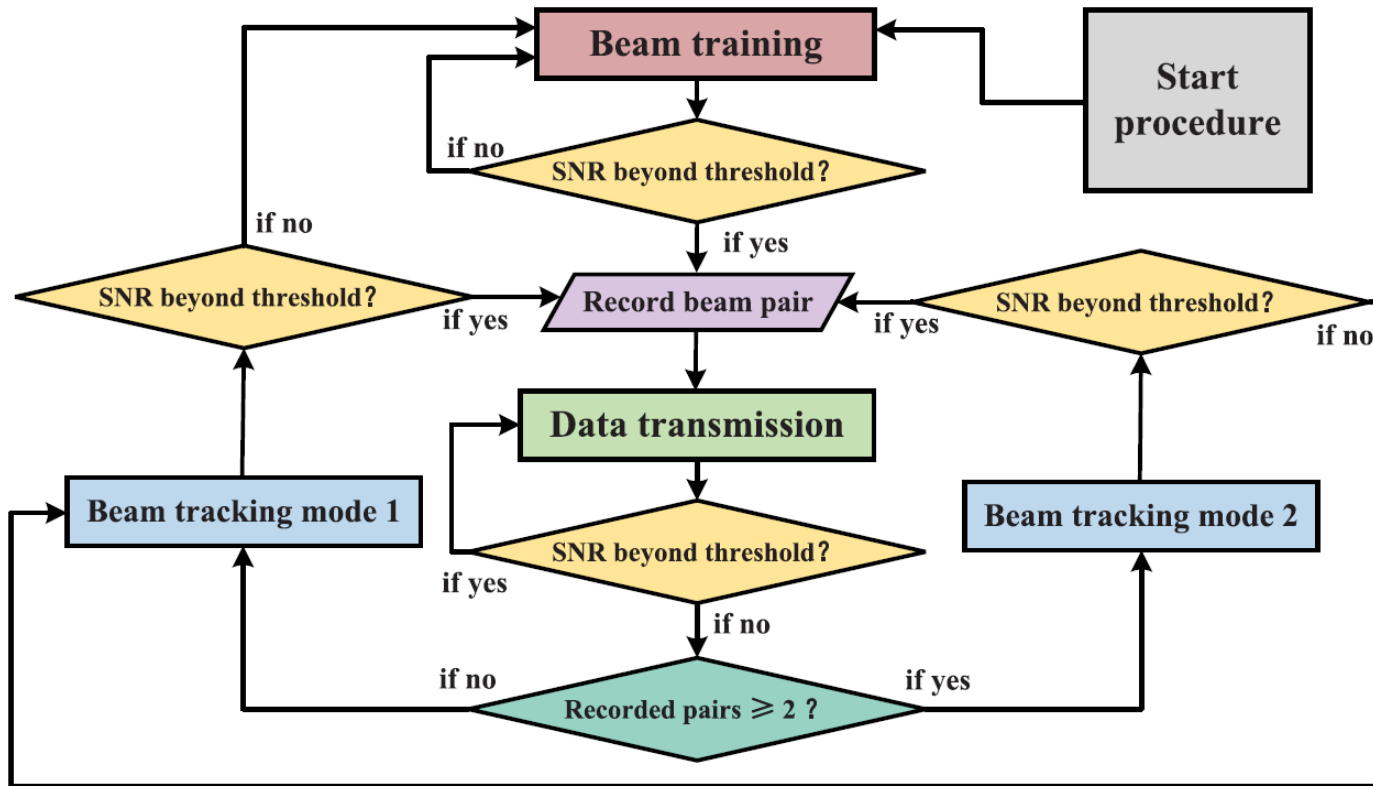
We only need **one beam test**, but not stable.

Mode 1 is stable Mode 2 is faster.

Unified Procedure for Training and Tracking



A unified procedure combines the training and tracking protocols.



- Our proposed procedure adopts **dynamic on-demand** beam training/tracking depending on the real-time quality of service.
- **If tracking mode 2 failed**, this procedure subsequently applies tracking mode 1.

Beam Training Codebook



Codebook Design

Codebook design aims to **optimize the weights of each codeword** to make its **beam pattern** cover the zone specified by the protocol.

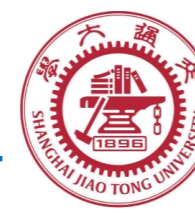
Beam pattern:

Beam pattern is characterized by the magnitude (or power) of the array factor, i.e.,

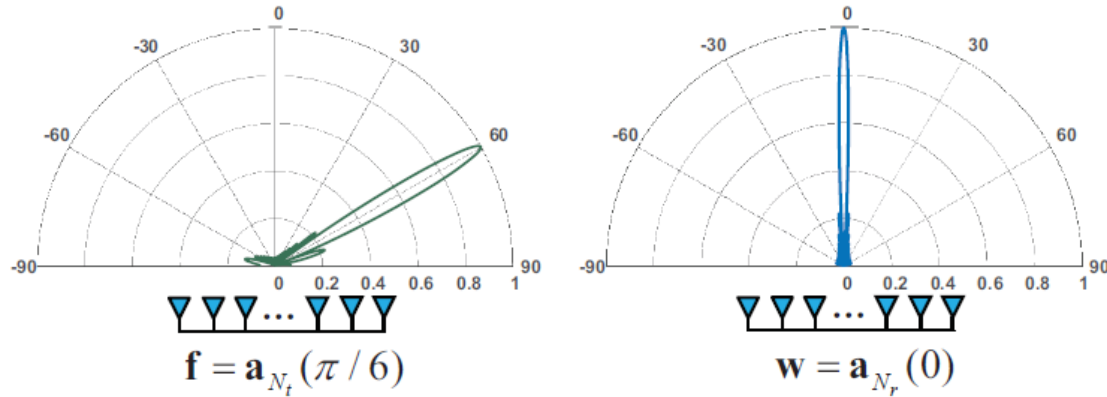
$$g(\phi, \mathbf{w}) = |\mathbf{w}^H \mathbf{a}(\phi)|, \quad \phi \in \left[-\frac{\pi}{2}, \frac{\pi}{2}\right]$$

- In the training protocol, the **narrow beams** in the bottom stage can be set as **array response vectors** whereas the **wide-beam design** is an **open problem**.

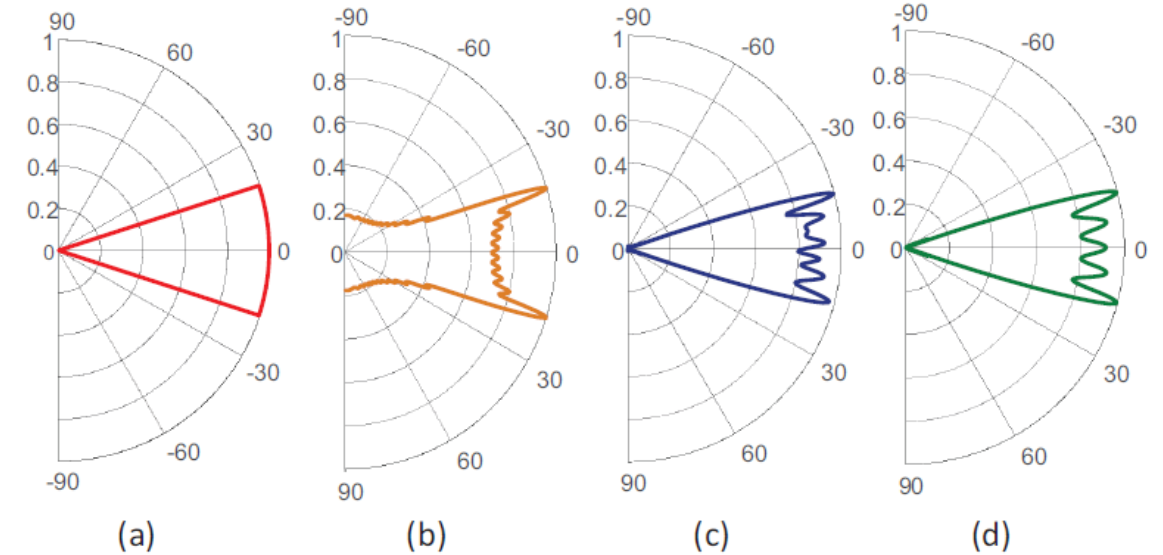
Beam Training Codebook



Codebook Design



Narrow Beam Patterns



Wide Beam Patterns

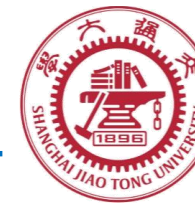
$N_t=32$: (a) ideal beam pattern. (b) beam pattern by ROP. (c) beam pattern in COP. (d) beam pattern by SNB-GP

(b) A. Alkhateeb, O. E. Ayach, G. Leus, and R. W. Heath, "Channel estimation and hybrid precoding for millimeter wave cellular systems," *IEEE J. Sel. Topic Signal Process.*, vol. 8, no. 5, pp. 831–846, Oct. 2014.

(c) K. Chen, C. Qi, and G. Y. Li, "Two-step codeword design for millimeter wave massive MIMO systems with quantized phase shifters," *IEEE Trans. Signal Process.*, vol. 68, pp. 170–180, 2020.

(d) S. Noh, M. D. Zoltowski, and D. J. Love, "Multi-resolution codebook and adaptive beamforming sequence design for millimeter wave beam alignment," *IEEE Trans. Wireless Commun.*, vol. 16, no. 9, pp. 5689–5701, Sep. 2017.

Codebook Optimization



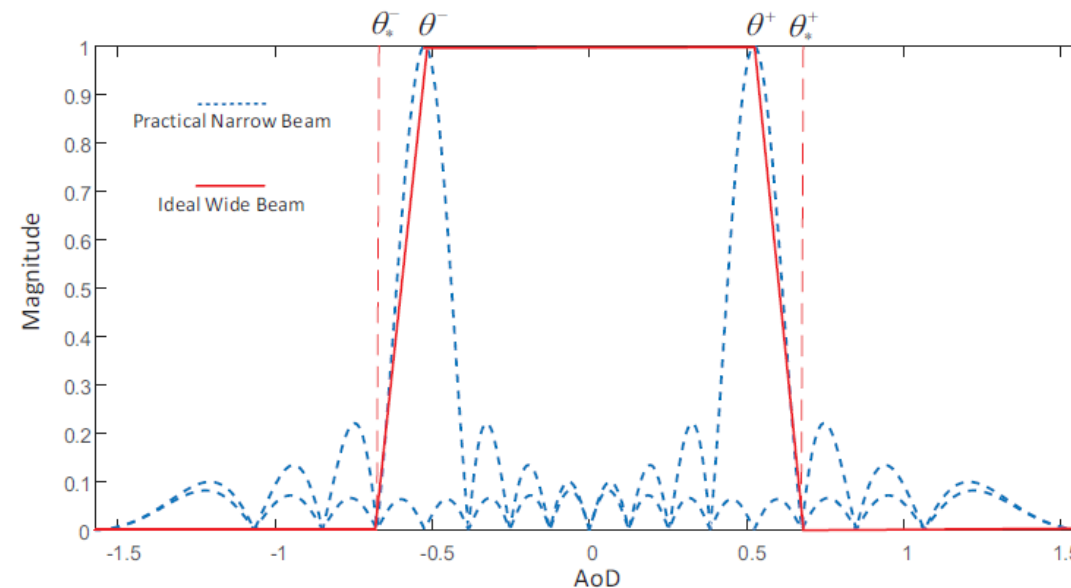
Existing approaches are **heuristic**, we proposed a **optimization-based method**, which is referred to as successive convex approximation (SCA)-based auxiliary target pursuit (**SCA-ATP**).

To tackle this problem, we propose a **BPE metric** to characterize the gap between the practical beam pattern and the ideal one. Specifically, given a codeword $\omega(\theta^-, \theta^+)$, its BPE can be expressed as

$$\begin{aligned} \varepsilon \{ \omega(\theta^-, \theta^+) \} & \triangleq \int_{\varphi \in [\theta^-, \theta^+]} \left| \gamma - \left| \mathbf{a}_{N_t}(\varphi)^H \omega(\theta^-, \theta^+) \right| \right|^2 d\varphi \\ & + \int_{\varphi \in [\theta_*^-, \theta^-] \cup [\theta^+, \theta_*^+]} \left| \mu(\varphi) - \left| \mathbf{a}_{N_t}(\varphi)^H \omega(\theta^-, \theta^+) \right| \right|^2 d\varphi \\ & + \int_{\varphi \in [-\frac{\pi}{2}, \theta_*^-] \cup [\theta_*^+, \frac{\pi}{2}]} \left| \mathbf{a}_{N_t}(\varphi)^H \omega(\theta^-, \theta^+) \right|^2 d\varphi, \end{aligned}$$

where $\mu(\varphi) \in \mathbb{R}$ is an arbitrary real variable with $0 \leq \mu(\varphi) \leq \gamma$. Hence, the wide-beam realization problem can be formulated as

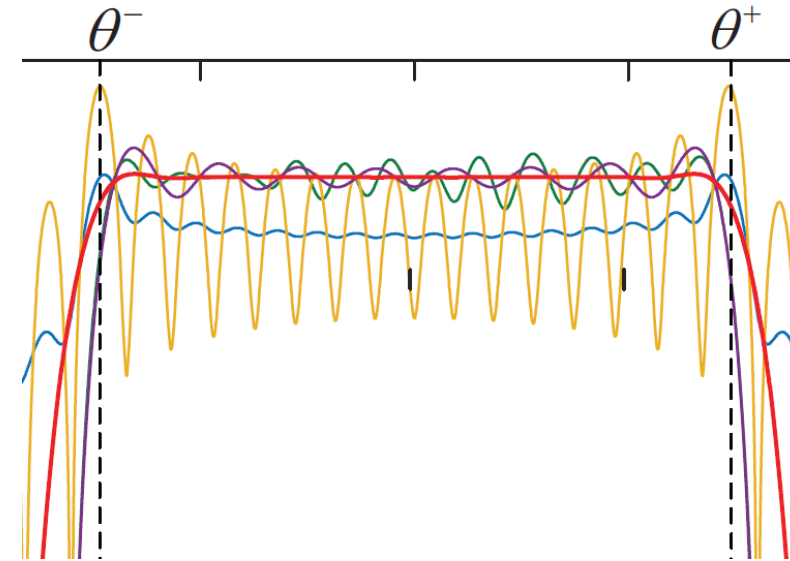
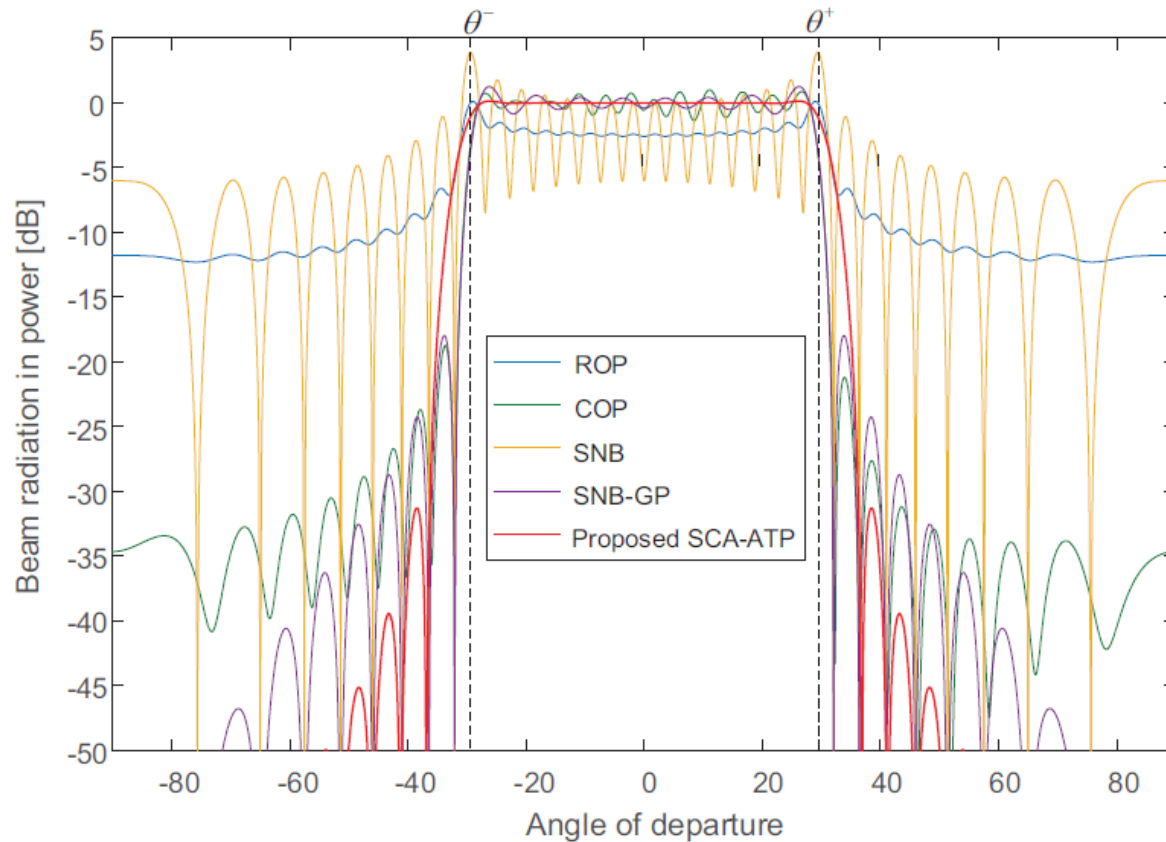
$$\begin{aligned} \text{(P1): } \quad & \min_{\omega(\theta^-, \theta^+), \mu(\varphi)} \varepsilon \{ \omega(\theta^-, \theta^+) \} \\ \text{s.t. } \quad & 0 \leq \mu(\varphi) \leq \gamma, \quad \varphi \in [\theta_*^-, \theta^-] \cup [\theta^+, \theta_*^+]. \end{aligned}$$



Codebook Optimization

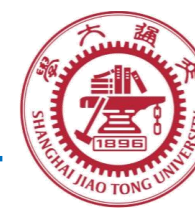


Codebook Design



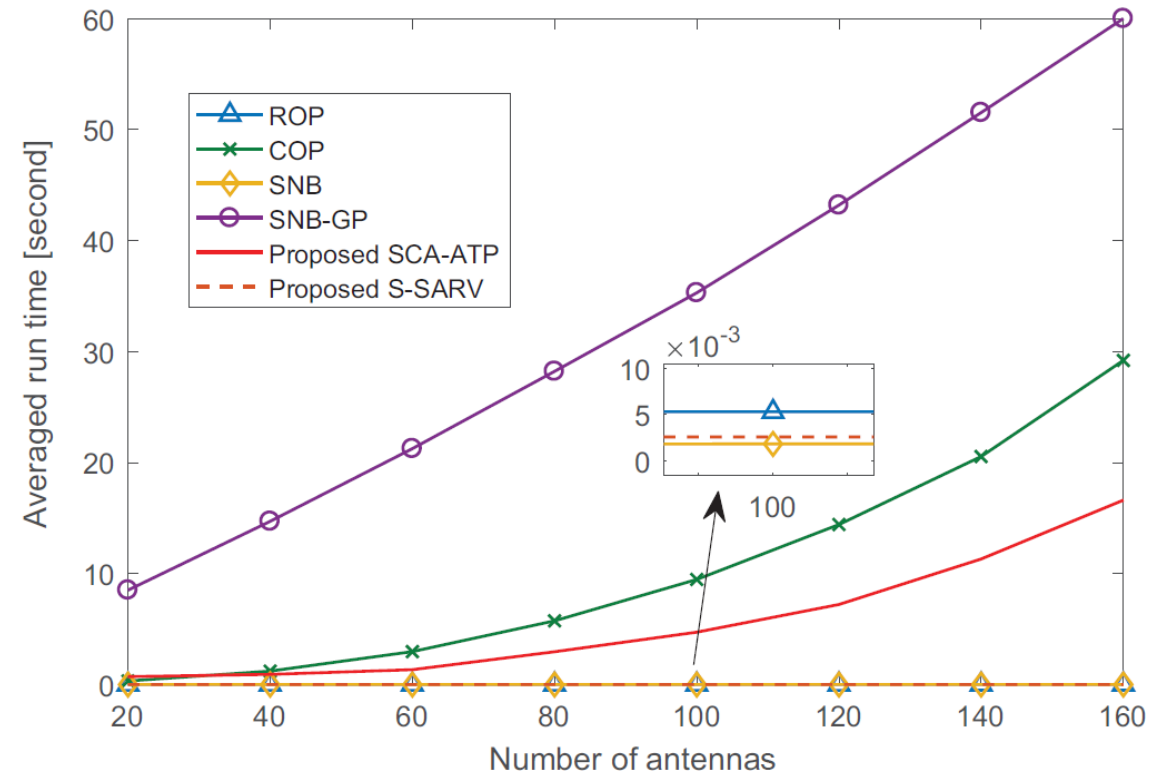
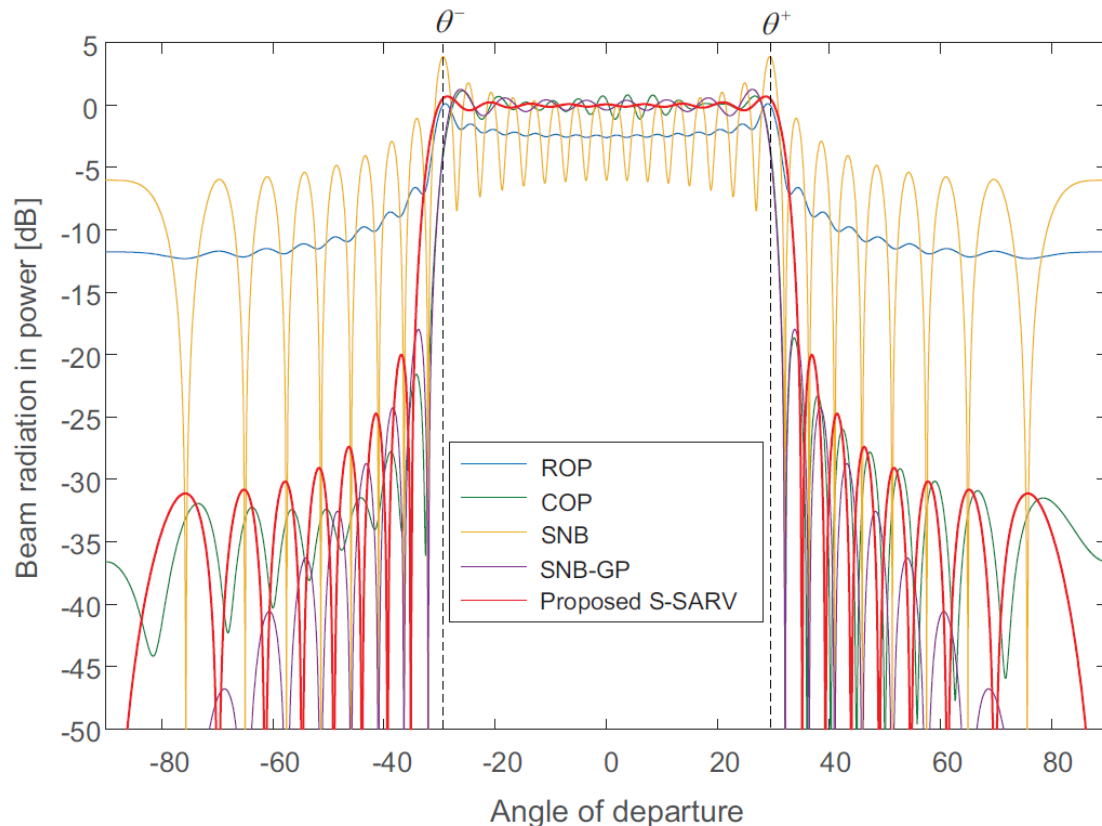
The beam pattern via SCA-ATP has a flatter main lobe and decent side-lobe suppression

Codebook Optimization

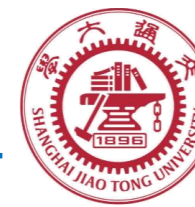


Codebook Design

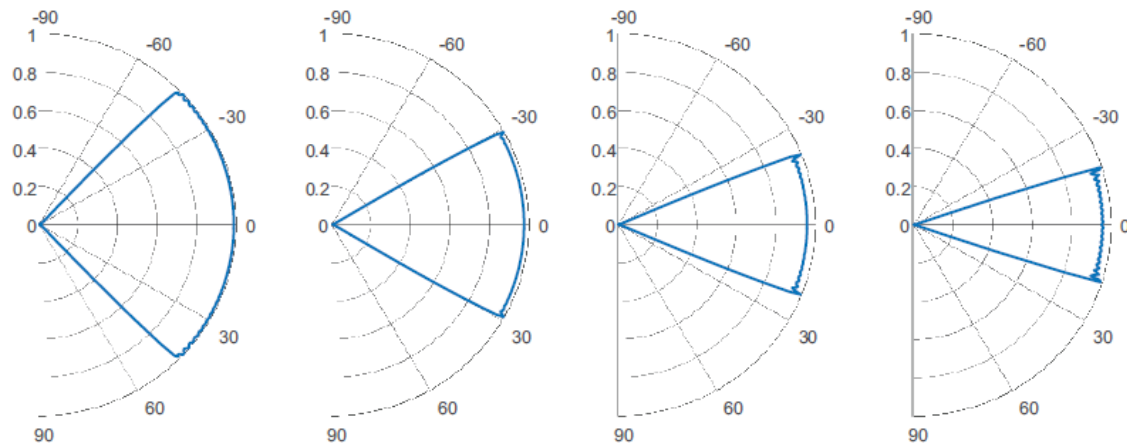
Although **SCA-ATP** yields a good performance, it cannot be used for real-time design due to the high complexity. In sight of this, we further propose an **S-SARV** method for the real-time design as a low-complexity solution.



Codebook Optimization



SCA-ATP



S-SARV

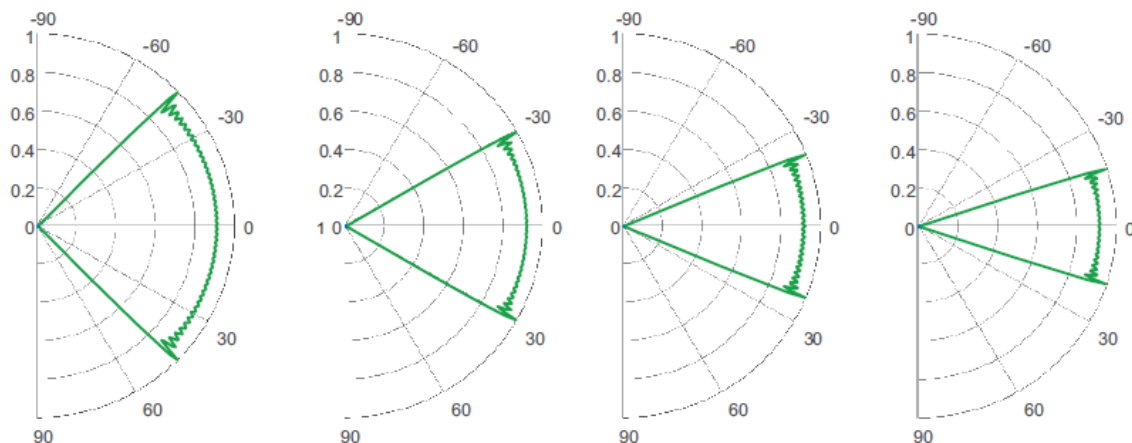


TABLE X

COMPARISON OF THE WIDE-BEAM APPROACHES.
MORE ★ REPRESENTS LOWER COMPLEXITY OR HIGHER PERFORMANCE

Wide-beam approaches	Complexity	Performance
ROP [135]	★★★★★	★★
COP [136]	★★	★★★★
SNB [137]	★★★★★	★
SNB-GP [119]	★	★★★★
SCA-ATP [138]	★★★	★★★★★
S-SARV [139]	★★★★★	★★★★

To the best of our knowledge, the beam pattern of the **SCA-ATP** is closest to the ideal one, and the **S-SARV** is the best approach to balance the performance and computational complexity.

Beam Estimation



Process the received signal after beam training to obtain the accurate estimated beam direction

Target

- Millidegree-level DoA estimation
- Millisecond-level DoA tracking

Existing solutions

- On-grid: estimation accuracy restricted by the grid resolution ✘
- Off-grid: cannot be directly applied to different hybrid beamforming architectures ✘

Received signal: $\mathbf{y} = \mathbf{W}^H \mathbf{H}[f, r, k] \mathbf{F} \mathbf{s} + \mathbf{W}^H \mathbf{n}$,

$$\text{THz channel: } \mathbf{H}[f, r, k] = \sum_{\ell=1}^L \alpha_{\ell}[f, r, k] \mathbf{a}_r(\theta_{\ell,r}[k], \phi_{\ell,r}[k]) \mathbf{a}_t(\theta_{\ell,t}[k], \phi_{\ell,t}[k])^H = \mathbf{A}_r[k] \mathbf{\Lambda}[k] \mathbf{A}_t^H[k]$$

Combining matrix: When $N_{RF} = 16, N_r = 1024$, Compression rate is $16/1024=1.56$

DAoSA-MUSIC Beam Estimation and Tracking

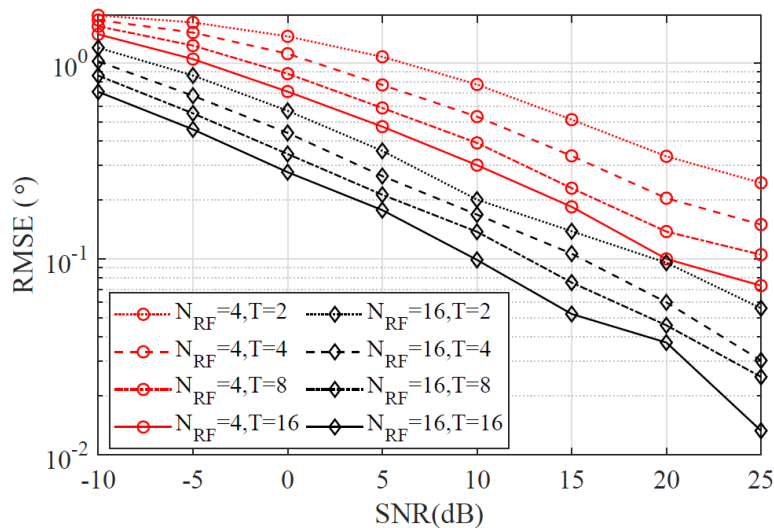


DAoSA-MUSIC estimation

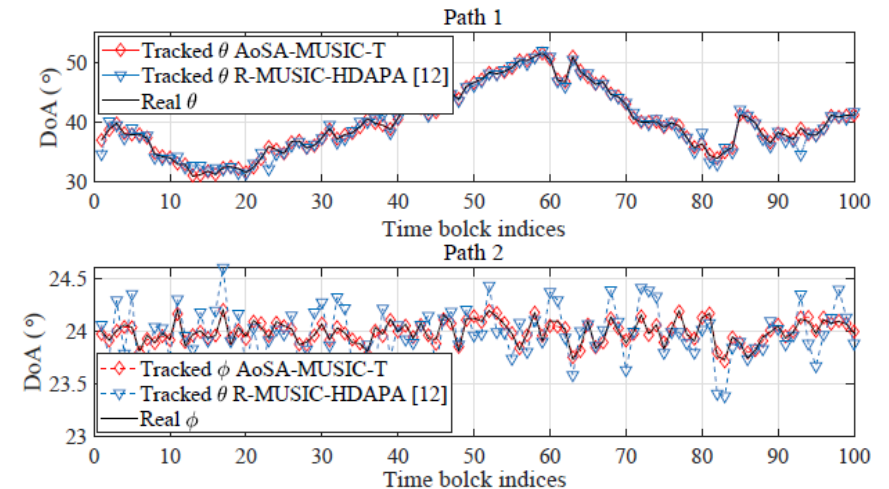
Design two stage coarse and refine training and signal reconstruction to handle the combining matrix

DAoSA-MUSIC-T tracking

Deploy correlations among tracking time slots with fifty-percent reduced training overhead



Millidegree-level estimation precision when SNR = 10 dB and $N_{RF}=16$



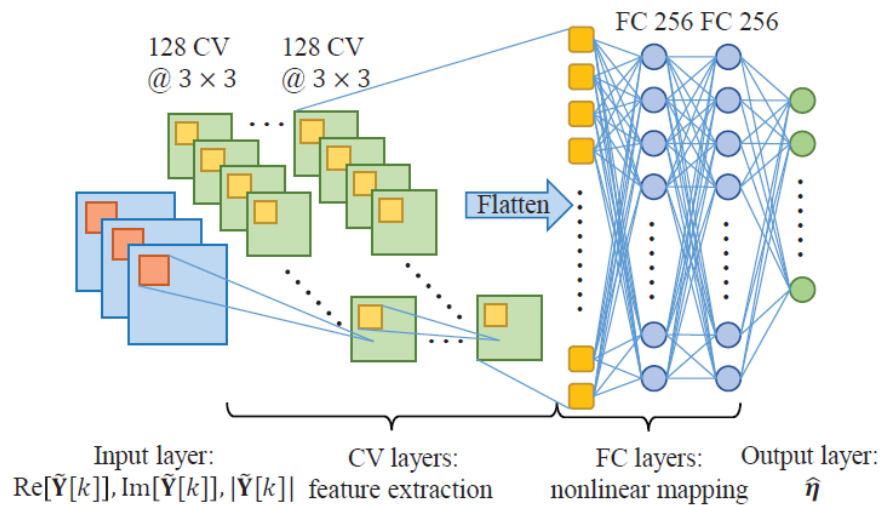
DL Beam Estimation



DCNN estimation

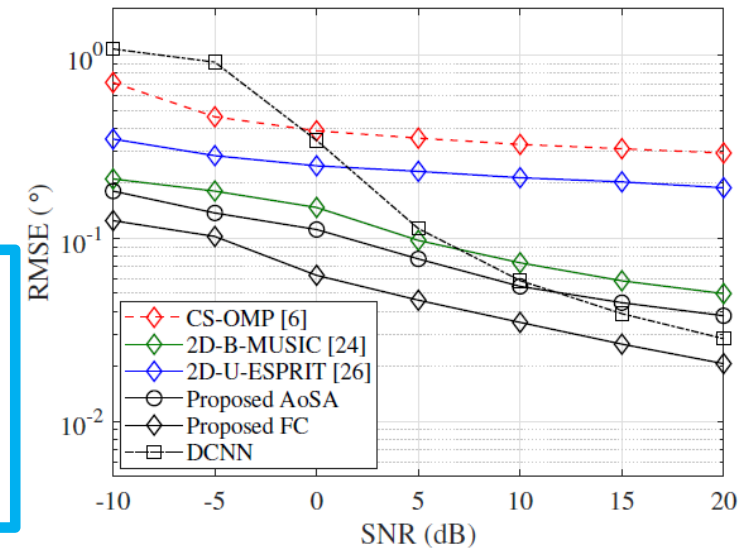
Design a DCNN network for DoA estimation, input the channel observation

Require coarse training only



DCNN network structure

0.1° estimation precision in milliseconds with coarse training only



Estimation RMSE comparison

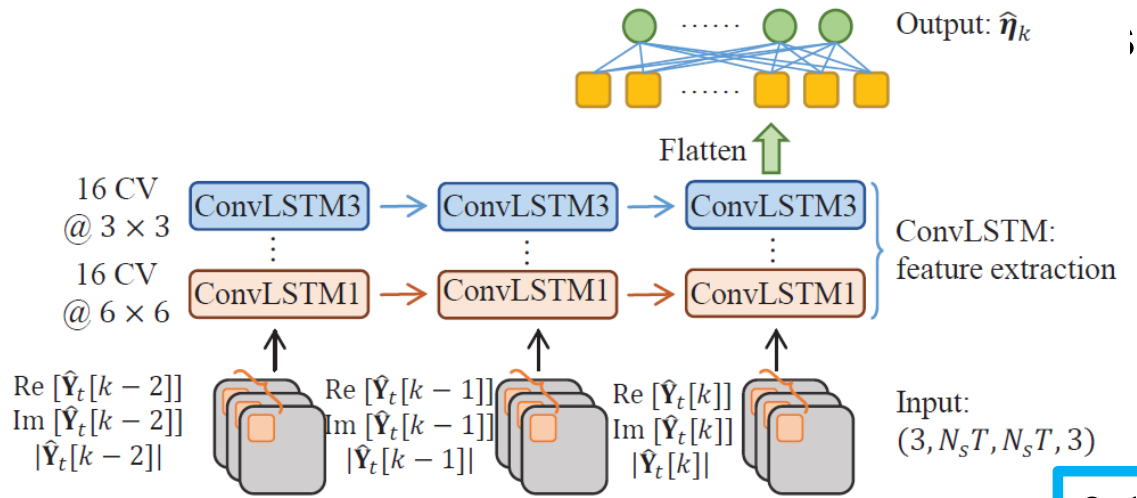
DL Beam Tracking



ConvLSTM tracking

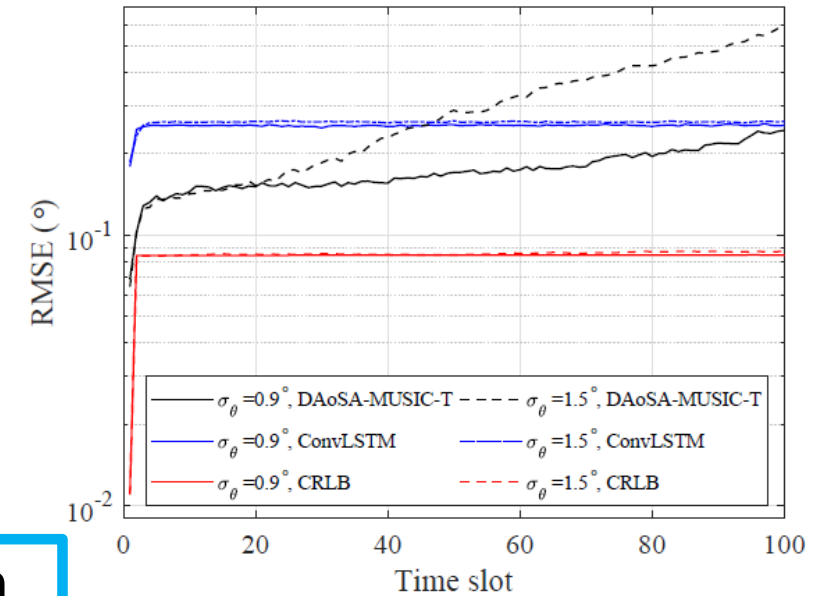
Design a ConvLSTM network for DoA tracking

Convolution layers: extract spatial correlations



ConvLSTM network structure

0.1° tracking precision with 50% reduced training overhead in ms

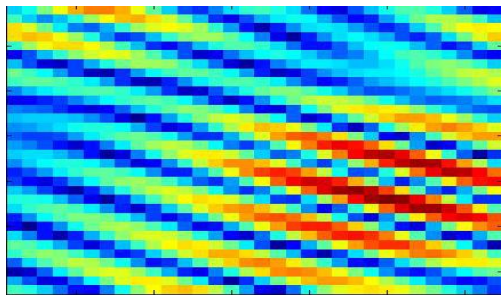
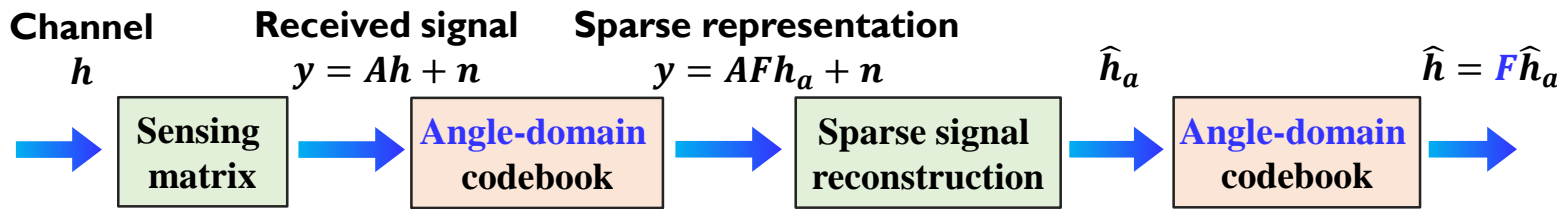


Tracking RMSE over time

Challenge of THz Near-Field Beam Estimation

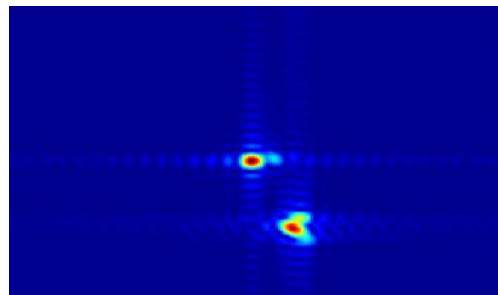


- Existing far-field beam estimation relies on the **angle-domain sparsity** exploited by the orthogonal **angle-domain codebook**, i.e., the DFT codebook
- The near-field angle-domain channels suffer from a severe **energy spread problem**

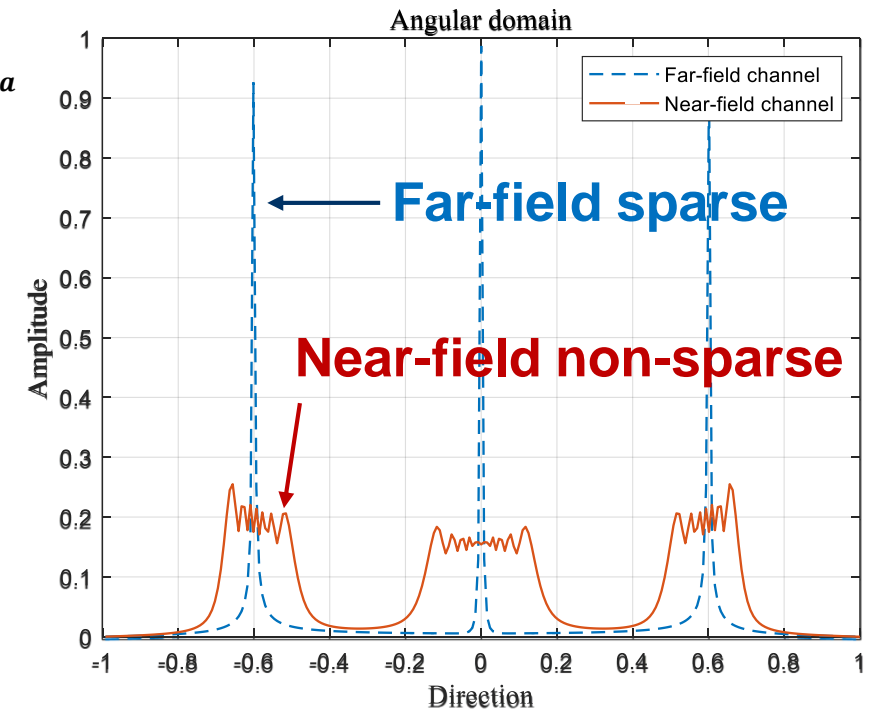


Far-field antenna-domain

Angle-domain codebook



Far-field angle-domain



The angle-domain codebook is not appropriate for near-field beam estimation

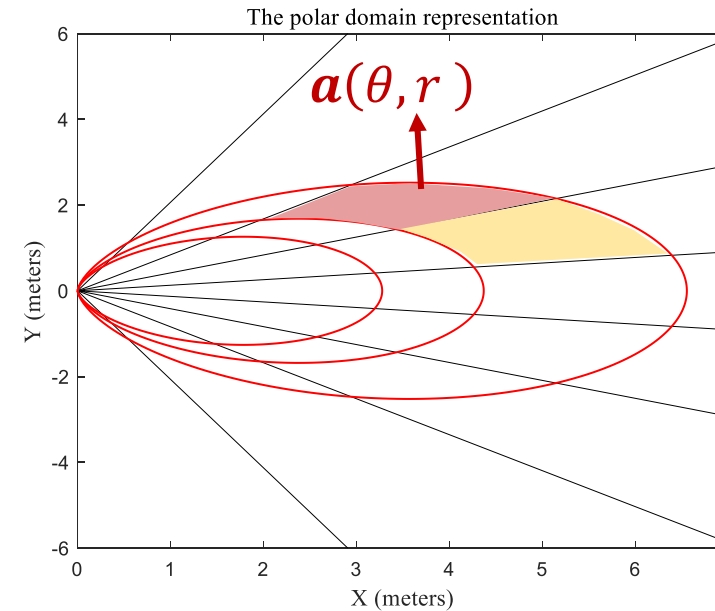
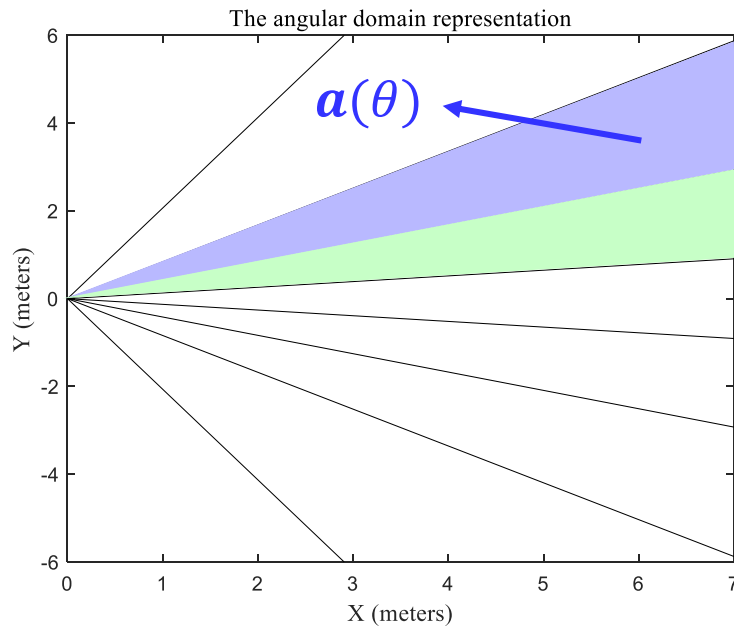
Near-Field Beam Codebook Design



- Far-field codebook: samples multiple **angle** grids in the **angle** domain
- Near-field codebook: samples multiple “**angle-distance**” grids in the **polar** domain

Angle-domain codeword $\mathbf{a}(\theta) = [e^{jn\pi\theta}]_{n=-N}^N$

Polar-domain codeword $\mathbf{a}(\theta, r) = [e^{jk\sqrt{r+n^2d^2-2r}nd\theta}]_{n=-N}^N$



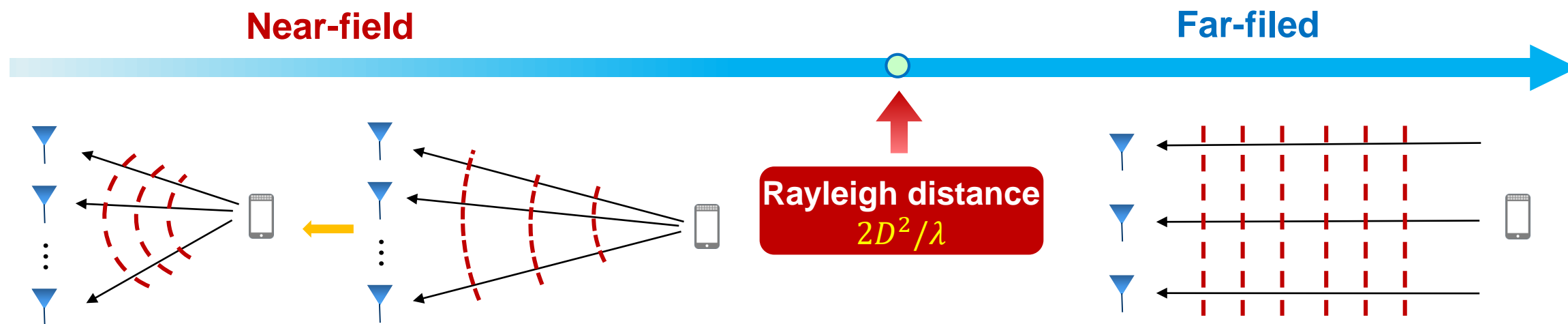
How to design the **additional distance sampling criterion** in polar-domain



The Distance-Sampling Criterion



- With the decrease of distance, the near-field effect becomes obvious and the **distance information gradually becomes significant**
- To exploit the near-field information, the grids can be **sampled sparsely far away from ELAA**, but should be **sampled densely near the ELAA**



A non-uniform distance-sampling criterion is preferred

Polar-Domain Codebook Based Beam Estimation



- Codebook design method: minimizing the largest mutual coherence of the codebook
- Based on the **Fresnel approximation**, we prove the following sampling criteria

Uniform angle sampling: $\theta_n = \frac{2n}{N} - \frac{N+1}{N}, \quad n = \{1, 2, \dots, N\}$

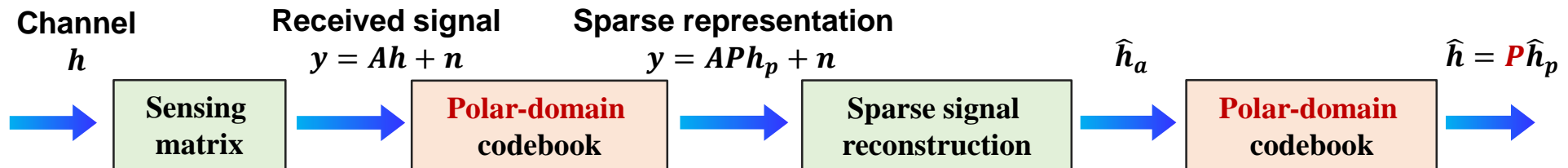
Non-uniform distance sampling: $r_{n,s} = \frac{1}{s} (1 - \theta_n^2) Z_\Gamma, \quad s = \{1, 2, \dots, S\}, \quad Z_\Gamma = \frac{M^2 d^2}{2\lambda\beta_\Gamma^2}$

The number of sampled distances

- The **polar-domain codebook** can be constructed as

$$P_n = [\mathbf{a}(\theta_n, r_{n,1}), \mathbf{a}(\theta_n, r_{n,2}), \dots, \mathbf{a}(\theta_n, r_{n,S})] \quad P = [P_1, P_2, \dots, P_N]$$

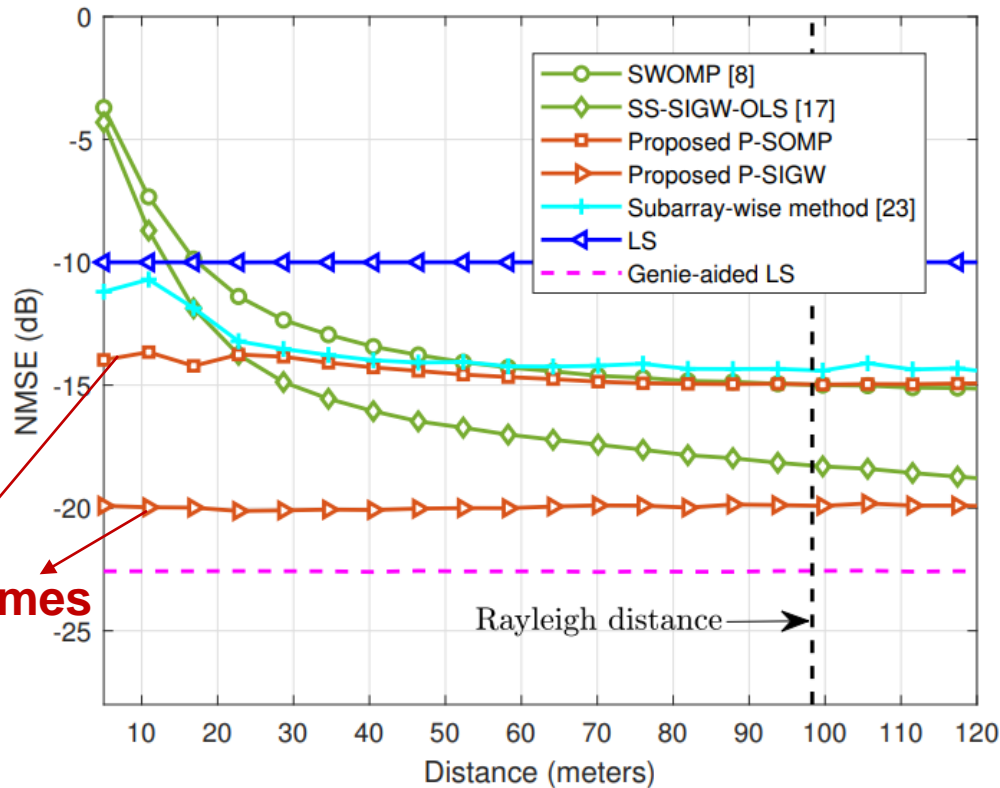
- Polar-domain codebook based near-field beam estimation



Simulation Result



● NMSE vs. Distance



Proposed schemes

Parameter	Value
Carrier	100 GHz
Bandwidth	400 MHz
Number of carriers	1024
Array Aperture	0.4 m
SNR	10 dB
Pilot overhead	0.5

Polar-domain codebook considerably **improves** the estimation accuracy in near-field

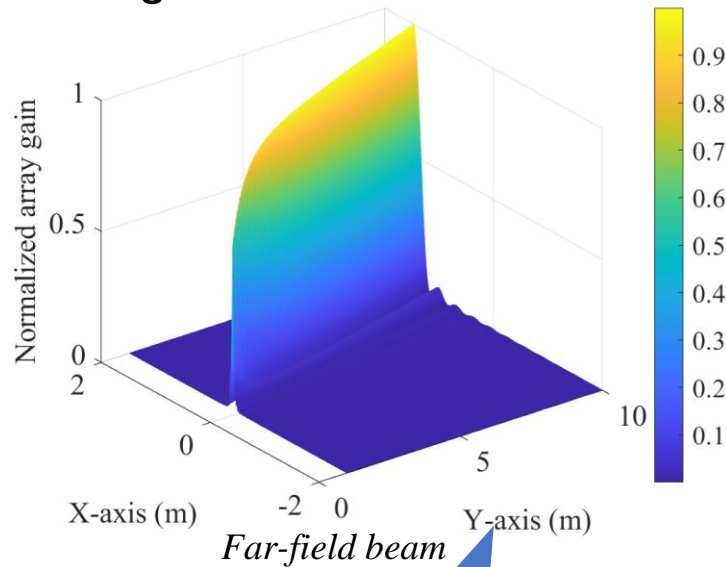
Challenge of THz Cross-field Beam Alignment



- Far-field beam alignment only in **angle domain**

$$w(\theta) = \exp\left(-j \frac{2\pi}{\lambda} nd \sin\theta\right) \Big|_{n=0}^{N-1}$$

- θ : angle

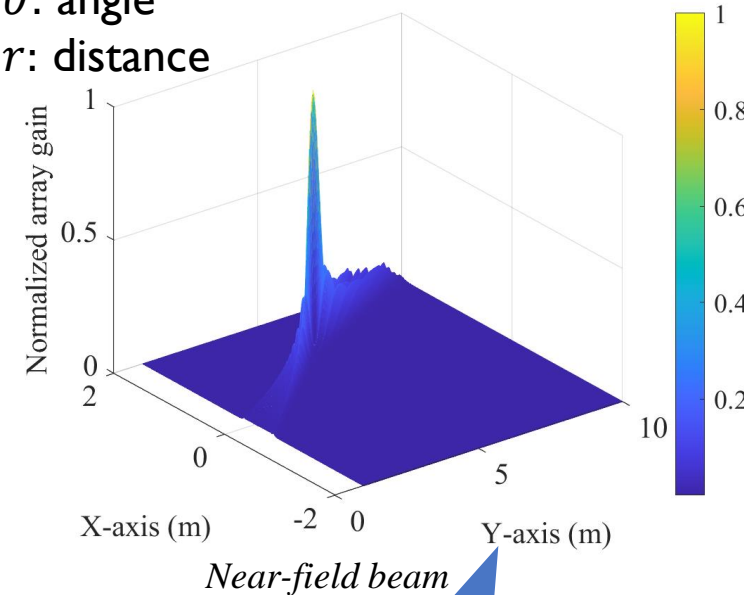


N^2 dimensional angle search

- Near-field beam alignment in **both angle and distance domains**

$$w(r, \theta) = \exp\left(-j \frac{2\pi}{\lambda} \sqrt{r + n^2 d^2 - 2r nd \sin\theta}\right) \Big|_{n=0}^{N-1}$$

- θ : angle
- r : distance



$N^2 D^2$ dimensional angle and distance search

N, D : number of beams in the angle and distance domains

Require efficient cross-field beam management method with high accuracy

Far-field Training with Estimation

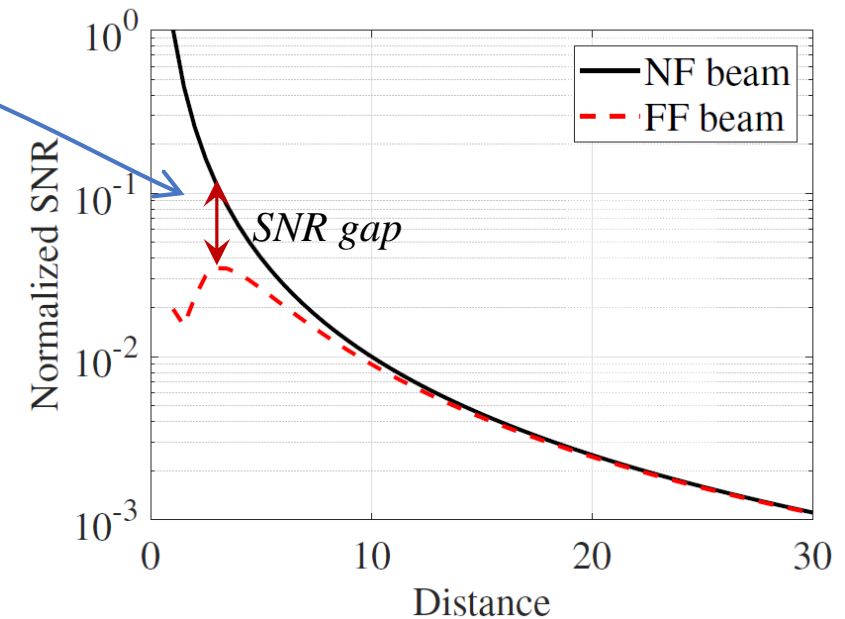


- **Far-field training**

- Aim of beam training: create directional beam with enhanced SNR to scan the spatial domain
 - Large propagation losses in THz band, the SNR is low without directional beams
- Although without distance alignment, far-field beam for training can be used in near-field as well, with sufficient SNR

- **Beam estimation**

- At short distance: exist SNR gap by using far-field and near-field beams due to distance domain beam misalignment
- Require low overhead beam management for precise distance and angle alignment

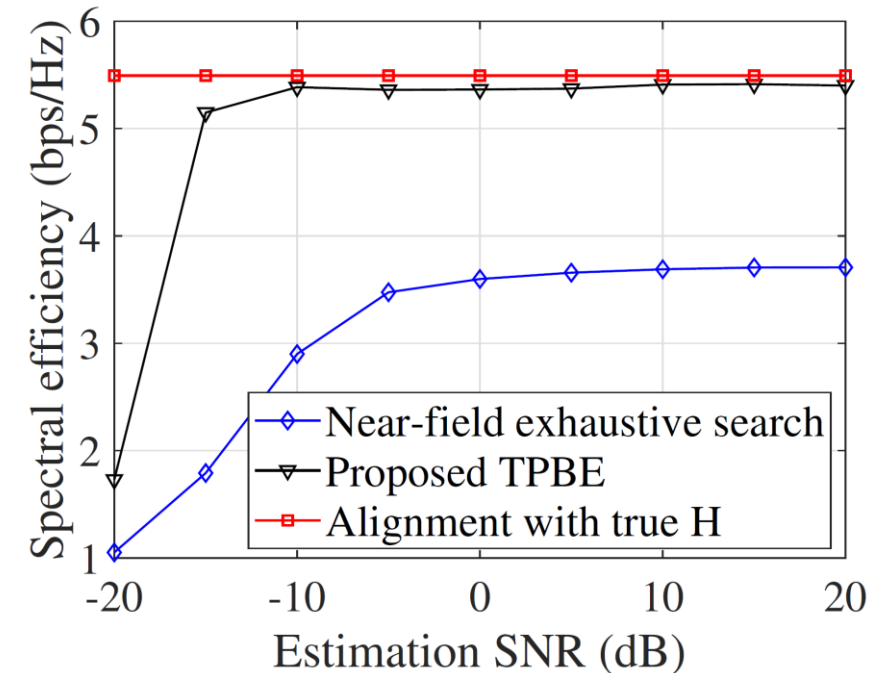


Compared to near-field (NF) beams, far-field (FF) beams enable enough SNR for training in near- and far-field

Performance Evaluation



- **Alignment performance**
 - TPBE achieves **near-perfect spectral efficiency**, 0.1 bps/Hz lower than alignment with true channel at SNR = 0 dB
- **Training overhead**
 - **30 times reduced** training overhead



Method	Near-field exhaustive search	Far-field exhaustive search	Proposed TPBE
Training overhead	$N_b N_u C_d$	$N_b N_u$	$N_b N_u$

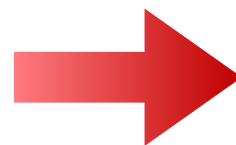
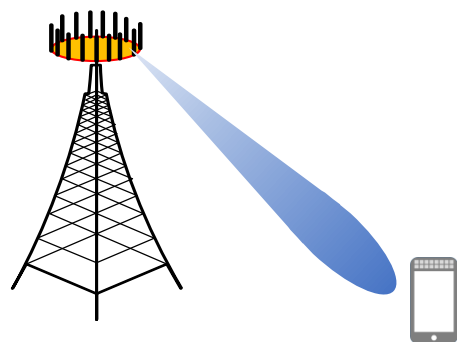
$C_d = 30$ times reduced

Challenge of THz Beam Tracking

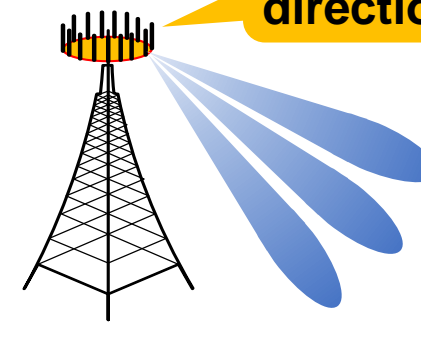


- Beam tracking:
 - Align the beam with a mobile user
- Technical challenge
 - The extremely narrow beam makes the pilot overhead of classical THz beam training unaffordable

Serially scanning



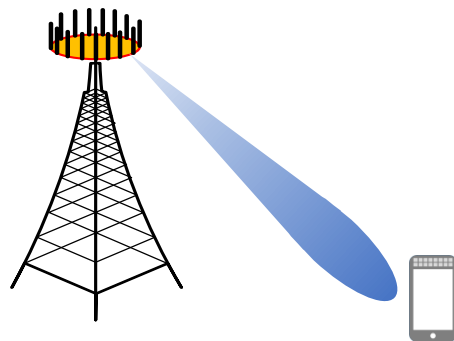
Can we scan multiple directions in parallel?



Beam Zooming based THz Beam Tracking

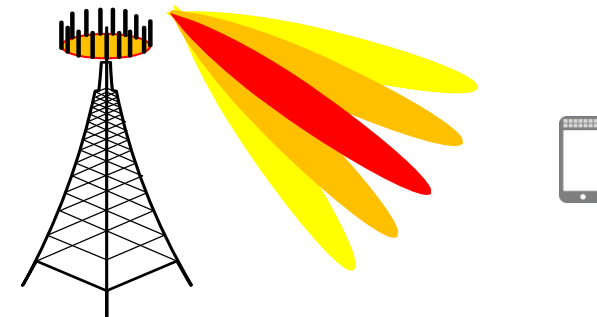


- Technical challenge
 - The extremely narrow beam makes the pilot overhead of classical THz beam training unaffordable
- Beam Zooming technology
 - Redirect the vision from mitigating beam split to benefiting from it
 - Elaborately design time delays in the delay-phase precoding structure.
 - Flexibly Control the angular coverage of frequency-dependent beams over the whole bandwidth



Searching **one** angle per time slot

Beam zooming

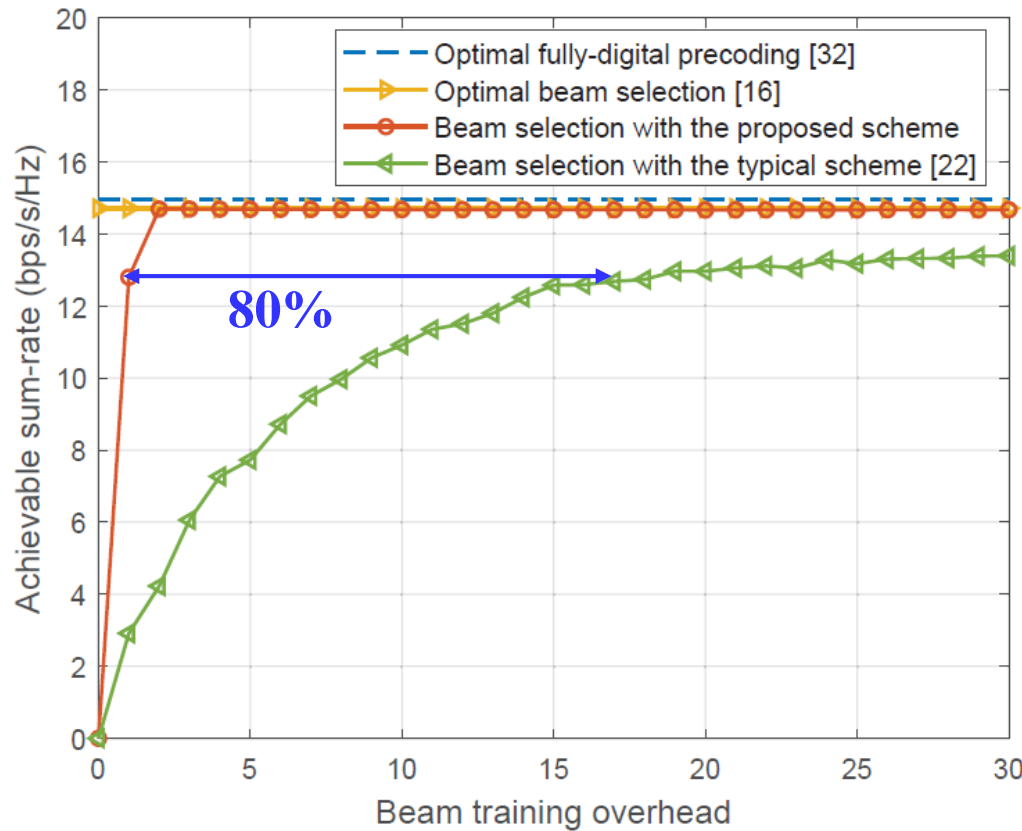


Searching **multiple** angles per time slot

Simulation Result



● Performance of Beam Tracking



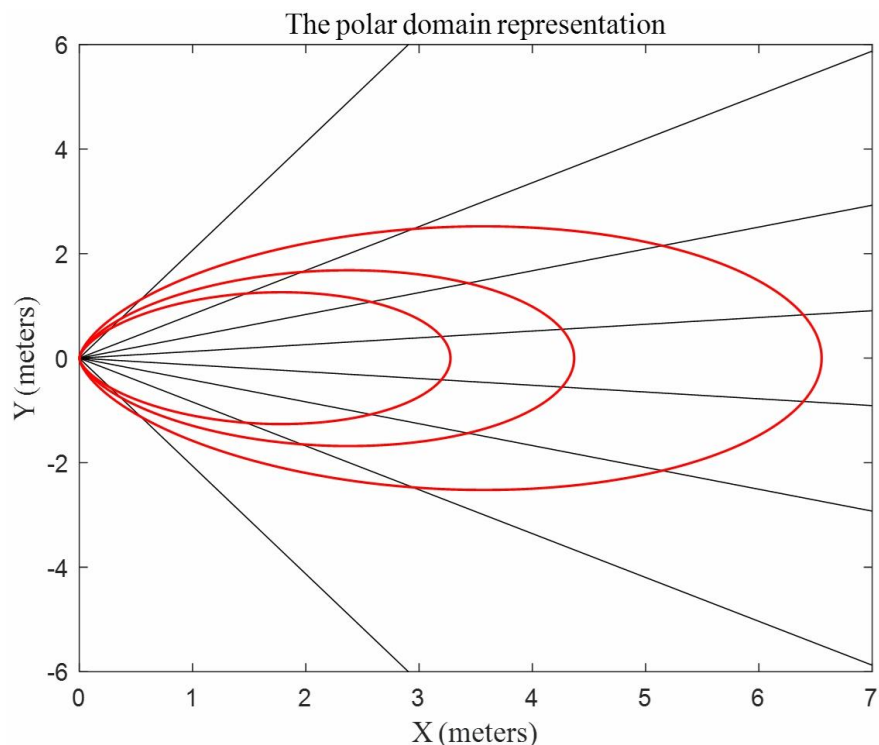
Parameter	Value
Carrier	100 GHz
Bandwidth	5 GHz
Number of carriers	1024
Number of antennas	256
SNR	10 dB

Remarkably reducing the pilot overhead by 80%

Challenge of Near-Field Beam Training



- Polar-domain codebook requires extra grids on the distance domain, leading to a substantial scaling of codebook size



Exhaustive Search

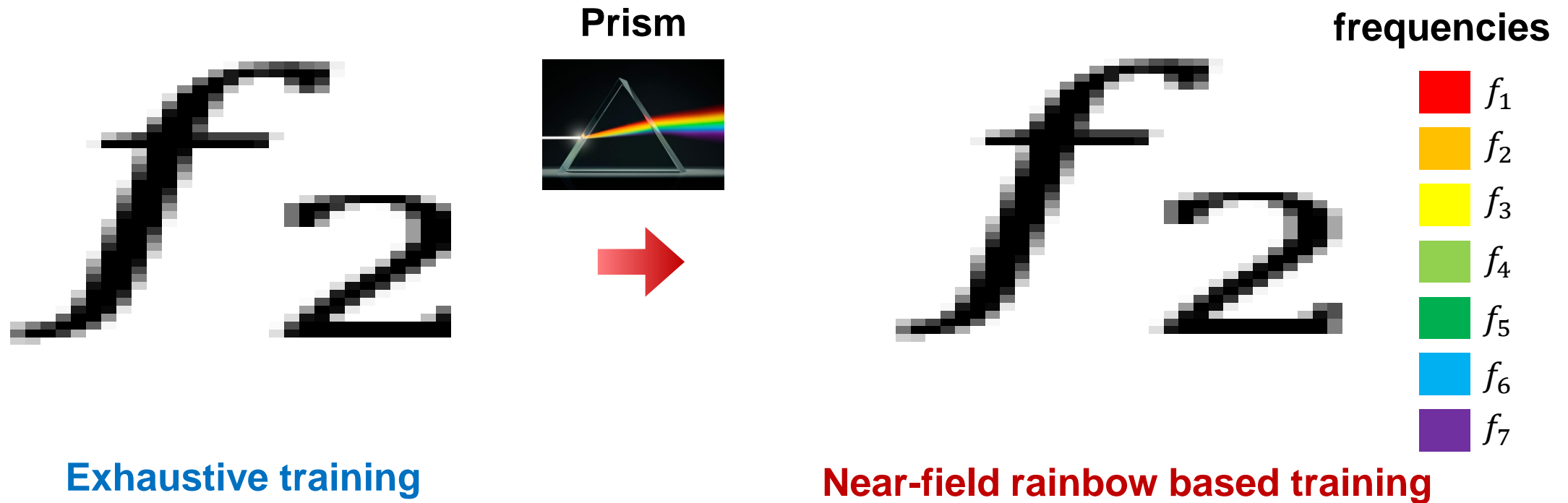
Parameter	Far-field codebook	Near-field codebook
Number of antennas	512	512
Carriers	100 GHz	100 GHz
Number of angle grids	512	512
Number of distance grids	1	20
Codebook size	512	10240

The overhead of near-field exhaustive beam training is unaffordable

Near-field Rainbow based Beam Tracking



- Time-delay circuits are able to control the degree of the near-field beam split effect
 - The optimal **distance** is searched in a **time division** manner
 - The optimal **angle** is searched in a **frequency division** manner



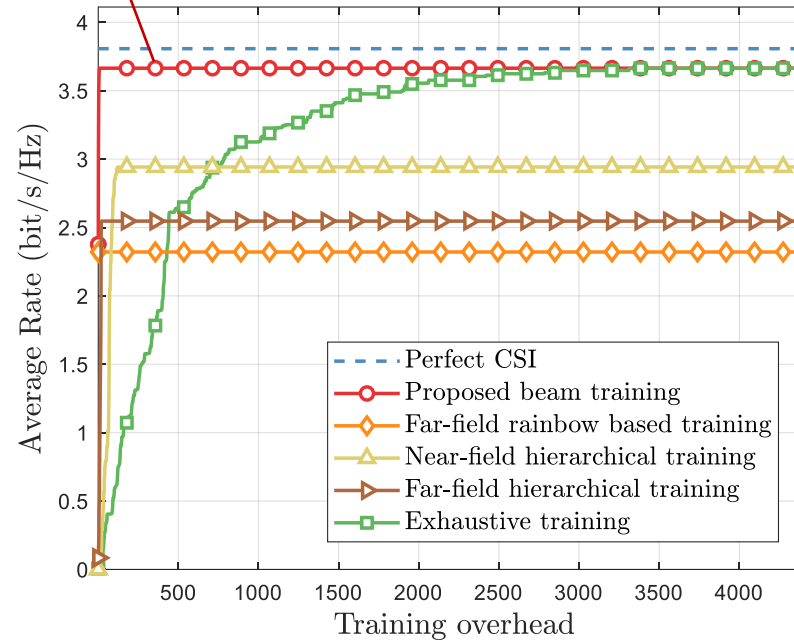
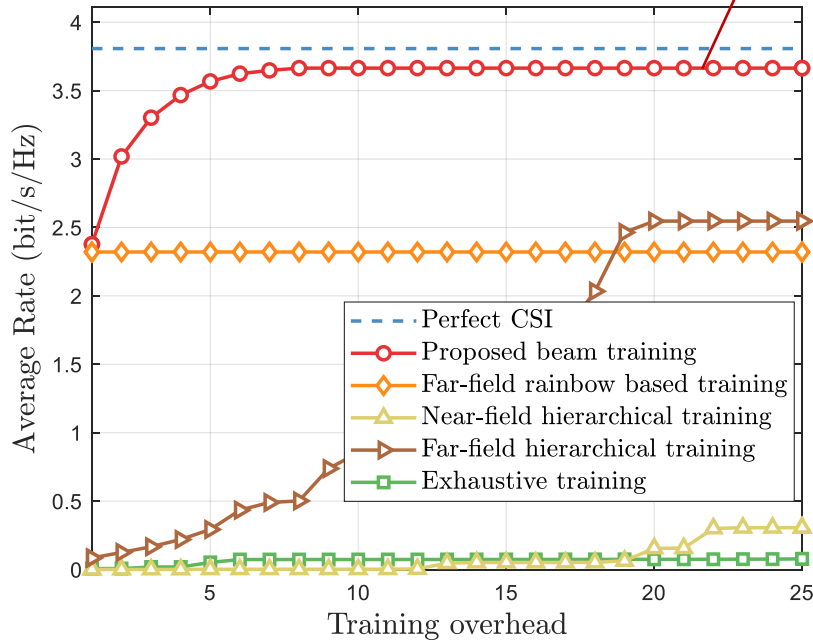
The pilot overhead is determined by the search of distance

Simulation Result



- Average achievable rate vs. training overhead

Proposed method



Parameter	Value
Carrier	60 GHz
Bandwidth	3 GHz
Antenna number	256
Distance	$U(3 \text{ m}, 40 \text{ m})$
Angle	$U(-\sin \frac{\pi}{3}, \sin \frac{\pi}{3})$

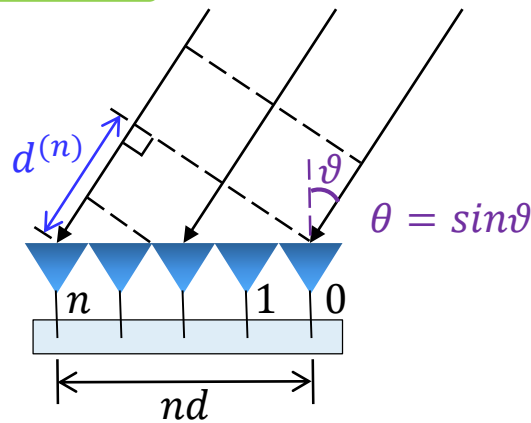
Our scheme achieves a near-optimal average rate with 8 training overhead

Comparison of far-field and near-field



- **Far-field:** The EM waves impinging on the antenna array can be approximately modeled as **planar waves**, where the phase of the EM wave is a **linear function** of the antenna index n
- **Near-field:** The EM waves have to be accurately modeled as **spherical waves**, where the phase of the EM wave is a **non-linear function** of the antenna index n

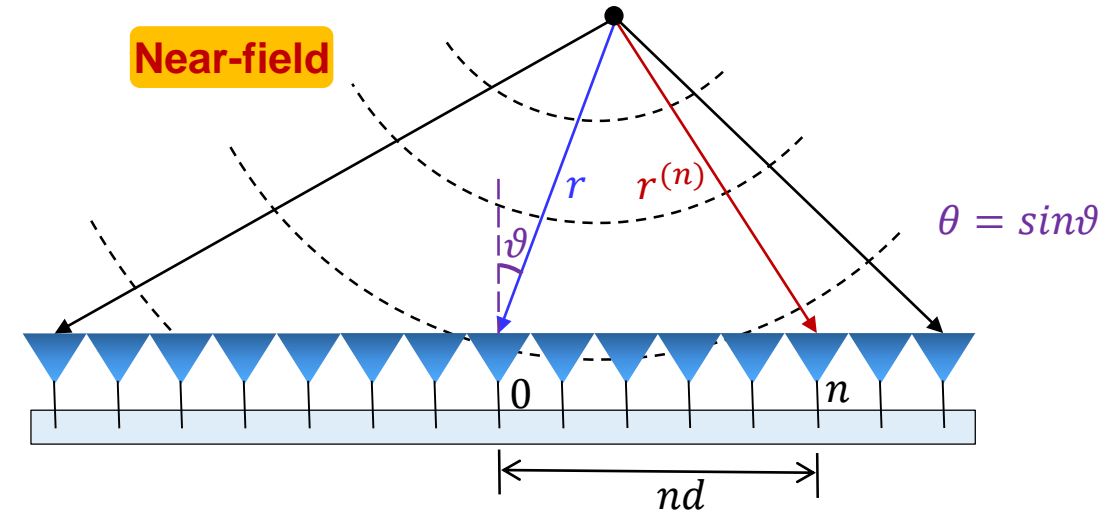
Far-field



Distance: $d^{(n)} = nd\theta$ Linear

Phase: $\phi_n^{\text{far}} = -\frac{2\pi d^{(n)}}{\lambda} = -\frac{2\pi}{\lambda} nd\theta$

Near-field



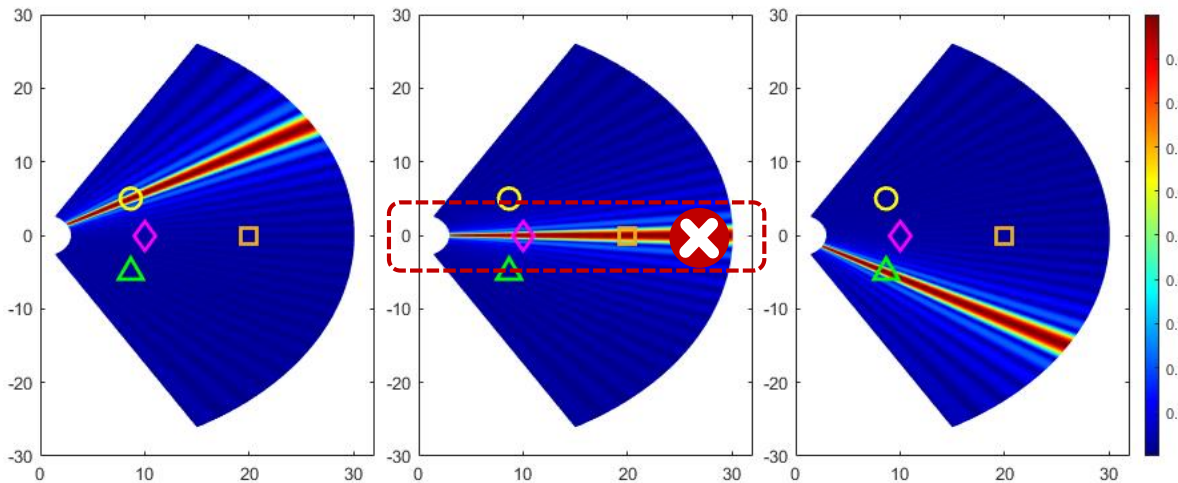
Distance: $r^{(n)} = \sqrt{r^2 + n^2 d^2 - 2n d r \theta}$ Non-linear

Phase: $\phi_n = \frac{2\pi(r^{(n)} - r)}{\lambda} = \frac{2\pi}{\lambda} (\sqrt{r^2 + n^2 d^2 - 2n d r \theta} - r)$
 $\approx -\frac{2\pi}{\lambda} nd\theta + \frac{1-\theta^2}{\lambda r} \pi n^2 d^2$ Near-field term

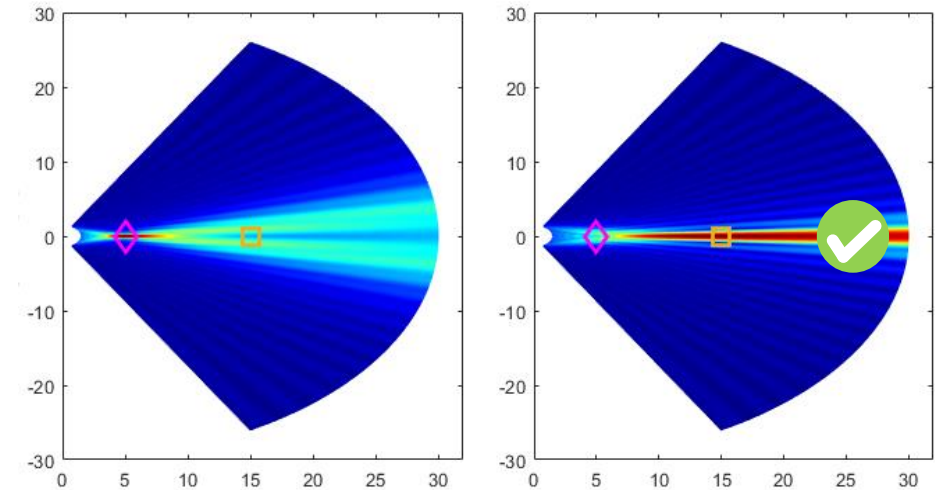
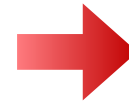
Challenge of SDMA for Far-Field Communication



- **Spatial division multiple access (SDMA)** is employed by massive MIMO to serve multiple users, but it fails to simultaneously serve users **at the same angle**
- Unlike **far-field beam steering** which focus on specific angles, near-field beam focusing is able to focus on specific location



Far-field beamsteering



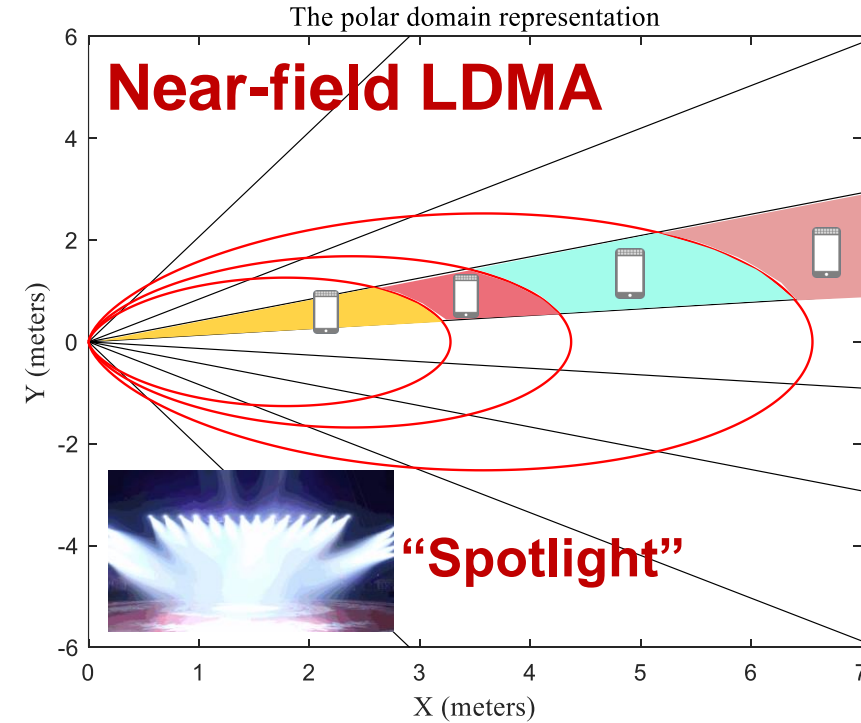
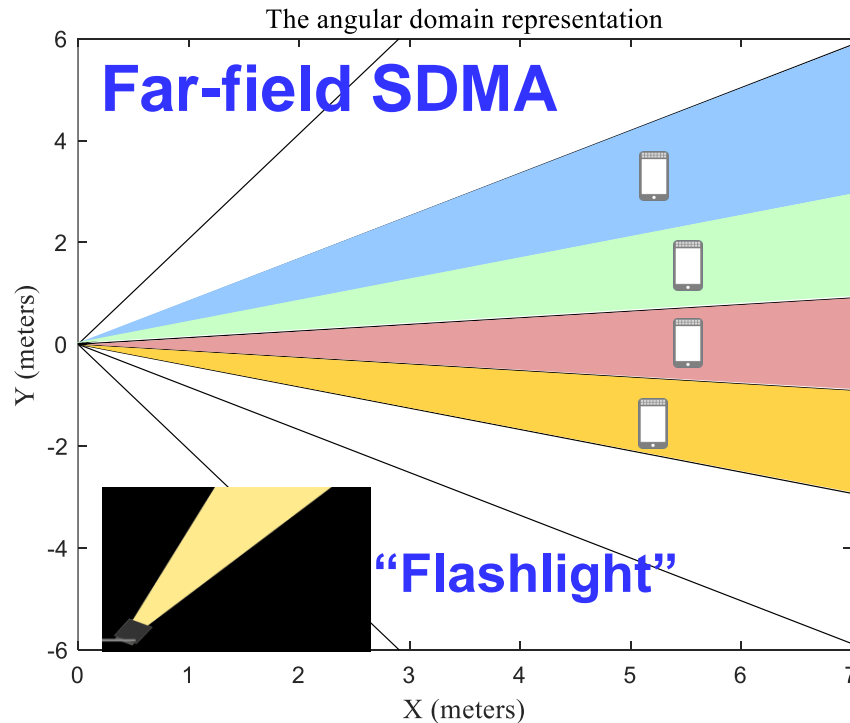
Near-field beamfocusing

Near-field beamfocusing has the potential to serve users at the **same** spatial angle

Multiple Access in Near-Field: SDMA or LDMA?



- Far-field SDMA: Users at different angles are served by orthogonal far-field beams
- Near-field location division multiple access (LDMA): Users at different locations can be simultaneously served due to property of near-field beam focusing



Compared with far-field SDMA, near-field LDMA provides new possibility for capacity improvement

Beamfocusing of Near-Field Beams



Lemma 1: The normalized array gain achieved by $w = a^*(\bar{r}, \theta)$ at any user location (r, θ) is obtained through **Fresnel approximation** as

$$f(r, \bar{r}, \theta) = \frac{1}{M} \left| \sum_{n=-N}^N e^{jk(\bar{r}^{(n)} - r^{(n)})} \right| \approx |G(\beta)| = \left| \frac{C(\beta) + js(\beta)}{\beta} \right|$$

where $\beta = \sqrt{\frac{M^2 d^2 (1 - \theta^2)}{2\lambda} \left| \frac{1}{r} - \frac{1}{\bar{r}} \right|}$, $C(\beta) = \int_0^\beta \cos\left(\frac{\pi}{2} t^2\right) dt$ and $S(\beta) = \int_0^\beta \sin\left(\frac{\pi}{2} t^2\right) dt$ are **Fresnel functions**.

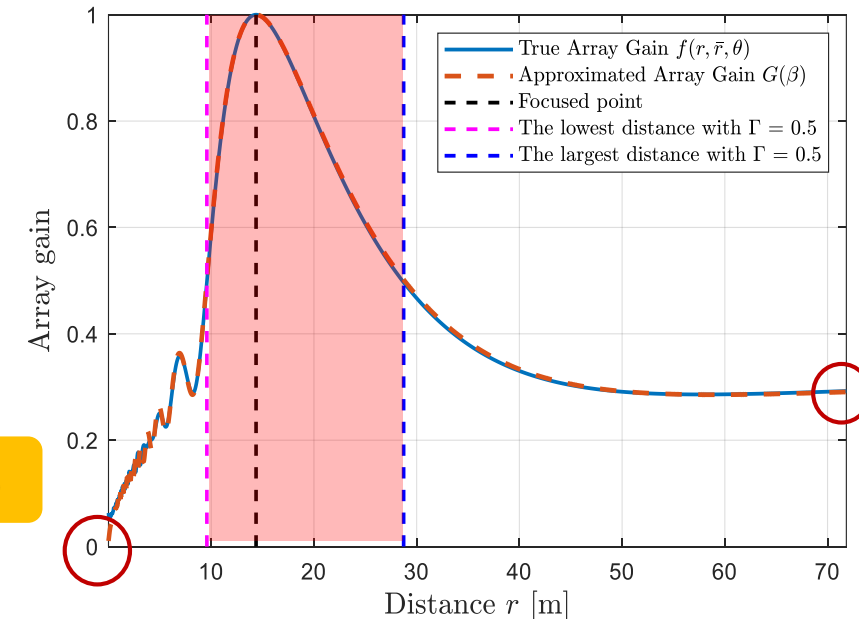
- Beamfocusing property of near-field beams

- Similar to the beam-width in angular domain of far-field beams, near-field beams possess **depth-of-focus** in distance domain

$$r \in \left[\frac{\bar{r} D^2 (1 - \theta^2)}{D^2 (1 - \theta^2) + 2\lambda \beta_\Gamma^2 \bar{r}}, \frac{\bar{r} D^2 (1 - \theta^2)}{D^2 (1 - \theta^2) - 2\lambda \beta_\Gamma^2 \bar{r}} \right]$$

3dB depth-of-focus: $r_d = \frac{4\lambda \beta_\Gamma^2 \bar{r}^2 D^2 (1 - \theta^2)}{D^4 (1 - \theta^2)^2 - 4\lambda^2 \beta_\Gamma^4 \bar{r}^2}$

$G(\beta_\Gamma) = 0.5$



Distance Domain Asymptotic Orthogonality



- Far-field orthogonality in **angular** domain

Phase: $\phi_n^{\text{far}}(\theta) = -\frac{2\pi}{\lambda}nd\theta$

Correlation: $f^{\text{far}} = |a^H(\theta_1)a(\theta_2)| = \frac{1}{N} \left| \frac{\sin(\frac{1}{2}Nkd(\sin \theta_1 - \sin \theta_2))}{\sin(\frac{1}{2}kd(\sin \theta_1 - \sin \theta_2))} \right|$

As $N \rightarrow \infty$, interference from different angles $I^{\text{far}} \rightarrow 0$ ($\theta_1 \neq \theta_2$)

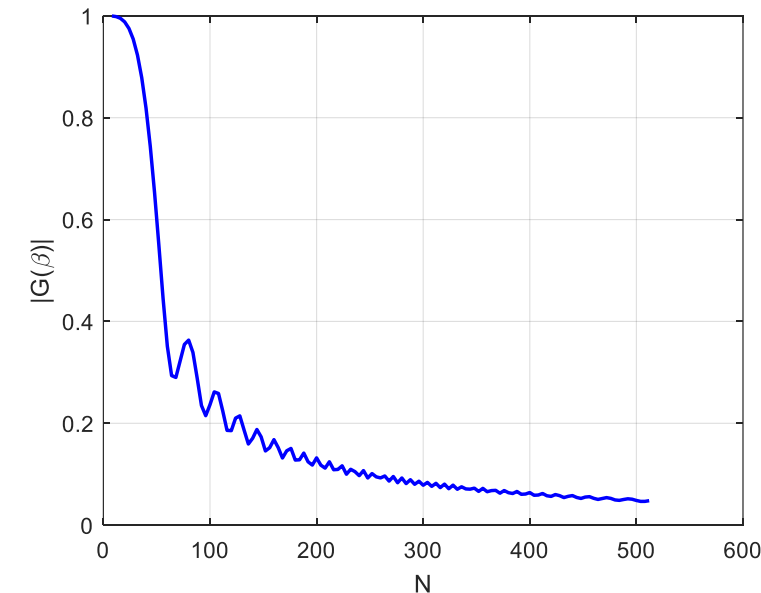
- Lemma 2: **Near-field orthogonality** in **distance** domain

Phase: $\phi_n^{\text{near}}(\theta) = -\frac{2\pi}{\lambda}nd\theta + \frac{1-\theta^2}{\lambda r} \pi n^2 d^2$

Correlation: $f^{\text{near}} = |a^H(\theta, r_1)a(\theta, r_2)| \approx |G(\beta)| = \left| \frac{C(\beta) + jS(\beta)}{\beta} \right|$

where $\beta = \sqrt{\frac{N^2 d^2 (1-\theta^2)}{2\lambda} \left| \frac{1}{r} - \frac{1}{\bar{r}} \right|}$

As $N \rightarrow \infty$, interference from different distances $I^{\text{near}} \rightarrow 0$ ($\forall \theta, r_1 \neq r_2$)

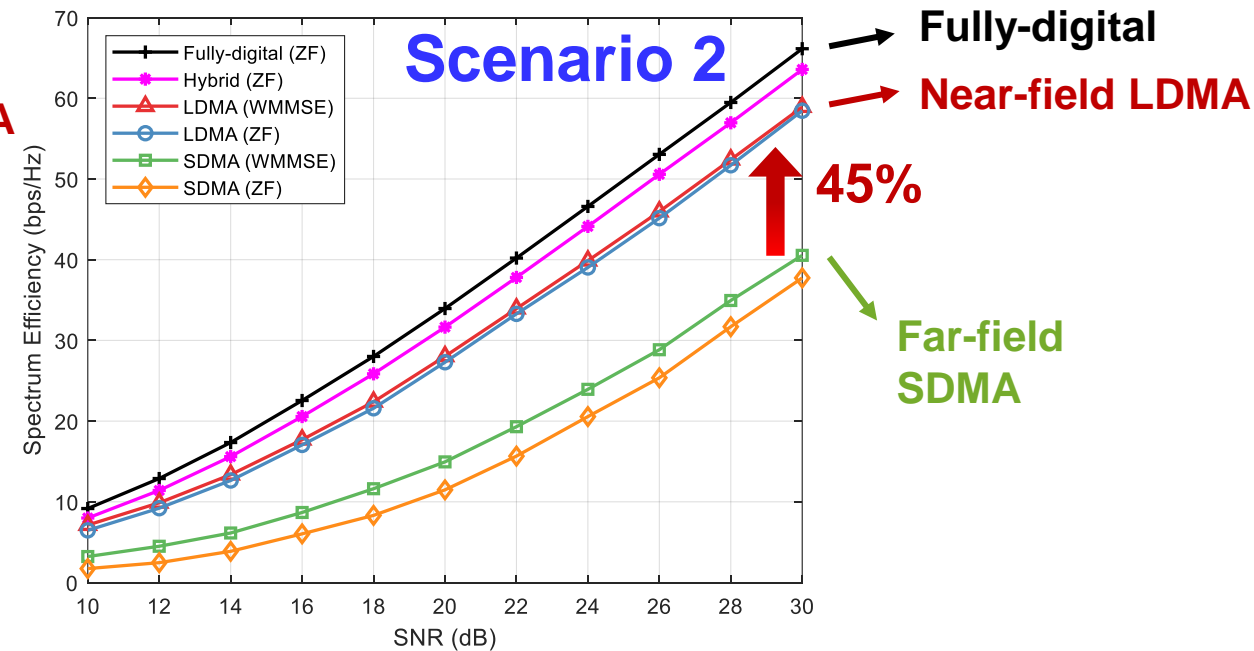
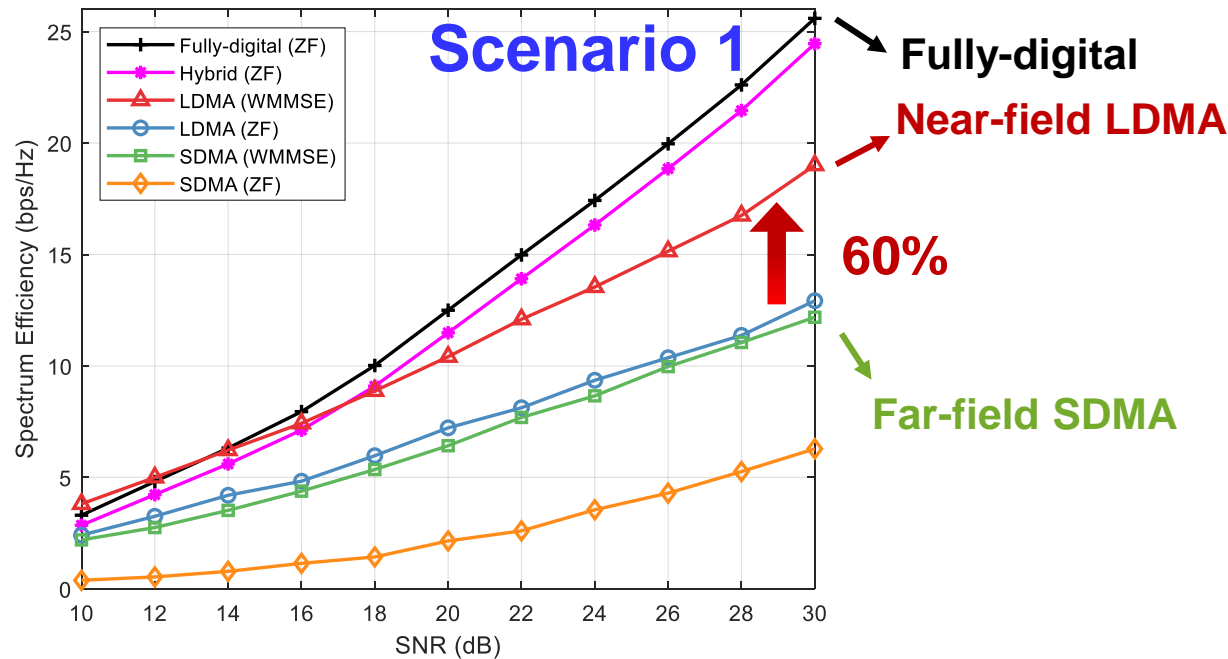


Simulation Results for LDMA



- Scenario 1: Users are **linearly distributed** along the same direction
- Scenario 2: Users are **uniformly distributed** within a cell

BS Antennas	UE Antennas	Frequency	UE Numbers	Elevation/ Azimuth Angle Range	Distance Range
256	1	30 GHz	20	$[-\pi/2, \pi/2]$	[4m, 100m]



Outline



- **Chapter 1: Introduction**
 - i. Evolution to 6G
 - ii. Applications
 - iii. Motivations for THz UM-MIMO
- **Chapter 2: THz UM-MIMO Systems**
 - i. Electronic and photonic approaches
 - ii. New material approaches
 - iii. THz UM-MIMO channel
- **Chapter 3: THz Beamforming Technologies**
 - i. Fundamentals of beamforming
 - ii. State-of-the-art and challenges on beamforming
 - iii. Far-field beamforming
 - iv. Near-field beamforming/beamfocusing
- **Chapter 4: THz Beam Management**
 - i. Fundamentals of beam management
 - ii. State-of-the-art and challenges on beam management
 - iii. Beam estimation/alignment
 - iv. Beam tracking
 - v. Beam-guided medium access
- **Chapter 5: Future Directions**
 - i. Cross far- and near-field beamforming
 - ii. IRS-assisted hybrid beamforming
 - iii. Beam management in IRS assisted systems
- **Conclusion**

Cross Far- and Near-field Communication



Recall Rayleigh distance is a classic boundary between far-field and near-field.

- In THz UM-MIMO system, the **increment of the number of antennas** and **decrease of wavelength** result in the **growth of the Rayleigh distance**

Rayleigh distance/m	0.1THz		0.3THz	
Antennas at Tx and Rx	1024-64	1024-1024	1024-64	1024-1024
ULA	1775	6291	591.9	2097
UPA	4.8	12.3	1.6	4.1
WSMS	262.8	307.2	87.6	102.4

WSMS is with 64λ subarray spacing and 4 subarrays

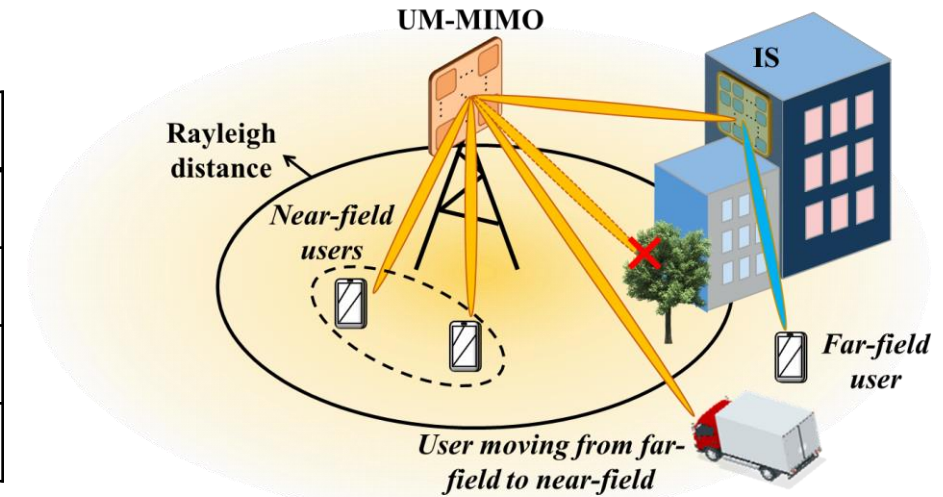


Illustration of THz Hybrid-field communications

- Typical communication distance at THz band **covers both far-field and near-field**

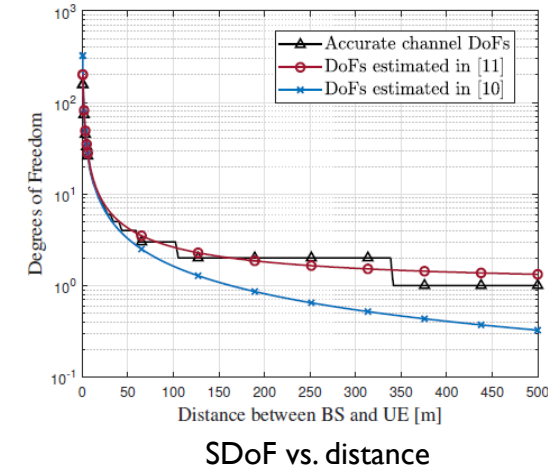
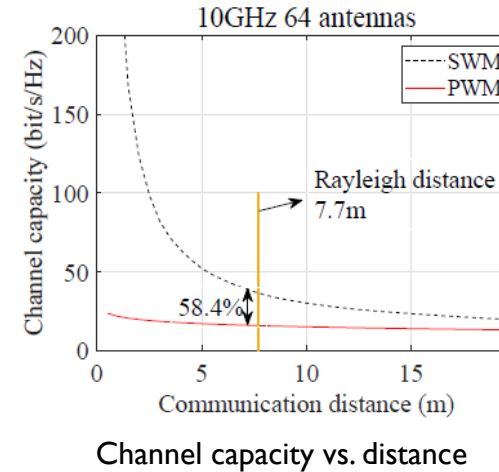
Practical Hardware Efficient Design



Decrement of distance → Increment of channel capacity

● Far-field

- Limited spatial multiplexing
 - **Less RF chains and phase shifters required**
 - **Lower hardware cost**



● Near-field

- Non-linear channel phases gives additional spatial degree-of-freedom (SDoF)
- To unleash spatial multiplexing
 - **More RF chains and phase shifters required**
 - **Higher hardware cost**

Difficult to **simultaneously meet** the cross-field spatial multiplexing and hardware cost requirements.

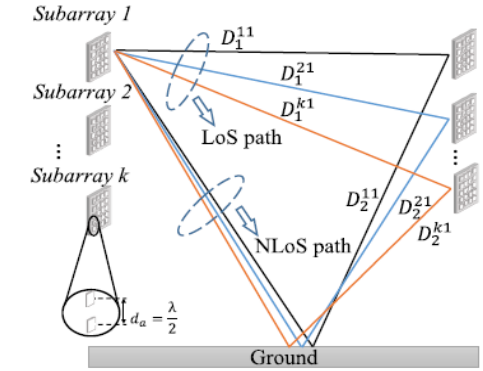
C. Han, Y.-H. Chen, L. Yan, Z. Chen, and L. Dai, “**Cross far- and near-field wireless communications in terahertz ultra-large antenna array systems,**” IEEE Wireless Communications, 2023.

Practical Hardware Efficient Design

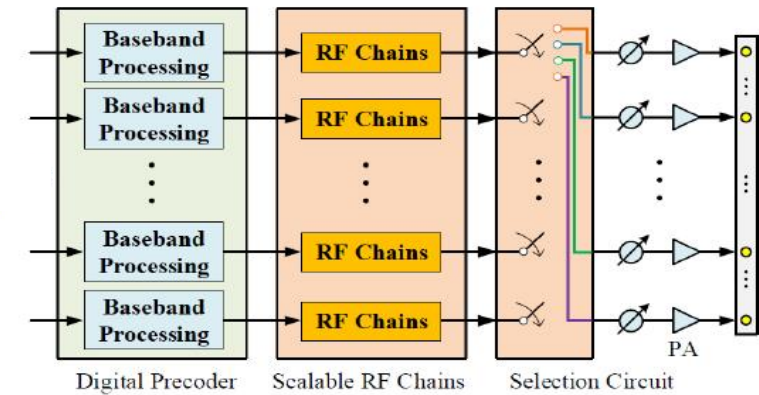


Two potential solutions:

- **Widely-Spaced Multi-Subarray (WSMS)**
 - Enlarge the near-field region to a typical communication distance
- **Distance-aware precoding structure (DAP)**
 - Insert a selection circuit between phase shifters and RF-chains
 - Flexibly activate/inactivate each RF-chain according to the SDoFs



WSMS structure



DAP architecture

The number of RF-chains and phase shifters of both structures are **larger than** structures for far-field transmission.

More efficient structure is needed to **balance spatial multiplexing and hardware cost** in cross-field transmission.

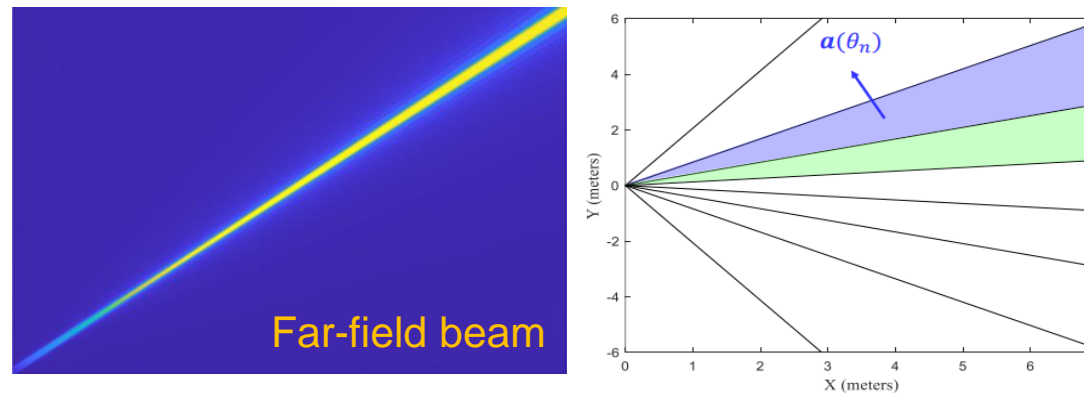
Cross-field Beam Training



Beam training is required to realize **narrow beam pair alignment** between Tx and Rx

- Far-field:

- **Angle domain beam** $[\mathbf{w}(\theta)]_n = \frac{1}{\sqrt{N}} \exp(-jk_c \delta_N^{(n)} d \sin \theta)$



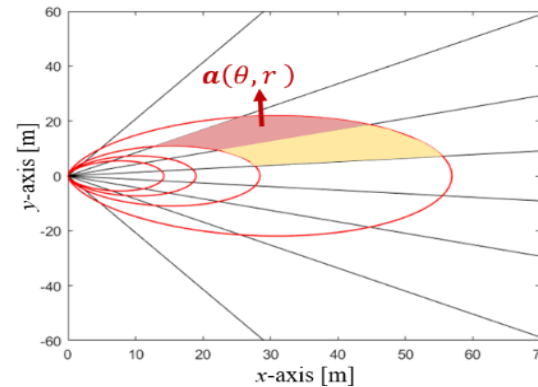
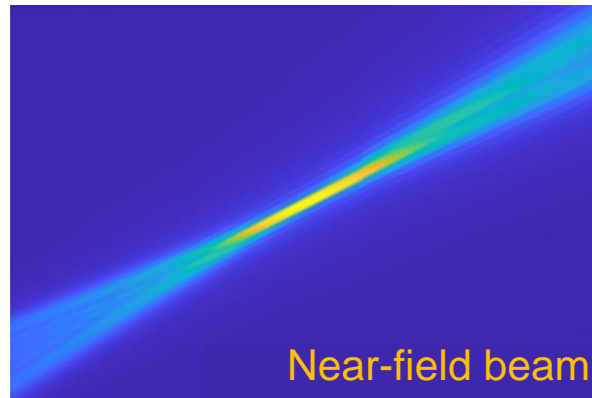
- Beams only process angular resolution
- Beam training only needs to search in the angular dimension
- Inaccurate in the near-field

Cross-field Beam Training



- Near-field:

- Joint angle and distance domains beam $[\mathbf{w}(r, \theta)]_n = \frac{1}{\sqrt{N}} \exp\left(-jk_c r \left(1 - \delta_N^{(n)} d \sin\theta\right)\right)$



- Additional distance domain beam resolution
- Beam training jointly searches in the angular and distance domains
- Significantly increases the training overhead

Codebook designs are different for cross-field beam training, and are not universally applicable.

Multi-user Communications and Networking



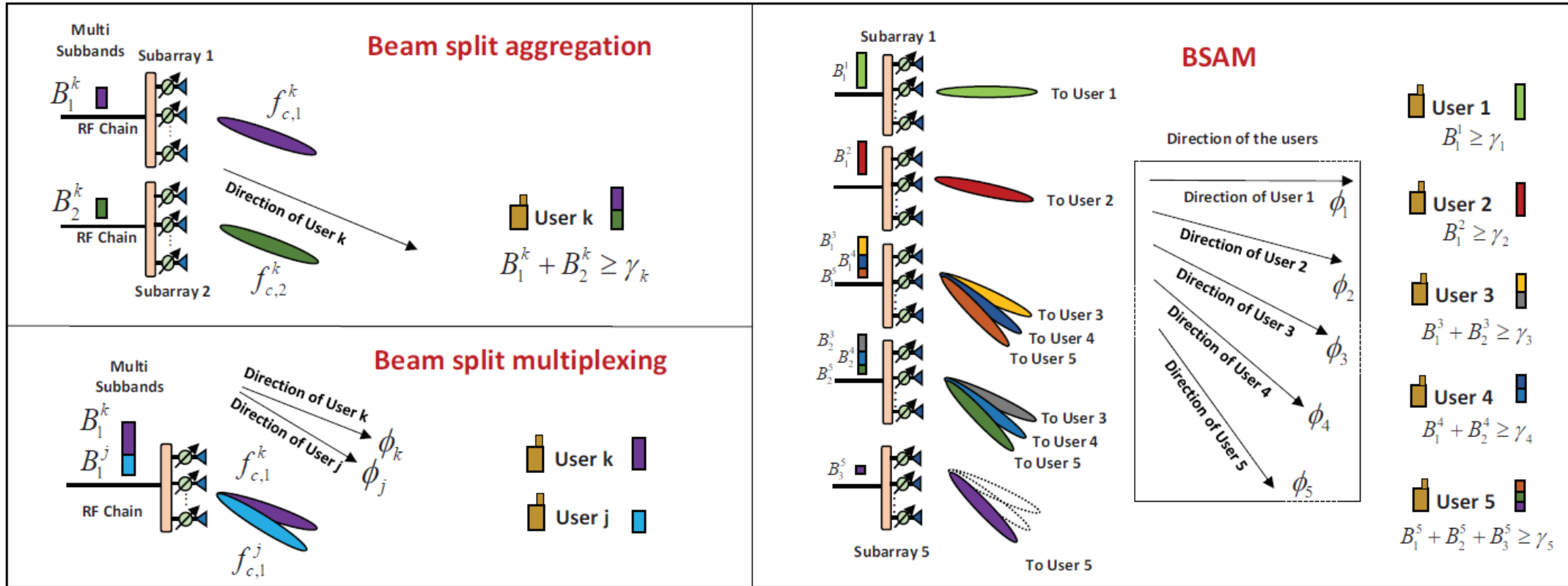
Lack of analysis on **medium access control (MAC) and networking** in THz cross-field communication.

- Far-field: spatial division multiple access (SDMA)
- Near-field: location division multiple access (LDMA)
 - Orthogonality in **both angular and distance domains** → increased precision of beamforming
 - **Employ near-field location-dependent beam focusing vectors** as analog precoders to serve different UEs located in different locations
 - Enhance the multiple accessibilities **by the distance dimension**
- How to unify the cross-field multiple access?
 - Account for distance and angular beam resolutions in different communication distances

Beam Split Aggregation and Multiplexing



BSAM is a general concept including beam split aggregation and multiplexing



beam split aggregation: each user might be served by multiple subarray on different sub-bands

beam split multiplexing: each subarray may serve multiple users on different sub-bands


Outline

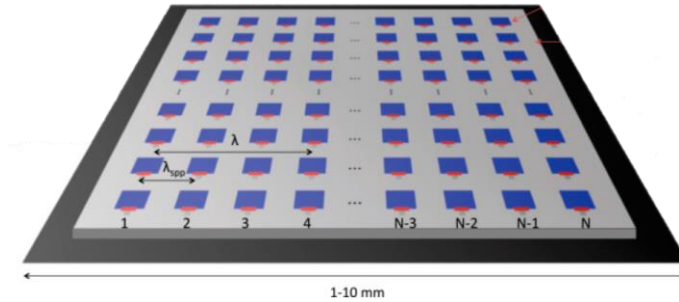


- **Chapter 1: Introduction**
 - i. Evolution to 6G
 - ii. Applications
 - iii. Motivations for THz UM-MIMO
- **Chapter 2: THz UM-MIMO Systems**
 - i. Electronic and photonic approaches
 - ii. New material approaches
 - iii. THz UM-MIMO channel
- **Chapter 3: THz Beamforming Technologies**
 - i. Fundamentals of beamforming
 - ii. State-of-the-art and challenges on beamforming
 - iii. Far-field beamforming
 - iv. Near-field beamforming/beamfocusing
- **Chapter 4: THz Beam Management**
 - i. Fundamentals of beam management
 - ii. State-of-the-art and challenges on beam management
 - iii. Beam estimation/alignment
 - iv. Beam tracking
 - v. Beam-guided medium access
- **Chapter 5: Future Directions**
 - i. Hybrid far- and near-field beamforming
 - ii. IRS-assisted hybrid beamforming
 - iii. Beam management in IRS assisted systems
- **Conclusion**

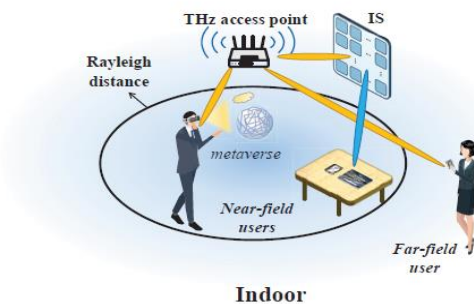
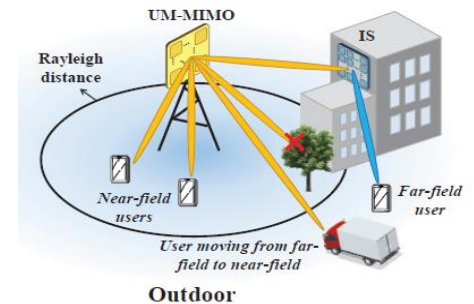
Conclusion



- **UM-MIMO** is essential for the viability of terahertz communication.
 - Large array gain
 - Multiplexing gain  Compensate Loss
- Lots of ideas and algorithms have been proposed for THz band communication. To ensure the practical values, these designs should sufficiently consider **the characteristics of terahertz devices and channels**.



- As an important future direction, the **cross near- and far- field communication** will bring a new paradigm of communication.





IEEE/CIC International Conference on Communications in China
10-12 August 2023 // Dalian, China
Integrating Space-Air-Ground-Sea Communications



**Thank you very much
for your attention!**

Chong Han

Shanghai Jiao Tong University

chong.han@sjtu.edu.cn

Linglong Dai

Tsinghua University

dail@tsinghua.edu.cn

Zhi Chen

University of Electronic Science and
Technology of China

chenzhi@uestc.edu.cn